USGS
science for a changing world

Prepared in cooperation with the Bureau of Reclamation

Hydrogeologic Conceptual Model of Groundwater Occurrence and Brine Discharge to the Dolores River in the Paradox Valley, Montrose County, Colorado

Scientific Investigations Report 2023–5094

U.S. Department of the Interior
U.S. Geological Survey

Cover. Paradox Valley, Montrose County, Colo., view looking northwest toward the La Sal Mountains (Used with permission from Wark Photography).

Hydrogeologic Conceptual Model of Groundwater Occurrence and Brine Discharge to the Dolores River in the Paradox Valley, Montrose County, Colorado

By Suzanne S. Paschke, M. Alisa Mast, Philip M. Gardner, Connor P. Newman, and Kenneth R. Watts

Prepared in cooperation with the Bureau of Reclamation

Scientific Investigations Report 2023–5094

U.S. Department of the Interior
U.S. Geological Survey

U.S. Geological Survey, Reston, Virginia: 2024

Suggested citation:
Paschke, S.S., Mast, M.A., Gardner, P.M., Newman, C.P., and Watts, K.R., 2024, Hydrogeologic conceptual model of groundwater occurrence and brine discharge to the Dolores River in the Paradox Valley, Montrose County, Colorado: U.S. Geological Survey Scientific Investigations Report 2023–5094, 58 p., https://doi.org/10.3133/sir20235094.

Associated data for this publication:
Gardner, P.M., and Newman, C.P., 2023, Recharge temperatures and groundwater-age models for the Paradox Valley alluvial aquifer, 2011, Colorado: U.S. Geological Survey data release, https://doi.org/10.5066/P9FMWX2J.

Newman, C.P., 2021, Water-level and pumping data, water-level models, and estimated hydraulic properties for the Paradox Valley alluvial aquifer in Montrose County, Colorado, 2013: U.S. Geological Survey data release, https://doi.org/10.5066/P9NV5U6F.

Paschke, S.S., and Mast, M.A., 2024, Geospatial datasets developed for a hydrogeologic conceptual model of brine discharge to the Dolores River, Paradox Valley, Colorado: U.S. Geological Survey data release, https://doi.org/10.5066/P9CJQDDU.

U.S. Geological Survey [USGS], 2020a, USGS water data for the nation: U.S. Geological Survey National Water Information System database, at https://doi.org/10.5066/F7P55KJN.

ISSN 2328-0328 (online)

Acknowledgments

The authors thank Andrew Nicolas, Bureau of Reclamation Facility Operations Specialist for the Paradox Valley Field Office, and Don Barnett of the Colorado River Salinity Control Forum for their contributions to Paradox Valley investigations.

The authors also thank U.S. Geological Survey colleagues Chuck Heywood, Laura Bexfield, and Geoff Delin for providing thoughtful reviews on previous versions of this report.

Contents

Figures

Tables

Conversion Factors

U.S. customary units to International System of Units

Multiply	By	To obtain
	Length	
inch (in.)	2.54	centimeter (cm)
inch (in.)	25.4	millimeter (mm)
foot (ft)	0.3048	meter (m)
mile (mi)	1.609	kilometer (km)
	Area	
acre	4,047	square meter (m^2)
acre	0.4047	hectare (ha)
acre	0.004047	square kilometer (km^2)
square mile (mi^2)	259.0	hectare (ha)
square mile (mi^2)	2.590	square kilometer (km^2)
	Density	
pound per cubic foot (lb/ft^3)	0.01602	gram per cubic centimeter (g/cm^3)
	Flow rate	
foot per day (ft/d)	0.3048	meter per day (m/d)
	Mass	
ton, short (2,000 lb)	0.9072	metric ton (t)
ton, long (2,240 lb)	1.016	metric ton (t)
	Hydraulic conductivity	
foot per day (ft/d)	0.3048	meter per day (m/d)
	Hydraulic gradient	
foot per mile (ft/mi)	0.1894	meter per kilometer (m/km)
	Resistivity	
ohm feet (Ωft)	0.3048	ohm meters (Ωm)

International System of Units to U.S. customary units

Multiply	By	To obtain
	Length	
centimeter (cm)	0.3937	inch (in.)
millimeter (mm)	0.03937	inch (in.)
meter (m)	3.281	foot (ft)
kilometer (km)	0.6214	mile (mi)
	Area	
square meter (m^2)	0.0002471	acre
hectare (ha)	2.471	acre
square hectometer (hm^2)	2.471	acre
square kilometer (km^2)	247.1	acre
hectare (ha)	0.003861	square mile (mi^2)
square kilometer (km^2)	0.3861	square mile (mi^2)

Multiply	By	To obtain
	Density	
gram per cubic centimeter (g/cm^3)	62.4220	pound per cubic foot (lb/ft^3)
	Flow rate	
meter per day (m/d)	3.281	foot per day (ft/d)
cubic meter per second (m^3/s)	35.31	cubic foot per second (ft^3/s)
	Mass	
metric ton (t)	1.102	ton, short (2,000 lb)
metric ton (t)	0.9842	ton, long (2,240 lb)
	Hydraulic conductivity	
meter per day (m/d)	3.281	foot per day (ft/d)
	Hydraulic gradient	
meter per kilometer (m/km)	5.27983	foot per mile (ft/mi)
	Resistivity	
ohm meters (Ωm)	3.28	ohm feet (Ωft)

Temperature in degrees Celsius (°C) may be converted to degrees Fahrenheit (°F) as follows:

$$°F = (1.8 \times °C) + 32.$$

Temperature in degrees Fahrenheit (°F) may be converted to degrees Celsius (°C) as follows:

$$°C = (°F - 32) / 1.8.$$

Datum

Vertical coordinate information is referenced to the North American Vertical Datum of 1988 (NAVD 88) and the National Geodetic Vertical Datum of 1929.

Horizontal coordinate information is referenced to the North American Datum of 1983 (NAD 83).

Altitude, as used in this report, refers to distance above the vertical datum.

Supplemental Information

Specific conductance is given in microsiemens per centimeter at 25 degrees Celsius (µS/cm).

Concentrations of chemical constituents in water are given in milligrams per liter (mg/L).

Concentrations of dissolved gases are given in cubic centimeters at standard temperature and pressure per gram of water (ccSTP/g).

Water year is the 12-month period from October 1 through September 30. The water year is designated by the year in which it ends.

Results for measurements of stable isotopes of an element (with symbol E) in water, solids, and dissolved constituents commonly are expressed as the relative difference in the ratio of the number of the less abundant isotope (iE) to the number of the more abundant isotope of a sample with respect to a measurement standard.

Abbreviations

δ^2H	hydrogen-2/hydrogen-1 isotopic ratio
$\delta^{18}O$	oxygen-18/oxygen-16 isotopic ratio
AEM	aerial electromagnetic survey
ccSTP/g	cubic centimeters at standard temperature and pressure per gram of water
CDWR	Colorado Division of Water Resources
CO_2	carbon dioxide
DIC	dissolved inorganic carbon
FWBI	freshwater-brine interface
GIS	geographic information systems
GMWL	Global Meteoric Water Line
K	hydraulic conductivity
Ma	mega-annum, millions of years before present
NWIS	USGS National Water Information System
Pmc	percent modern carbon
PVU	Paradox Valley Unit
Reclamation	Bureau of Reclamation
SC	specific conductance
TDS	total dissolved solids
TU	tritium units
USGS	U.S. Geological Survey

Hydrogeologic Conceptual Model of Groundwater Occurrence and Brine Discharge to the Dolores River in the Paradox Valley, Montrose County, Colorado

By Suzanne S. Paschke, M. Alisa Mast, Philip M. Gardner, Connor P. Newman, and Kenneth R. Watts

Abstract

Salinity, or total dissolved solids (TDS), of the Colorado River is a major concern in the southwestern United States where the river provides water to about 40 million people for municipal and industrial use and is used to irrigate about 5.5 million acres of land. Much of the salinity in the Colorado River Basin is derived from natural interactions of surface water and groundwater with various geologic materials (rocks, soils, and alluvial deposits). The Dolores River in southwest Colorado is a major tributary of the Colorado River that historically accounts for about 6 percent of the salinity load to the Upper Colorado River Basin with the Paradox Valley being the primary source of salinity to the Dolores River. The Paradox Valley, one of several salt-anticline valleys in the region, is a fault-bounded topographic basin aligned with and exposing an underlying salt-anticline core. Salt deposits in the Pennsylvanian Paradox Formation of the Hermosa Group form an elongated salt diapir oriented northwest to southeast that is up to 12,000 feet (ft) thick beneath the present valley floor. Surface erosion, groundwater circulation, and weathering during Tertiary and Quaternary valley formation contributed to development of a cap rock, collapse features, breccia, and brine at the top of the exposed salt diapir. Today (2023), brine occurring in the brecciated cap rock and underlying salt deposits is in hydraulic connection with an overlying freshwater alluvial aquifer, and depending on seasonal river stage and hydrologic conditions, the brine discharges to the Dolores River causing the observed increase in salinity as the river crosses the Paradox Valley.

To reduce salinity concentrations in the Dolores River, the Bureau of Reclamation (Reclamation) operates the Paradox Valley Unit (PVU). The PVU project consists of nine shallow brine pumping wells near the Dolores River and one deep disposal well where the brine is injected for disposal. When operational, the PVU pumping wells extract brine from the base of the alluvial aquifer that is piped and injected into a deep disposal well about 3 miles southwest of the PVU. The PVU became fully operational July 1, 1996, and by 2015, operation of the PVU had reduced salinity concentrations in the Dolores River by as much as 70 percent compared to pre-PVU conditions. In response to a 4.5 magnitude earthquake, injection operations, and thus PVU pumping, were ceased from March 2019 to June 2022. A trial period of PVU operation began in June 2022 with a reduced injection rate, and thus PVU pumping rate, of about two-thirds capacity to gather additional information and guide future operational decisions.

In cooperation with Reclamation, the U.S. Geological Survey (USGS) developed this report to present the current (2023) understanding of groundwater and brine occurrence and discharge to the Dolores River in the Paradox Valley. Results from the compilation of spatial datasets, groundwater sampling and age dating, and aquifer tests are presented to provide improved understanding of the Paradox Valley hydrogeology, to supply datasets for a numerical groundwater-flow and brine-transport model, and to support future operations of the PVU. The hydrogeologic data provided herein, along with the most recent loading analysis for the Dolores River in the Paradox Valley, and a previous conceptual model for brine discharge to the river are used to present a conceptual understanding of groundwater occurrence in the Paradox Valley.

Introduction

Salinity, or total dissolved solids (TDS), of the Colorado River is a major concern in the Colorado River Basin of the southwestern United States. The Colorado River and its tributaries provide water to about 40 million people for municipal and industrial use and irrigate about 5.5 million acres of land in the United States (Bureau of Reclamation [Reclamation], 2020). Salinity in the Upper Colorado River Basin is derived primarily from surface-water and groundwater interactions of water with various geologic materials (including rocks, soils, and alluvial deposits) (Tuttle and Grauch, 2009). Water-use processes, including irrigation, reservoir evaporation, and municipal and industrial wastewater discharges, can also increase salinity concentrations and accelerate the release of dissolved solids to streams (Tuttle and Grauch, 2009). During water year 1991, about 57 percent of the salinity load

in the Colorado River upstream from its confluence with Green River was from natural geologic sources (Kenney and others, 2009).

The Dolores River is a major tributary of the Colorado River historically accounting for about 6 percent of the salinity load to the Colorado River, and the primary source of salinity to the Dolores River is the Paradox Valley of southwest Colorado (Kenney and others, 2009) (fig. 1). The Paradox Valley is a fault-bounded topographic basin outlining the geologic structure and exposing the collapsed core of a salt-valley anticline that underlies the valley (Hite and Lohman, 1973). The salt-anticline core is composed of an elongated northwest-to-southeast trending salt diapir of the Pennsylvanian Paradox Formation of the Hermosa Group (herein Paradox Formation) (Cater and Craig, 1970). The Paradox Formation salt diapir is up to 12,000 feet (ft) thick beneath the Paradox Valley (King and others, 2014).

The apparent paradox of the Paradox Valley is that the Dolores River crosses the valley perpendicular to—and about midway along—the valley rather than flowing parallel to the anticlinal axis of the Paradox Valley (Hite and Lohman, 1973; Gutiérrez, 2004) (fig. 1). This drainage pattern is observed across other salt-valley anticlines in the region and is attributed to antecedent valley formation during the Tertiary and Quaternary (Hite and Lohman, 1973). During the regional epeirogenic uplift that began in the Miocene (Epis and others, 1980), streams of the Colorado Plateau eroded through the underlying strata while maintaining their ancient courses forming antecedent valleys that were superimposed on the landscape (Cater and Craig, 1970; Hite and Lohman, 1973; Gutiérrez, 2004). Surface erosion, groundwater circulation, and weathering during valley formation further contributed to development of a cap rock, collapse features, breccia, and brine at the top of the exposed salt diapir as described in the "Geologic Setting and Development of the Paradox Valley" section of this report

Because of its salt content, brine occurring in the brecciated cap rock and salt deposits is denser than the freshwater that occurs in the overlying alluvial aquifer. The heavy brine density creates upward hydraulic gradients, which drive upward and lateral flow of brine into the base of the alluvial aquifer and to the Dolores River, and this discharge of brine causes the observed increase in salinity as the river crosses the valley (Mast and Terry, 2019). River stage varies seasonally in response to the annual cycle of spring snowmelt runoff and winter low-flow (base flow) conditions, and this variation in river stage affects thickness of the freshwater lens in the alluvial aquifer as well as brine discharge (Mast, 2017). Brine discharge to the river is minimized during spring and summer high-flow conditions when river stage is highest, and the freshwater-brine interface is depressed beneath the riverbed (Mast and Terry, 2019). Brine discharge to the river is greatest during the winter low-flow months when river stage is lowest and the freshwater-brine interface rises to the land surface, with as much as 70 percent of the annual salinity gain across the valley occurring from December through March (Mast, 2017).

Paradox Valley Unit

To reduce salinity concentrations in the Dolores River, Reclamation operates the Paradox Valley Unit (PVU) in the Paradox Valley. The PVU project consists of nine shallow pumping wells near the Dolores River that extract brine from the base of the alluvial aquifer and one deep disposal well where the brine is injected for disposal (fig. 1). The PVU is a Reclamation project authorized by the Colorado River Basin Salinity Control Act of 1974 (Public Law 93–320) to construct salinity-control projects in the Colorado River Basin (Reclamation, 2022). The nine PVU pumping wells are located adjacent to the river along its southeast bank (fig. 1) and are completed below the freshwater-brine interface and above the base of the alluvial aquifer at depths that range from 48 to 106 ft below land surface (Reclamation, 1978). Brine is pumped at a total rate of about 0.5 cubic feet per second (ft^3/sec), and the PVU pumping lowers the freshwater-brine interface beneath the river thereby reducing discharge of brine to the river. The pumped brine is collected and piped to a deep disposal well (the injection well) about 3 miles (mi) southwest of the PVU where it is injected into the Mississippian Leadville Limestone at depths of 14,068 to 15,857 ft below land surface (Watts, 2000; Block and others, 2015) (fig. 1).

The PVU system was developed in the 1970s and 1980s with a test phase of intermittent pumping and injection occurring from 1991 to 1993 (Reclamation, 1978; Block and others, 2015). Regular operation of the PVU began July 1, 1996 (Block and others, 2015). The period of PVU operation prior to July 1, 1996, is herein described as the pre-PVU period, and the period of PVU operation after July 1, 1996, is herein described as the post-PVU period. Continued operation of the PVU supports reduction of the salinity load of the Dolores and Colorado Rivers (Mast, 2017). However, earthquake seismicity induced by PVU injection has increased since 2016 (Denlinger and O'Connell, 2020) and, on March 4, 2019, injection operations, and thus PVU pumping, were immediately suspended after the occurrence of a 4.5 magnitude earthquake in the region (the largest to date attributed to PVU operations) (Reclamation, 2022). Except for a short pumping period in the spring 2020, PVU operations remained ceased from March 2019 to June 2022 (Reclamation, 2022). On June 1, 2022, the PVU temporarily resumed operations for a six-month trial period with a reduced injection rate of 115 gallons per minute, or about 67 percent of past operations, to gather additional information and guide future operational decisions (Reclamation, 2022).

The effect of the PVU on the salinity loading to the Dolores River is based on analysis of continuous measurements of specific conductance (SC) and streamflow from two U.S. Geological Survey (USGS) streamgages on the Dolores

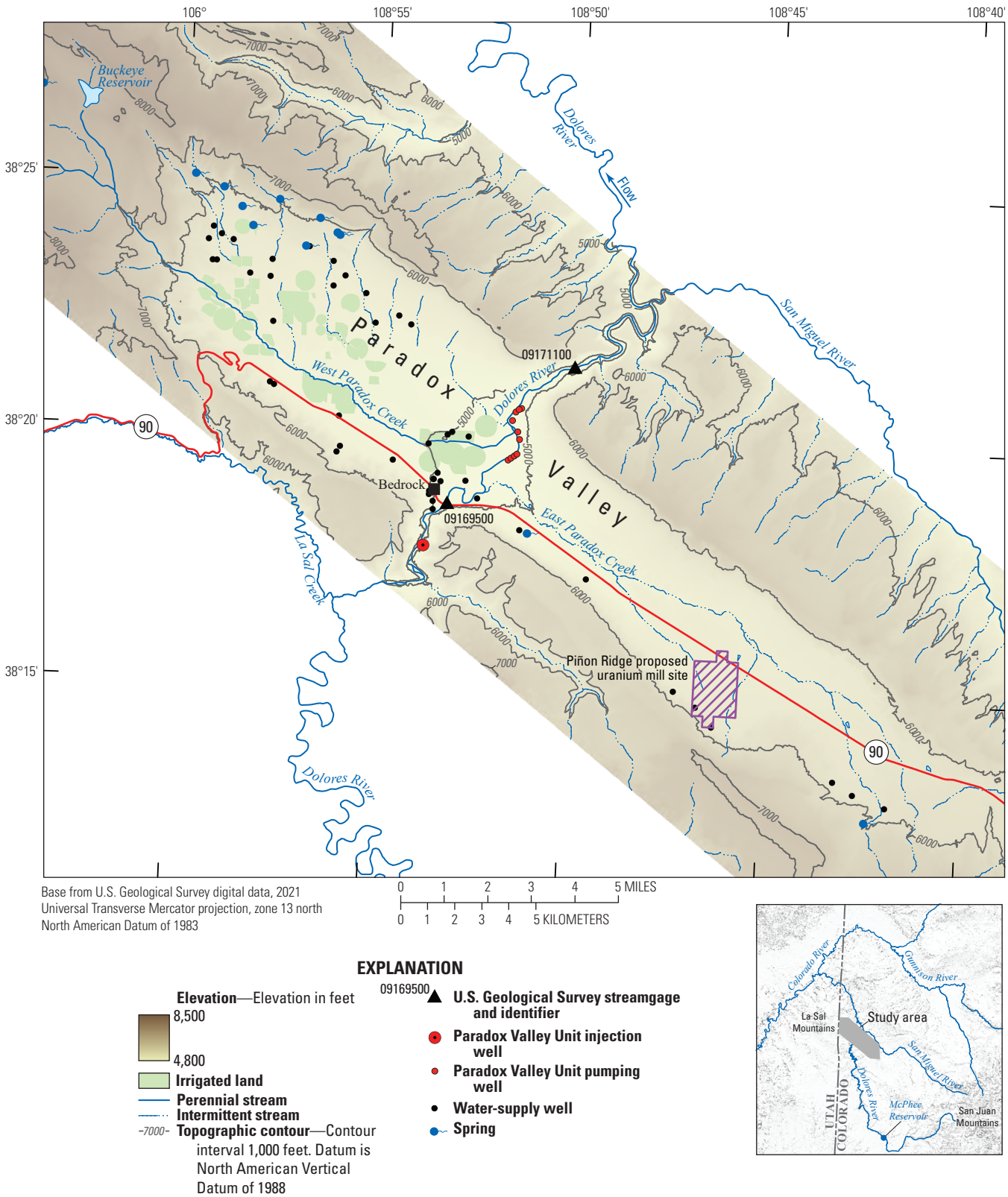

Figure 1. Locations of Paradox Valley Unit pumping and injection wells, irrigated areas, Piñon Ridge proposed uranium mill site, springs, selected water-supply wells, and U.S. Geological Survey streamgages in the Paradox Valley, Montrose County, Colo. (Colorado's Decision Support System, 2020; Colorado Department of Public Health and Environment, 2020; Colorado Oil and Gas Conservation Commission, 2020; Reclamation, 2022; U.S. Geological Survey, 2020a; Paschke and Mast, 2024).

River that bracket the Paradox Valley. The site Dolores River at Bedrock, Colorado (USGS streamgage 09169500) is located upstream from the PVU where the river enters the southern side of the valley, and the site Dolores River near Bedrock, Colorado (USGS streamgage 09171100) is located downstream from the PVU where the river exits the northern side of valley (U.S. Geological Survey, 2020a; fig. 1). Salinity load is computed based on continuous measurements of SC and streamflow at the two USGS streamgages and on monthly water-quality samples analyzed for TDS; both types of data were used to develop regressions between TDS concentrations and SC, which are then used to compute TDS load at each streamgage (Mast, 2017). The increase in TDS loading to the Dolores River between the two streamgages is termed the "net load" and is served to the National Water Information System (NWIS) database (U.S. Geological Survey, 2020a) for the downstream streamgage Dolores River near Bedrock (USGS streamgage 09171100). Prior to PVU test operations that began in 1991, the average annual increase in TDS load of the Dolores River across the Paradox Valley was estimated at about 137,900 tons per year (Mast, 2017). The average annual increase in TDS load of the Dolores River across the Paradox Valley during the post-PVU period from 1996 to 2015 was 43,300 tons per year, which represents a TDS load reduction of 94,600 tons per year or about a 70 percent reduction in TDS loading to the Dolores River compared to pre-PVU conditions (Mast, 2017).

Purpose and Scope

The purpose of this report is to present results of USGS data-collection efforts that began in 2009 and, in combination with more recent studies, to present a conceptual understanding of the hydrogeology in the Paradox Valley. The investigations of the groundwater system, conducted by the USGS in cooperation with Reclamation, provide improved understanding of brine discharge to the Dolores River, provide datasets that support a numerical groundwater-flow and brine-transport model (Heywood and others, 2024a; 2024b), and inform future operations of the PVU. The report presents details regarding hydrogeology of the Paradox Valley including results and interpretations from data compilation, aquifer mapping, groundwater-quality sampling, and aquifer testing. During 2009, groundwater-quality and groundwater-level data, maps, and geographic information systems (GIS) datasets were compiled to support conceptual understanding of the Paradox Valley hydrogeology as described in the "Hydrogeology Data Compilation" section of this report. Associated published products include generalized maps of the base of the alluvial aquifer (the top of the weathered bedrock surface), the top of the salt in the Paradox Formation, and the extent and altitude of the alluvial-aquifer water table (Paschke and Mast, 2024). In June 2011, groundwater-quality samples were collected from springs, domestic and irrigation wells, and PVU pumping wells in the valley, and the samples were analyzed for a suite of groundwater-age tracers and other constituents as described in the "Groundwater-Sample Collection and Analysis" section of this report. Analytical results for the groundwater samples are presented by Gardner and Newman (2023), are described in the "Groundwater Quality and Geochemical Indicators of Recharge Sources and Groundwater Age" section of this report, and contribute to understanding of general water quality, recharge, mixing, and groundwater-flow paths within part of the study area. In 2013, the USGS measured groundwater levels in PVU pumping and observation wells as a large-scale aquifer pumping test as described in the "2013 Aquifer Testing and Analysis" section of this report, and the analyzed results are presented in the "Results of 2013 Aquifer Testing" section of this report as estimates of alluvial-aquifer hydraulic conductivity (Newman, 2021). In addition, results from a 2011 aerial electromagnetic survey (Ball and others, 2015; 2020) are presented to illustrate the extent of the Paradox Valley brine. The most recent TDS loading analysis for the Dolores River in the Paradox Valley (Mast, 2017; Heywood and others, 2024a), the brine-discharge conceptual model developed by Mast and Terry (2019), and the hydrogeologic data provided by Paschke and Mast (2024) are used to present a conceptual model of groundwater occurrence in the Paradox Valley.

Previous Investigations

Previous investigations related to the hydrogeology of the Paradox Valley include geologic, geophysical, and hydrogeologic assessments. Because uranium deposits occur in the Late Jurassic Morrison Formation in the vicinity of the Paradox Valley, the geology of the area was originally mapped at a 1:24,000 scale during the late 1940s and early 1950s. Geologic maps of the Paradox Valley and adjoining areas include: Cater (1954, 1955a, 1955b, and 1955c), Cater and others (1955), McKay (1955), Withington (1955), Shoemaker (1956), Carter and Gualtieri (1957), and Carter and others (1958). Cater and Craig (1970) describe the structure and stratigraphy of the Colorado portion of the salt-anticline region. Doelling (2002 and 2004) mapped the geology of the areas northeast and southeast of the La Sal Mountains and presented the maps in a GIS format. Williams (1964) compiled maps showing the geology, structure, and uranium deposits of the Moab 1° × 2° quadrangle. Day and others (1999) prepared a geospatial model of the Colorado portion of the Moab 1° × 2° quadrangle. Elston and Shoemaker (1961) presented a map showing the generalized altitude of the top of the salt in the Paradox Formation in the salt-anticline region of Colorado and Utah.

Freethey and Cordy (1991) and Geldon (2003a; 2003b) described the regional hydrogeology of Paleozoic and Mesozoic rocks in the Upper Colorado River Basin, including the Paradox Valley. Weir and others (1983) described the hydrology of the Dolores River Basin, including a water budget for the basin. Hite and Lohman (1973) appraised salt deposits in the structural Paradox basin for waste emplacement and provided information on the evolution of salt

anticlines and groundwater occurrence in the salt of the Paradox Formation. Gutiérrez (2004) provided additional perspectives on the dissolution and collapse of evaporite deposits with respect to the formation of salt valleys of the Colorado Plateau.

Data collected along the Dolores River during planning and development of the PVU (Reclamation, 1978) included small-scale maps of the altitude of the top of a collapsed brecciated gypsum layer (collapse breccia) within the top of the salt in the Paradox Formation. This collapse breccia feature beneath the Dolores River in the center of the valley is mapped herein as part of the alluvial aquifer, because the breccia and alluvium are considered contemporaneous deposits (Gutiérrez, 2004). The planning report for the PVU (Reclamation, 1978) includes drilling and construction logs of test wells and piezometers, results from aquifer tests, and water-quality data for freshwater and brine from the alluvial aquifer.

Hydrologic, geologic, and geophysical investigations in an 880-acre area in the southeastern part of the valley were done during permitting of the Piñon Ridge proposed uranium mill site (fig. 1) (Geological Associates, 2007; Golder Associates Inc., 2008b, 2009; Kleinfelder, 2008, 2009) and provided hydrogeologic data for the southeastern part of the Paradox Valley. Few hydrogeologic data were previously available for this area.

Konikow and Bedinger (1978) presented a conceptual model of groundwater flow (above the salt in the Paradox Formation) in the Paradox Valley. They discussed strategies for salinity control and described the types of data needed to (1) better understand groundwater flow, (2) predict hydrologic responses to salinity-control processes, and (3) characterize natural variations in recharge and discharge conditions. The conceptual understanding of groundwater flow in the Paradox Valley presented in the "Hydrogeologic Framework" section of this report includes ideas from the conceptual model of Konikow and Bedinger (1978).

Three additional recent USGS studies in the valley contribute to the understanding of groundwater flow and brine discharge in the Paradox Valley, and results from those studies are incorporated into this report. In October 2011, a helicopter-borne aerial electromagnetic (AEM) survey was conducted to assess the distribution of brine in the upper 985 ft of the subsurface. Results from that study were published by Ball and others (2015, 2020) and provided data useful in mapping the freshwater-brine interface for October 2011 as described in the "Extent of Brine and Freshwater-Brine Interface in the Paradox Valley" section of this report. From 2015 to 2016, the USGS assisted Reclamation in updating regressions describing the relation between SC measured at USGS streamgages upstream and downstream from the PVU and TDS concentrations measured in stream samples and collected monthly at the same locations (Mast, 2017). Results from the regression analysis were used to develop estimates of TDS loads to the Dolores River from 1982 to 2015 (Mast, 2017) and through 2020 (Heywood and others, 2024a) to better understand the seasonal signals of brine discharge.

From 2016 to 2018, the USGS, in cooperation with Reclamation, conducted a geophysical and hydrologic study to improve characterization of processes controlling spatial and temporal variations in brine discharge to the Dolores River (Mast and Terry, 2019). Three geophysical surveys were conducted in March, May, and September 2017, and water levels were monitored in selected ponds and groundwater wells from November 2016 to May 2018 (Mast and Terry, 2019). Mast and Terry (2019) also estimated TDS loading to the Dolores River and developed conceptual models of brine discharge to the Dolores River at three different spatial scales.

Methods

A conceptual understanding of the Paradox Valley hydrogeology was developed through review of previous work, compilation of the available hydrogeologic information, analysis of aquifer-test results, and analysis of groundwater-quality and age information as described in this section.

Hydrogeologic Data Compilation

Hydrogeologic data compilation included the review of previous work and collection of available hydrologic and geologic datasets. Gridded datasets for annual and monthly precipitation amounts for 1980–2017 were retrieved from the Parameter-elevation Regressions on Independent Slopes Model (PRISM) climate data website (PRISM Climate Group, 2021) and extracted for the Paradox Valley. Diversion data, irrigated areas, irrigation methods, and crop-planting information were retrieved from the Colorado's Decision Support System (Colorado's Decision Support System, 2020), a water data management system developed by the Colorado Division of Water Resources (CDWR). Hydrogeologic data and documents for the Piñon Ridge proposed uranium mill site in the southeastern part of the Paradox Valley were retrieved from the Colorado Department of Public Health and Environment (Colorado Department of Public Health and Environment, 2020). Well-construction and test reports as well as locations for permitted wells as of 2011 were compiled from the CDWR online well-permit database (Colorado's Decision Support System, 2020). Locations, drilling reports, and geophysical logs of oil and gas test wells in and near the Paradox Valley as of 2011 were retrieved from the Colorado Oil and Gas Information System (Colorado Oil and Gas Conservation Commission, 2020). Documents, reports, and data collected during planning, testing, and operation of the PVU were supplied by Reclamation (Reclamation, 2022). Well-construction information and groundwater levels for groundwater wells in and near the study area also were retrieved from the USGS National Water Information System (NWIS)

database (U.S. Geological Survey, 2020a). Locations of springs in the Paradox Valley and their land-surface altitudes were estimated from USGS 7.5-minute topographic maps for the study area.

Hydrogeologic maps showing the generalized altitude of (1) the top of the bedrock or base of the alluvial deposits, (2) the top of the salt in the Paradox Formation, and (3) the alluvial aquifer water table were prepared for this study using GIS software, Esri ArcMap version 10.3 (Esri, 1999–2009). In addition, a map showing the saturated thickness of the alluvial aquifer and the estimated extent of saturated alluvium was derived from the top of bedrock and water-table altitude maps. The final maps and datasets and processing steps used to develop them, described in the following paragraph, are published in a USGS data release (Paschke and Mast, 2024).

Hydrogeologic maps presented in this report are considered generalized because of sparse spatial distributions and poor accuracy for location and altitude of many control points. Locations and altitudes of control points at the PVU and Piñon Ridge site were surveyed and are considered accurate. Locations and altitudes of many water wells and of older abandoned oil-gas wells generally were reported to the center of 40-acre tracts and have maximum possible location errors of about 933 ft (284 m). When altitude of the land surface was not reported for a control point, the altitude was estimated using a digital elevation model (U.S. Geological Survey, 2020b). Consequently, wells with poor location accuracy also have poor altitude accuracy. With the exceptions of observation wells at the PVU, groundwater levels are not routinely measured in the Paradox Valley. Reported groundwater levels from water-well construction and test reports submitted to CDWR (Colorado's Decision Support System, 2020) were used in conjunction with groundwater levels from the USGS NWIS database (U.S. Geological Survey, 2020a), PVU operational records, and a previous water-table map of the PVU (Reclamation, 1978) to prepare a generalized map of the water table in the northwestern part of the Paradox Valley. Because these datasets span a timeframe of about 50 years, groundwater-level measurements used in preparing this map are not contemporaneous, and the water-table surface is generalized. The water-table surface was not mapped in the southeastern end of the valley because the alluvium is unsaturated (Golder Associates Inc., 2009). Saturated thickness of the alluvial aquifer and the extent of saturated alluvium were derived by subtracting the generalized water-table altitude surface from the altitude at the base of the alluvium (top of bedrock) surface (Paschke and Mast, 2024).

2013 Aquifer Testing and Analysis

Aquifer tests were conducted at the PVU by the USGS in 2013 using both slug-test (Butler, 1997) and pumping-test (Kruseman and de Ridder, 1990) methods. Slug tests were completed in March 2013, and data collection related to pumping tests was conducted from March through May 2013. Data are available in a USGS data release (Newman, 2021).

2013 Slug Tests

In general, slug tests consist of instantaneous displacement of the water table by introduction and extraction of a known volume, known as a slug. Displacement can be caused by introduction of a solid cylinder or addition of water (Butler, 1997). Water-level displacement during slug testing is measured, and hydraulic properties of the aquifer may then be estimated by comparing testing data with analytical solutions (Bouwer and Rice, 1976). Slug tests are typically only representative of a small volume of the aquifer in the immediate vicinity of the tested well (Freeze and Cherry, 1979).

Slug testing in 2013 was conducted at the 8E25 and 3E25 observation well locations (fig. 2). Each location has a pair of wells, one at a shallow (S) depth and one at a deeper (D) depth for a total of four wells used for testing: 8E25-S, 8E25-D, 3E25-S, and 3E25-D (table 1). Pressure transducers were set to record depth of water below the measuring point and water temperature at 1-second intervals. Only slug-testing data from 8E25-D were usable for subsequent analysis because data from other wells indicated that instantaneous water-level displacement was not achieved. Data from well 8E25-D were evaluated using the Bouwer-Rice (Bouwer and Rice, 1976) and the Springer-Gelhar (Springer and Gelhar, 1991) methods as implemented in the software AQTESOLV (Duffield, 2007). The Bouwer-Rice method is widely applied for slug testing (Butler, 1997), and the Springer-Gelhar method is used when water-level displacement shows oscillatory behavior (Springer and Gelhar, 1991), which was observed in the dataset. Hydraulic properties were calculated using the software AQTESOLV (Duffield, 2007). Slug testing of 8E25-D consisted of two slug-in and two slug-out tests, each of which were analyzed using the Bouwer-Rice and Springer-Gelhar methods, resulting in eight initial slug-test solutions in AQTESOLV. One solution using the Springer-Gelhar method was removed because it did not display oscillatory behavior. The slug-test data and results for well 8E25-D (Newman, 2021) are described in the "Results of 2013 Aquifer Testing" section of this report.

2013 Pumping Test

There are a variety of methods for conducting pumping tests, but in general, these tests consist of pumping one or multiple wells at either constant or variable rates. Water-level displacement is measured in observation wells located at different distances from the pumped well(s). Hydraulic properties are then derived from comparison with analytical models similar to the approach used for slug testing

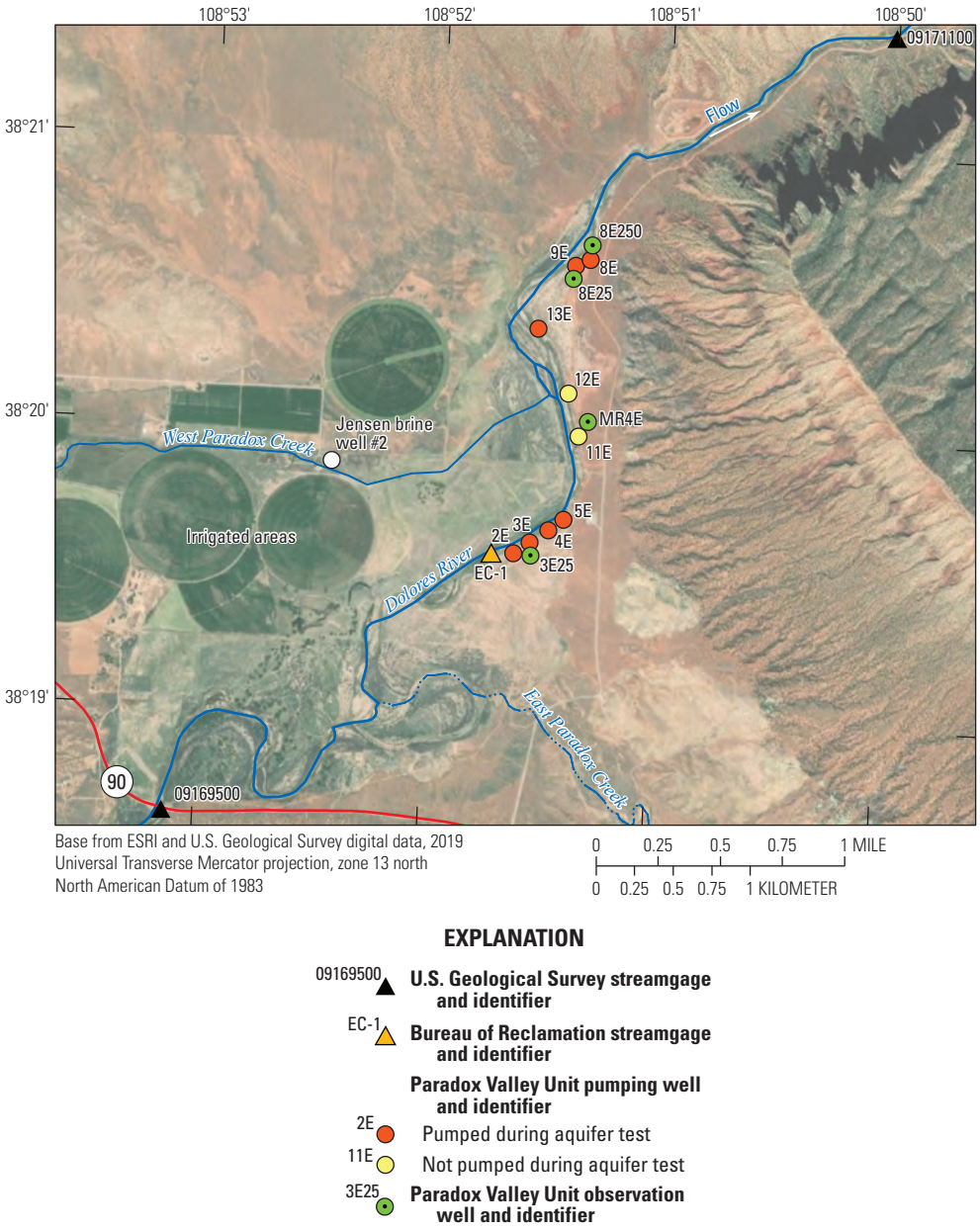

Figure 2. Locations of Paradox Valley Unit pumping and observation wells used for aquifer testing, the Jensen brine well #2 (original data available in Paschke and Mast, 2024), U.S. Geological Survey streamgages (U.S. Geological Survey, 2020a), and the Bureau of Reclamation EC-1 streamgage, in the Paradox Valley, Montrose County, Colo.

(Kruseman and de Ridder, 1990). In comparison to slug tests, the results of pumping tests are generally applicable to a greater volume of the aquifer material.

In 2013, a large-scale pumping test of the alluvial aquifer in the Paradox Valley was conducted by monitoring pressure (groundwater levels) in observation wells before and during operation of the PVU pumping wells (fig. 2). Observation wells for the pumping test conducted by this study were selected based on the depth of the screened interval and on proximity to the PVU pumping wells. Wells at four locations (3E25, MR4E, 8E250, and 8E25) were used during the pumping test (fig. 2). Three of the observation well locations (3E25, 8E250, and 8E25) are composed of shallow (S) and deep (D) wells drilled adjacent to one another. Well characteristics for the pumping and observation wells are listed in table 1. Water-level observation points were established by placing three pressure transducers at different depths within a single well pipe in the shallow observation wells (3E25-S, 8E250-S, 8E25-S, and MR4E), which allowed the evaluation of differences in hydraulic head at different depths in the aquifer.

Table 1. Summary of Paradox Valley Unit pumping and observation wells used in aquifer testing.

[Data from U.S. Geological Survey (2020a). Vertical datum is North American Vertical Datum of 1988. Latitude and longitude in decimal degrees are from horizontal datum North American Datum of 1983. USGS, U.S. Geological Survey; MP, measurement point; S, shallow; D, deep; NWIS, National Water Information System]

USGS identification number from NWIS	Well name	Well type	Latitude	Longitude	Altitude of MP (feet)
381935108513701	2E	Pumping	38.32629	−108.86041	4,943.26
381937108513301	3E	Pumping	38.32694	−108.85924	4,941.98
381940108512801	4E	Pumping	38.32770	−108.85788	4,943.12
381942108512501	5E	Pumping	38.32835	−108.85682	4,942.23
382036108512001	8E	Pumping	38.34355	−108.85563	4,939.08
382035108512401	9E	Pumping	38.34319	−108.85667	4,939.25
382022108513301	13E	Pumping	38.33936	−108.85925	4,941.37
381937108513303	3E25-S	Observation	38.32700	−108.85929	4,942.36
381937108513302	3E25-D	Observation	38.32700	−108.85929	4,942.42
381959108512202	MR4E	Observation	38.33317	−108.85608	4,941.65
382036108512302	8E250-S	Observation	38.34320	−108.85638	4,938.10
382036108512301	8E250-D	Observation	38.34320	−108.85637	4,941.29
382037108512102	8E25-S	Observation	38.34349	−108.85579	4,939.72
382037108512101	8E25-D	Observation	38.34349	−108.85579	4,939.52

For the calculation of hydraulic properties, the shallowest of the three transducers was chosen from each shallow observation well to represent the observation point for aquifer-test analysis (table 2). Only one transducer was placed in each of the three deep wells (3E25-D, 8E250-D, and 8E25-D).

Pressure transducers were set to record depth to water below the measuring point and to measure water temperature at 60-second intervals. Data collection was initiated in March 2013, when the PVU pumping wells were inactive, to provide a baseline understanding of groundwater levels in the absence of pumping. On April 17, 2013, extraction from PVU pumping wells was reinitiated. Pumping occurred at seven wells within the well field in the immediate vicinity of the observation wells as shown in figure 2. Groundwater levels were monitored in observation wells with pressure transducers (table 2) from March to May 2013 to evaluate hydraulic responses to pumping. Discharge data for PVU pumping wells were obtained from Reclamation (John Adams, Reclamation, written commun., August 2013) and are provided along with the observation data in a USGS data release (Newman, 2021).

Because numerous pumping wells were pumped at variable rates throughout the test, water-level modeling was used to evaluate the effect of pumping interference and to assign water-level displacements in observation wells to specific pumping signals or to an aggregation of pumping signals. Water-level modeling is a technique where patterns in water-level displacements are statistically evaluated in comparison to external stresses in the groundwater system such as barometric effects, streamflow variation, and pumping (Bakker and Schaars, 2019). Water-level modeling has

Table 2. Summary of water-level observation points used in aquifer testing at the Paradox Valley Unit.

[Data from U.S. Geological Survey (2020a). Vertical datum is North American Vertical Datum of 1988. MP, measurement point; S, shallow; D, deep]

Well name	Observation point name	Observation point depth below MP (feet)	Observation point altitude below land surface (feet)
3E25-D	3E25-D_Deep	35.30	4,911.02
3E25-S	3E25-S_15	15.01	4,930.35
8E25-D	8E25-D_Deep	33.70	4,908.53
8E25-S	8E25-S_14	15.43	4,927.02
8E250-D	8E250-D_Deep	26.15	4,915.14
8E250-S	8E250-S_14	14.04	4,927.28

been identified as being useful in aquifer testing to detect small drawdowns (Garcia and others, 2013). In this analysis, water-level modeling was used to assign observation-well water-level displacements to single pumping wells or to groups of pumping wells, as opposed to assigning water-level displacements based only on distances between observation wells and pumping wells. This approach is more robust for characterizing heterogeneous aquifers where pumping interferences may occur. Water-level modeling also discriminates between pumping stresses and streamflow stresses (Bakker and Schaars, 2019).

Water-level modeling was conducted using the Pastas package implemented in Python 3.7 (Collenteur and others, 2019). Modeling was conducted using an iterative approach where the first simulated stress on groundwater levels was net recharge (precipitation minus evapotranspiration). The second simulated stress was streamflow variation based on stream depth measured at EC-1, a streamgage location monitored by Reclamation (fig. 2). This stress was added to the net recharge stress in the model. The third simulated stress was pumping rate, which was added to the model containing net recharge and streamflow. Pumping rate from each possible combination of pumping wells was added in a separate model for each observation point to quantify the proportion of the water-level displacements attributable to specific pumping wells. For example, different water-level models were completed for pumping stress from well 2E alone; then wells 2E and 3E; wells 3E and 4E; wells 2E, 3E, and 4E; until each possible combination of pumping wells was evaluated. There are 127 possible combinations of pumping wells. Each observation point therefore has 129 water-level models that are considered: one considering net recharge only; one considering net recharge plus streamflow; and one each considering net recharge, streamflow, and pumping stress from the 127 possible combinations of pumping wells.

Based on the results of this water-level model analysis, discharge from the pumping well (or combination of pumping wells) that caused the greatest water-level change at an observation point was selected to calculate hydraulic properties. This process uses the discharge from pumping wells with the greatest effect on water-level displacements in computing hydraulic properties of the aquifer, while ignoring the stresses from other pumping wells. The effectiveness of the approach depends on whether numerous pumping stresses control water-level displacements at an observation point, or whether water-level displacement is primarily controlled by discharge from a single well. In the latter instance, the approach used in this analysis is expected to result in reasonable approximations of hydraulic properties. Model input files for water-level modeling are included in Newman (2021).

Following the assignment of pumping stresses responsible for most water-level displacement, water-level displacement and pumping-rate data were used to calculate hydraulic properties using the "pumpingtest" package of R (R Core Team, 2020). Input parameters were derived from well logs of the pumping wells and from measured land-surface distances between wells from GIS measurements. Two analytical approaches were used to explore potential variability in calculated hydraulic properties: the Boulton (1963) and Theis (1935) solutions. These solutions are most applicable to unconfined anisotropic and confined isotropic aquifers, respectively. The hydrologic system in the study area is layered, with the shallow observation wells completed in an alluvial aquifer and the deep observation wells completed in the transition zone between the underlying collapse breccia and the alluvial aquifer (Reclamation, 1978). Application of the Boulton and Theis solutions therefore evaluates the possible range in hydraulic properties given different possible boundary conditions.

Additionally, Hunt and Scott (2005) found that the Boulton solution contains the Theis solution, indicating that hydraulic property values derived from this solution may be the most widely applicable. The Boulton and Theis solutions are applied using the "pumpingtest" package by importing water-level displacement data for each observation point and pumping-rate data for the well(s) that were indicated to have the greatest proportion of explained variance for the observation point in question. Using the water-level displacement and the pumping rate, the "pumpingtest" package computes the hydraulic conductivity (K) according to the Boulton and Theis analytical solutions. Pumping-test data and results (Newman, 2021) are described in the "Results of 2013 Aquifer Testing" section of this report. Model input files for the pumpingtest package are included in Newman (2021).

Groundwater-Sample Collection and Analysis

Groundwater samples were collected by the USGS at nine sites in the study area in June 2011 including one spring, five domestic wells, one irrigation well, and two PVU pumping wells (table 3). Sites were selected to represent the range of chemical water types and anticipated ages of groundwater found within the study area. Results for all sample analyses are available from the USGS NWIS database (U.S. Geological Survey, 2020a) using the USGS identification numbers from table 3. The application of environmental tracers to estimate groundwater age is described in Appendix 1, and the groundwater-age calculations for noble gases and carbon isotopes are provided in a USGS data release (Gardner and Newman, 2023).

Water samples were collected from six wells using the existing submersible pumps and from one well (site 3) using a portable submersible pump. Samples were collected from a spring and a flowing well (site 4) under natural free-flowing conditions. Water samples from pumped wells were collected from an outlet as close to the wellhead as possible and after a minimum of three casing volumes of water had been pumped from the well.

Field measurements during water-sample collection included SC, pH, water temperature, concentration of dissolved oxygen, and total-dissolved-gas pressure.

Table 3. Site information for groundwater sites sampled during June 2011 in the Paradox Valley, Montrose County, Colo.

[Data from U.S. Geological Survey (2020a). Altitude is in feet above North American Vertical Datum of 1988. Hydrostratigraphic units from table 4. USGS, U.S. Geological Survey; bls, below land surface; DA, Dakota aquifer; AA, alluvial aquifer; CMCU, Chinle-Moenkopi confining unit; PVU, Paradox Valley Unit; —, not applicable or available; NWIS, National Water Information System]

Site number (fig. 12)	USGS identification number from NWIS	Site type	Altitude (feet)	Well depth (feet bls)	Screened interval (feet bls)	Hydrostratigraphic unit
1	382446109022101	Spring	7,152	—	—	DA
2	382351108590601	Domestic well	5,571	77.7	67.1–77.7	AA-CMCU[1]
3	382344108583701	Domestic well[2]	5,534	30.5	—	AA-CMCU[1]
4	382306108581701	Irrigation well[2]	5,439	19.8	6.1–19.8	PAA
5	382313108570501	Domestic well	5,412	57.9	—	CMCU[1]
6	381950108534001	Domestic well[2]	4,953	18	16.8–19.8	AA
7	381954108523801	Domestic well[2]	4,944	10.4	6.1–10.4	AA
8	381935108513701	PVU pumping well 2E[2]	4,945	77.5	11.3–23.6	AA
9	382036108512001	PVU pumping well 8E[2]	7,152	48.0	10.1–14.6	AA

[1]Hydrostratigraphic unit estimated from depth and geologic map in Cater and Craig (1970).

[2]Sample had rotten egg smell indicating presence of hydrogen sulfide gas.

Field parameters were measured using a calibrated multi-parameter probe following USGS protocols (U.S. Geological Survey, 2008). Samples for major constituents were filtered with a 0.45-micrometer (µm) capsule filter and analyzed at the USGS National Water Quality Laboratory in Denver, Colo., using approved methods (Fishman and Friedman, 1989). Unfiltered samples for stable isotopes of oxygen and hydrogen were collected in 60-milliliter glass vials with polyseal caps and analyzed by the USGS Stable Isotope Laboratory in Reston, Va. Unfiltered samples for tritium analyses were collected in polyethylene bottles and analyzed by the University of Utah Dissolved Gas Service Center in Salt Lake City, Utah. Samples for carbon-14 were filtered (0.45 µm) and collected in glass bottles. The bottles were filled from the bottom and allowed to overflow for several volumes to minimize contact of the samples with the air. Bottles were then sealed with polyseal caps and analyzed by the National Ocean Sciences Accelerator Mass Spectrometry Facility at the Woods Hole Oceanographic Institution in Woods Hole, Mass.

Dissolved-gas samples for noble gases were collected either as water samples sealed in copper tubes, as described by Stute and Schlosser (2000), or as gas samples collected with diffusion samplers similar to those described by Gardner and Solomon (2009) and Sanford and others (1996). The copper-tube method consists of attaching a 30-inch (in)-long section of 3/8-in-diameter copper tubing to a sampling port at the wellhead, allowing the tube to flush with well water until all air bubbles have been evacuated, then sealing both ends with clamps. The diffusion sampler method was used at sites where in-situ placement was possible for a minimum period of 24 hours. The diffusion sampler is constructed of 1/8-in-diameter copper tubing and a semipermeable gas diffusion membrane. After 24 hours, when the gases in the diffusion sampler had presumably equilibrated with the dissolved gases in the sample water, the sampler was removed from the well or spring and immediately sealed. Dissolved-gas concentrations were analyzed by the University of Utah Dissolved Gas Service Center using both quadrupole and sector-field mass spectrometers (University of Utah, 2022). The analysis provides the relative mole fractions of gases dissolved in a sample; the dissolved-gas concentrations are calculated using Henry's Law relations and field measurements of total dissolved-gas pressure and water temperature (University of Utah, 2022).

Hydrogeology of the Paradox Valley

The hydrogeology of the Paradox Valley can be generally characterized as an unconfined freshwater aquifer in alluvial deposits associated with present-day stream channels underlain by brine that occurs in the alluvial aquifer, near-surface brecciated cap rock, and underlying salt deposits of the Paradox Formation. Aquifer dynamics are complex because of geologic structures related to the collapsed salt anticline, brine density, and interaction between the brine and the freshwater system associated with the Dolores River and the alluvial aquifer. The "Hydrogeology of the Paradox Valley" section of this report provides detailed information on the physiography, hydrology, geology, and groundwater occurrence and quality of the Paradox Valley, and the results are synthesized in the "Conceptual Model of Groundwater Occurrence and Brine Discharge in the Paradox Valley" section of this report.

Physiography and Topography

The Paradox Valley is a topographic basin about 25 mi long and 3–5 mi wide (Fenneman, 1931) located in Montrose County, Colo., near the Colorado-Utah border (fig. 1). The landscape of the area is characterized by plateaus dissected by canyons with large topographic relief resulting from rapid downcutting by the Colorado River and its tributaries through relatively flat-lying resistant sandstones during the Tertiary and Quaternary (Hite and Lohman, 1973). The Paradox Valley, on the southeast flank of the La Sal Mountains, is oriented along the northwest to southeast axis of the underlying salt anticline, and the floor of the Paradox Valley has an altitude of about 4,900 ft and is relatively flat compared to the surrounding uplands (fig. 1). The paradox of the Paradox Valley is that the Dolores River crosses the salt-anticline valley perpendicular to its northwest to southeast trend and about midway along the valley axis. The Dolores River enters and leaves the Paradox Valley through deep canyons incised through the surrounding Paleozoic and Mesozoic rocks (Mast, 2017). Uplands at the northwestern end of the Paradox Valley and mesas on the northeastern and southwestern sides of the valley rise about 1,000 ft above the valley floor. Major land uses in the valley include rangeland and about 2,700 acres of irrigated cropland and pastureland located northwest of the river (Mast, 2017).

Climate and Streamflow

Climate of the Paradox Valley is semi-arid (Cater and Craig, 1970). Annual precipitation over the valley floor averaged 13.5 in for the period from 1980 to 2017 and ranged from a minimum of 7.0 in. in 1989 to a maximum of 18.5 in. in 1983 (PRISM Climate Group, 2021) (fig. 3*A*). Precipitation is generally greatest during the summer months occurring as rain with monthly average precipitation ranging from 0.4 in during June to about 1.5 in during August. Annual precipitation shown in figure 3*A* was in general greatest and most consistent during the 1980s with precipitation declines and greater annual variation observed since 1990. Average annual evaporation from free-water surfaces during 1961–2007 has been estimated at about 38 in (Golder Associates Inc., 2008a). Because the potential for evaporation substantially exceeds precipitation in the semi-arid climate, the opportunity for infiltration of precipitation on the valley floor as groundwater recharge is limited. Evaporative salts are observed at the land surface in the Paradox Valley near the river (Mast and Terry, 2019) suggesting evapotranspiration from plants as well as evaporation from the near-surface brine and water table are active processes in the valley.

The Dolores River and West Paradox Creek are the only perennial streams in the Paradox Valley (fig. 1). East Paradox Creek, which drains the southeastern part of the valley, is ephemeral. The Dolores River originates in the San Juan Mountains southeast of the valley and joins the Colorado River near the Colorado-Utah state line. The Dolores River drains an area upstream from the Paradox Valley of about 2,024 square miles (mi^2), and streamflow in the river is largely derived from snowmelt runoff from higher altitudes in the San Juan Mountains. Streamflow in the Dolores River upstream from the Paradox Valley has been regulated by releases from McPhee Reservoir (about 110 mi upstream) since July 1984, when the McPhee Dam was completed (Voggesser, 2001; fig. 1). Surface-water diversions for irrigation upstream from Paradox Valley (about 5,000 acres of irrigated land) and outside of the Dolores River Basin (about 74,600 acres of irrigated land) also affect streamflow in the Dolores River. West Paradox Creek originates in the upland areas flanking the La Sal Mountains northwest of the Paradox Valley (fig. 1). Streamflow in West Paradox Creek is regulated by Buckeye Reservoir, which stores water diverted from the eastern flank of the La Sal Mountains into the Dolores River drainage. Water released from Buckeye Reservoir to West Paradox Creek is then diverted for irrigation in the Paradox Valley. Surface water is also diverted from the Dolores River upstream from the town of Bedrock for supplemental irrigation in the valley.

Streamflow for the Dolores River in the Paradox Valley is measured at two USGS streamgages that bracket flow as the river crosses the valley (Mast, 2017). The site Dolores River at Bedrock (USGS streamgage 09169500) is located upstream from the PVU where the river enters the valley, and the site Dolores River near Bedrock (USGS streamgage 09171100) is located downstream from the PVU where the river exits the valley (U.S. Geological Survey, 2020a; fig. 1). Average annual streamflow at the downstream streamgage Dolores River near Bedrock for 1985 to 2017 ranged from a minimum of 27 ft^3/s in 2002 to 711 ft^3/s in 1993 (fig. 3*B*). Periods of low streamflow generally correspond to periods of less than mean precipitation (fig. 3*A*), although streamflow patterns for the Dolores River would likely relate more closely to precipitation conditions in the San Juan Mountains where the river originates. In general, streamflow in the Dolores River has declined during the period of record reflecting upstream reservoir operations and more frequent periods of drought during the past two decades. For example, average annual streamflow for the wetter period from 1985 to 1999 was 364 ft^3/s, which was nearly three times greater than the average streamflow of 135 ft^3/s for the period 2000 to 2017. On a seasonal scale, Dolores River streamflow generally exhibits an annual cycle of peak runoff during the spring snowmelt season from late March through June followed by a low-flow (base flow) period during the winter months from November through February (Mast, 2017). Localized summer rain storms can generate peak flows during the summer months. Streamflow at the downstream site is generally greater than at the upstream site for the period 1980 to 2015, with the simulated streamflow gain between the two sites ranging from about 3 to 4 ft^3/s (Heywood and others, 2024a; 2024b).

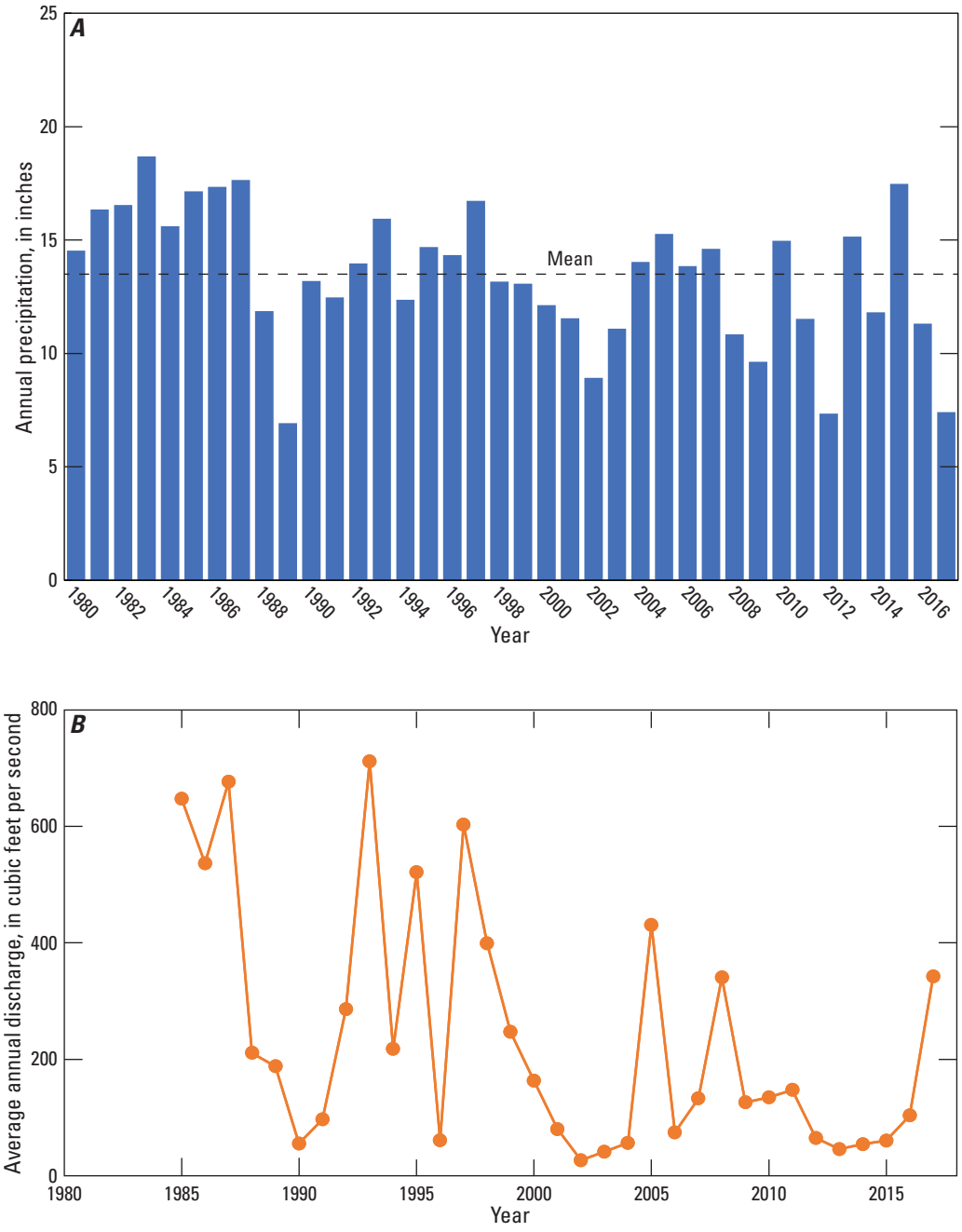

Figure 3. *A*, annual and mean precipitation amount in the Paradox Valley, Montrose County, Colo.,1980–2017 (PRISM Climate Group, 2021) and *B*, average annual streamflow for Dolores River near Bedrock (U.S. Geological Survey streamgage 09171100; U.S. Geological Survey, 2020a).

Hydrogeologic Framework

This section of the report provides an overview of the geologic setting compiled from previous studies followed by descriptions of the hydrogeologic units of primary interest in the Paradox Valley. Hydrogeologic units discussed in this report are based on the stratigraphic nomenclature of Hunt (1958, 1969); Cater and Craig (1970); Epis and others (1980); Freethey and Cordy (1991); Geldon (2003a); Gutiérrez, 2004; and Cohen and others (2013) (table 4).

Geologic Setting and Development of the Paradox Valley

The Paradox Valley is one of several northwest to southeast trending salt-anticline valleys in the Paradox fold and fault belt of the structural Paradox basin (Kelley, 1958; Cater and Craig, 1970; Hite and Lohman, 1973; Gutiérrez, 2004). The Paradox basin is an ancient depositional and structural basin in southeastern Utah and southwestern Colorado located southwest of the Uncompahgre Plateau uplift and defined by the maximum extent of evaporite salt deposits in the Pennsylvanian Paradox Formation of the Hermosa Group (Hunt, 1958; Hite and Lohman, 1973) The salt-anticline valleys parallel the anticlinal axis of the Uncompahgre Plateau, a large uplift almost 100 mi long and 25 mi wide, located 25 mi northeast of the La Sal Mountains (fig. 4) (Hunt, 1958). In addition to the Paradox Valley, other salt-anticline valleys in the region include Sinbad Valley, Gypsum Valley, Salt-Cache Valley, Fisher Valley, Castle Valley, Moab-Spanish Valley, and Lisbon Valley (fig. 4) (Gutiérrez, 2004).

Castle Valley and Paradox Valley are located along the same northwest to southeast structural trend (fig. 4) and are separated by Oligocene laccolith intrusions that form the La Sal Mountains (Hunt, 1958; Gutiérrez, 2004). Laccoliths are convex-up rock bodies with a known or assumed flat floor formed when magma intrudes into sedimentary rocks, spreads horizontally along layers, and forms a dome. The cores of several distinctive mountain groups in the Paradox Valley region, including the La Sal Mountains, were formed by magmatic intrusions about 25 millions of years before present (Ma) that created domed laccolith structures (Hunt, 1969). Uplift and erosion of the region that began during the Miocene (Cater and Craig, 1970) created the present-day mountains and valleys of the region (Hunt, 1969) (table 4).

Salt-anticline valleys were formed by regional tectonics that caused the upwelling and plastic deformation of the Paradox Formation (Hunt, 1958; Cater and Craig, 1970; Gutiérrez, 2004). Initial development of salt anticlines was contemporaneous with deposition of the Paradox Formation in the Pennsylvanian with subsequent movement through geologic time in response to regional tectonics including accumulation of overlying sediment and renewed movement along Proterozoic basement structures (Cater and Craig, 1970; Baars and Doelling, 1987; Gutiérrez, 2004). Collapse of the crests of the salt anticlines and subsequent exposure at the land surface occurred in two stages apparently widely separated in time (Cater and Craig, 1970). The first stage was associated with regional Late Cretaceous faulting and folding during the Laramide orogeny of the Rocky Mountains, (Hunt, 1969; Cater and Craig, 1970; Epis and others, 1980). During this first stage of anticline collapse, the crests of anticlines in places were dropped, as grabens, as much as several hundred feet in response to extensional tectonics (Cater and Craig, 1970; Gutiérrez, 2004). It appears that at no time during this initial stage of collapse were the salt cores of the anticlines exposed at the land surface, and, by the beginning of the Miocene, the top of the salt core was likely buried under nearly 5,000 ft of sediments (Cater and Craig, 1970).

The second stage of valley formation, which resulted in the present-day topography, was initiated during epeirogenic uplift of the entire Colorado Plateau that began during the Miocene about 15–20 Ma and continued into the Quaternary (about 2 Ma to present) (Hunt, 1958, 1969; Cater and Craig, 1970; Gutiérrez, 2004). Prior to epeirogenic uplift of the Colorado Plateau, erosion had reduced much of the area to a surface of low relief; uplands had been leveled and basins filled, with the domed La Sal and other laccolithic mountain masses likely rising above this surface (Cater and Craig, 1970). The ancestral Dolores River and other drainages were meandering, slow-moving streams, and the onset of regional uplift signaled a radical change for streams draining the area (Cater and Craig, 1970). As epeirogenic uplift progressed, erosion rates increased, and streams began downcutting. Some streams in the area adjusted courses to the changing structure of the underlying rocks, while others, such as the Dolores River, maintained their ancient meandering channels as downcutting proceeded in an antecedent manner (Hunt, 1969) such that their channel patterns were superimposed into the underlying strata (Cater and Craig, 1970). The Dolores River, which has not changed its course since the Miocene about 10–12 Ma (Hunt, 1969), flowed perpendicular to the Paradox Valley anticline cutting across and through the structure (Cater and Craig, 1970).

Downcutting of the Dolores River and associated groundwater circulation eventually breached the rocks overlying the salt anticline in the Paradox Valley exposing the top of the exposed salt diapir to weathering, dissolution, and collapse (Cater and Craig, 1970; Gutiérrez, 2004; King and others, 2014). As the superimposed river dissected the anticline and exposed the salt core, groundwater circulation was enhanced, and karst features developed at the top of the exposed salt diapir Gutiérrez, (2004). The river became an area of groundwater discharge, and the karst features created by the dissolution of subsurface salt created areas of subsidence (Gutiérrez, 2004). One such area of collapse is noted as collapse breccia in the center of the Paradox Valley (Reclamation, 1978), and the subsidence and collapse of this feature is considered contemporaneous with deposition of Quaternary alluvial deposits (Gutiérrez, 2004).The river, tributaries, and associated groundwater circulation also

Table 4. Stratigraphic and hydrogeologic units of the Paradox Valley, Montrose County, Colo.

[Cap rock of the Paradox Formation is a karstic residuum composed primarily of gypsum and clay from which the sodium chloride has been dissolved by groundwater (Gutiérrez, 2004). Ma, mega-annum, millions of years before present]

Era	Period	Epoch	Ending geologic age of period or epoch (in Ma)	Stratigraphic unit	Hydrogeologic unit
Cenozoic	Quaternary	Holocene	0	Alluvial, eolian, talus, and landslide deposits	Alluvial aquifer
		Pleistocene	[3]0.012	Lake deposits? terrace gravels and fanglomerate	
	Tertiary	Pliocene	[5]2		
		Miocene	[5]5		
		Oligocene	[3]23		
		Eocene	[4,5]38		
		Paleocene	[3]56		
Mesozoic	Cretaceous	Upper	[3]66	Mancos Shale	Mancos confining unit[1]
				Dakota Sandstone	Dakota aquifer[1]
		Lower	[3]100	Burro Canyon Formation	
	Jurassic	Upper	[3]145	Morrison Formation (Brushy Basin Member)	Morrison confining unit[1]
				Morrison Formation (Salt Wash Member)	Morrison aquifer[1]
				Summerville Formation of San Rafael Group	Curtis-Stump confining unit[1]
				Entrada Sandstone of San Rafael Group (Slick Rock Member)	Entrada-Preuss aquifer[1]
				Entrada Sandstone of San Rafael Group (Dewey Bridge Member)	
		Lower	[3]175	Navajo Sandstone of Glen Canyon Group	Navajo-Nugget aquifer[1]
				Kayenta Formation of Glen Canyon Group	
				Wingate Sandstone of Glen Canyon Group	
	Triassic	Upper	[3]201	Chinle Formation	Chinle-Moenkopi confining unit[1]
		Lower	[3]247	Moenkopi Formation	
Paleozoic	Permian	Upper	[3]254	Cutler Formation	Canyonlands aquifer[2]
	Pennsylvanian-Permian			Honaker Trail Formation of the Hermosa Group	
	Pennsylvanian		[3]290	Cap rock of the Paradox Formation[6] of Hermosa Group	Four Corners confining unit[2]
				Salt of the Paradox Formation of Hermosa Group	
				Pinkerton Trail Formation of Hermosa Group	
				Molas Formation	

[1]Freethey and Cordy (1991).

[2]Geldon (2003a).

[3]Cohen and others (2013).

[4]Hunt (1969).

[5]Epis and others (1980).

[6]Gutiérrez (2004).

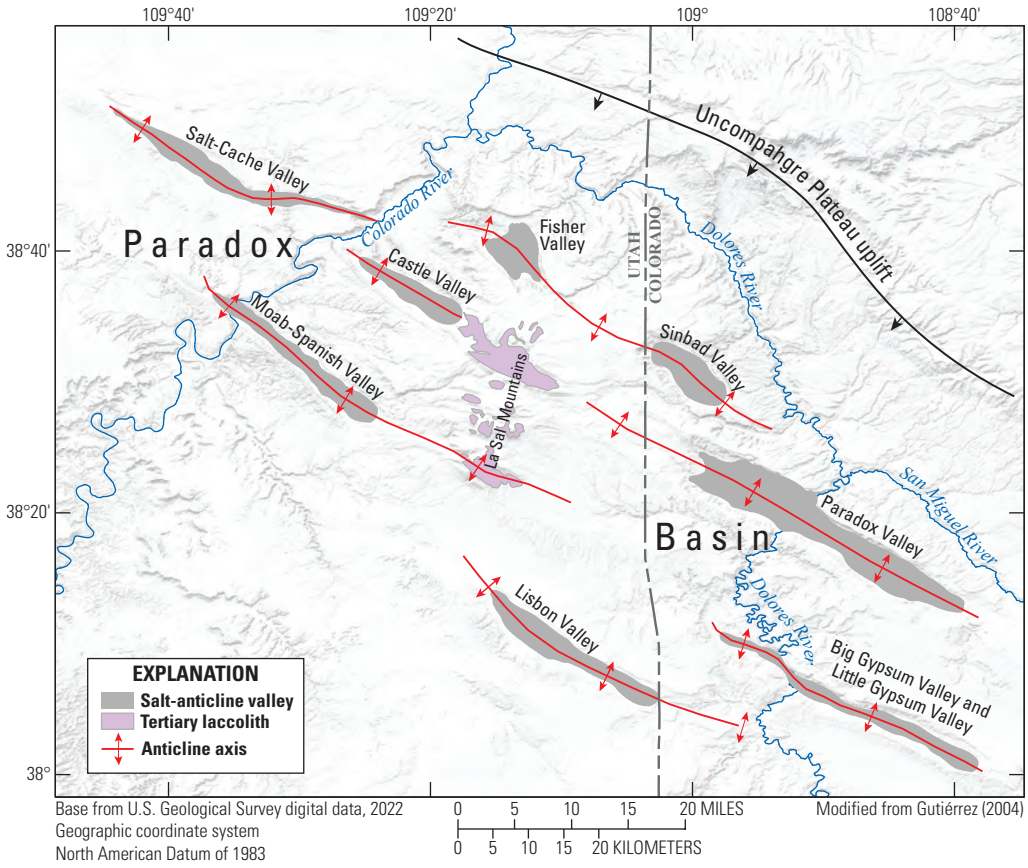

Figure 4. Geographic distribution of salt-anticline valleys in the Paradox basin fold and fault belt (modified from Gutiérrez, 2004).

contributed to development of a cap rock at the top of the exposed salt of the Paradox Formation (Cater and Craig, 1970; Gutiérrez, 2004). The cap rock, which is found in the valley bottom beneath younger sediments, is a karstic residuum left behind from the dissolution of salt (Gutiérrez, 2004). The cap rock is largely devoid of sodium chloride and contains a high proportion of gypsum and clay (Reclamation, 1978; Gutiérrez, 2004). During the Pleistocene glacial intervals, increased precipitation, runoff, and recharge enhanced streamflow, erosion rates, and groundwater circulation contributing to further salt dissolution, collapse, and the development of brine at the top of the exposed salt deposits in the Paradox Valley (Hunt, 1969; Cater and Craig, 1970; Konikow and Bedinger, 1978; Baars and Doelling, 1987; Gutiérrez, 2004).

Sedimentary rocks exposed at the surface in the Paradox Valley and surrounding uplands range in age from Pennsylvanian (Paradox Formation) to Late Cretaceous (Dakota Sandstone and Mancos Shale) (table 4; fig. 5). Evaporite deposits of the Paradox Formation at the core of the anticline are the oldest rocks, which are exposed along the floor of the Paradox Valley southeast of the Dolores River and to a lesser extent in the northwest part of the valley (fig. 5, 6). Younger Paleozoic and Mesozoic rocks were eroded from the crest of the anticline but remain exposed around the valley perimeter where they generally dip away from the anticline axis. The shale confining units of the Triassic Chinle and Moenkopi Formations overlie the Paradox Formation and form the flanks of the salt-anticline. The Jurassic Wingate Sandstone of the Glen Canyon Group forms cliffs that surround much of the Paradox Valley as well as canyons entering and exiting the valley (fig. 5). The Jurassic Entrada Sandstone of the San Rafael Group forms cliffs at higher altitudes around the valley, primarily to the north, and Mesozoic rocks of the Morrison Formation and Dakota Sandstone cap the mesas surrounding the valley (fig. 5). The youngest Mesozoic rocks are small remnants of Mancos Shale exposed in the uplands at the northwestern end of the valley (Carter and Gualtieri, 1965). Small and scattered outcrops of Tertiary terrace gravels and fanglomerate are exposed at some locations just outside the Paradox Valley (Cater and Craig, 1970). Quaternary eolian deposits blanket much of the valley floor but generally are less than about 10 ft thick. Quaternary alluvial deposits underlie eolian deposits and are thickest along the Dolores River and West Paradox Creek. Quaternary talus, colluvium,

Figure 5. Generalized surface geology of the Paradox Valley, Montrose County, Colo.

and landslide deposits occur on steeper slopes along the valley sides with some extending onto the valley floor. Northwest to southeast trending normal faults bound the graben collapse of the Paradox Valley and outline the core of the salt anticline (fig. 5).

Hydrogeologic Units

Hydrogeologic units in the Paradox Valley of primary interest to this work include unconsolidated Quaternary alluvial deposits on the valley floor and the salt of the Paradox Formation, which underlies the alluvial deposits (table 4). Mesozoic hydrogeologic units have been removed from the Paradox Valley by erosion and generally occur on topographic highs flanking the valley and dip away from the valley axis. Mesozoic sandstones can be highly jointed and fractured and, where incised by streams, are generally well drained (Freethey and Cordy, 1991). Low-permeability shales of the Permian Cutler Formation and Jurassic Chinle and Moenkopi Formations likely act as confining units where they directly overlie the salt of the Paradox Formation, underlie the alluvial aquifer, or form impermeable barriers where they comprise the valley walls (Konikow and Bedinger, 1978).

Figure 6. Paradox Valley, Montrose County, Colo., view looking northwest toward the La Sal Mountains (Used with permission from Wark Photography).

Quaternary Alluvial Deposits

Unconsolidated Quaternary alluvial, eolian, talus, landslide deposits, and fanglomerate (table 4) blanket much of the Paradox Valley floor (fig. 5). An unconfined water table occurs in the alluvial and aeolian deposits along the Dolores River and the northwestern part of the Paradox Valley and is hereinafter referred to as the alluvial aquifer. The talus, landslide, and fanglomerate deposits generally lie above the water table and are unsaturated. The eolian deposits consist of 10 ft or less of indistinctly bedded light-red silt and sand that has been partly reworked by water and mixed with sheet wash (Cater and Craig, 1970). The alluvial deposits along the Dolores River generally consist of a 5- to 15-ft thick, silty sand that overlies layers of sand, sand and gravel, gravel, and clay (Reclamation, 1978). Alluvial deposits overlie the salt of the Paradox Formation along the axis of the Paradox Valley anticline. Locally, alluvial deposits overlie the shale confining units of the Cutler, Moenkopi, and Chinle Formations along the sides of the valley and the Wingate Sandstone of the Glen Canyon Group at the northwestern end of the valley. Generally, a basal gravel in the alluvium occurs at the contact with the underlying Paradox Formation near the PVU (Reclamation, 1978).

The generalized configuration of the base of the alluvial aquifer (or top of bedrock) surface (fig. 7) was developed from previous maps of the top of the Paradox Formation near the PVU (Reclamation, 1978) as well as from available water-well drilling logs shown on figure 1 and as listed in Paschke and Mast (2024). The surface does not account for faulting, and because there are few data to define the base of the alluvial-aquifer surface, particularly in the valley southeast of the Dolores River, the map in figure 7 is considered generalized.

Thickness of the alluvial deposits varies substantially from a few feet to about 170 ft and is greatest in three areas of the Paradox Valley. The first area is near the center of the valley along the Dolores River, where a collapse feature in the underlying cap rock of the Paradox Formation is observed (fig. 7; Reclamation, 1978). The collapse feature is filled with breccia and contemporaneous alluvial sediments (Gutiérrez, 2004) in hydraulic connection with the surrounding alluvial aquifer as well as the underlying salt of the Paradox Formation (Reclamation, 1978). The collapse feature and breccia are

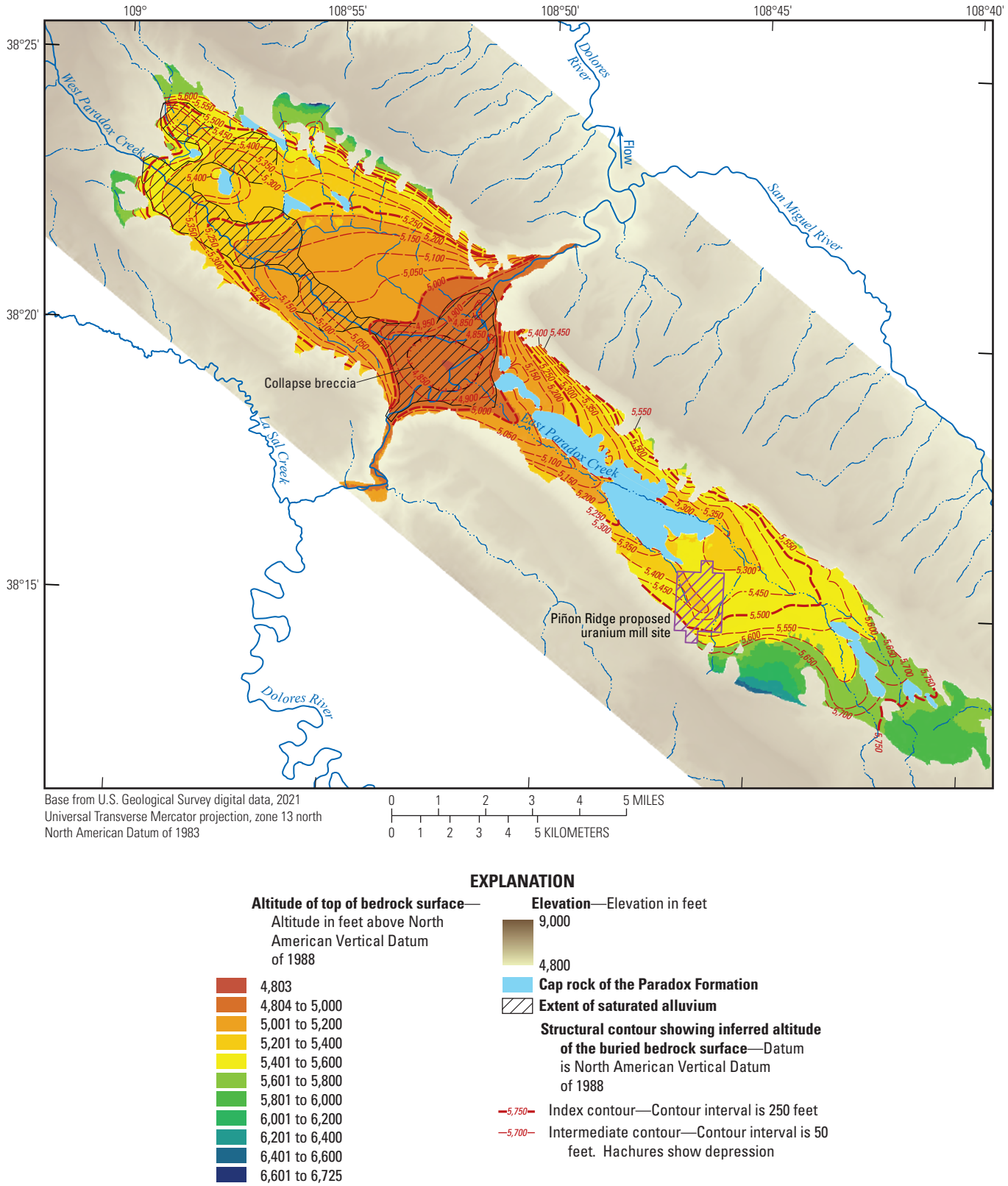

Figure 7. Generalized configuration and altitude of the top of bedrock surface (or base of the alluvial aquifer), location of the approximate center of the collapsed gypsum breccia (collapse breccia), and extent of the saturated alluvium in the Paradox Valley, Montrose County, Colo. (Reclamation, 1978; Paschke and Mast, 2024).

likely related to Quaternary underground karstification (dissolution and subsidence) of the salt of the Paradox Formation (Gutiérrez, 2004) and occur in an area of the Paradox Valley where the underlying salt is nearest to the surface. The second area is a bedrock trough near the northwestern corner of the valley that trends southeasterly for about 2 mi (fig. 7). This bedrock trough could be an erosional feature (buried channel), a graben, or a solution-collapse feature. The third area is a bedrock trough near the Piñon Ridge proposed uranium mill that trends northwesterly (fig. 7) and was identified as a graben (Golder Associates Inc., 2009). There is no alluvium on the valley floor where the Paradox Formation crops out and little to no alluvium southeast of the river.

Paleozoic Units

Paleozoic rocks in the Paradox Valley are classified into the regional Canyonlands aquifer and Four Corners confining unit (table 4). Rocks of the Canyonlands aquifer are exposed primarily on the northeastern side of the Paradox Valley, although the rocks thin toward the valley and faulting has offset bedding (Carter and Gualtieri, 1965; Cater and Craig, 1970). The Canyonlands aquifer is recharged by infiltration of precipitation and streamflow. In the subsurface, it is likely recharged by downward flow through overlying Mesozoic rocks (Lindner-Lunsford and others, 1989; Geldon, 2003b). Regionally, the salt in the Paradox Formation is considered a barrier to groundwater flow that restricts regional groundwater flow on opposite sides of the Paradox Valley (Geldon, 2003b).

Paradox Formation

In the study area, the Four Corners confining unit is composed of evaporite deposits of the Paradox Formation that form the core of the Paradox Valley anticline. The Paradox Formation underlies the alluvial aquifer near the Dolores River and is exposed along the floor of the Paradox Valley southeast of the river. The salt in the Paradox Formation is predominantly halite (70–80 percent) with interbedded shale, anhydrite and other evaporite minerals, and dolomite (Geldon, 2003a). The salt diapir at the center of the Paradox Valley anticline is up to 12,000 ft thick (King and others, 2014). A cap rock is present at the top of the salt that formed as circulating groundwater dissolved the more soluble minerals (potash and halite), leaving behind the less soluble minerals (anhydrite, gypsum, dolomite, and shale) (Gutiérrez, 2004). The cap rock, which is exposed on the floor of the Paradox Valley (fig. 5), has an estimated thickness (depth to the top of unweathered salt) ranging from about 400–500 ft near the Dolores River to about 1,300 ft at the southeastern end of the valley (Paschke and Mast, 2024).

In the center of the Paradox Valley is an apparent collapse feature (fig. 7) where the cap rock has been brecciated (broken up) by collapse and, in this report, is referred to as collapse breccia (Reclamation, 1978). The collapse breccia is similar in composition to the cap rock, is mixed with rock fragments and alluvial deposits, and is softer and more permeable than the cap rock in other locations where it is not brecciated (Reclamation, 1978). Because of the interbedding with alluvium, development of the collapse breccia is considered contemporaneous with deposition of Quaternary alluvial deposits in the Paradox Valley (Gutiérrez, 2004) and is described in drilling logs from wells and test holes at the PVU as “brecciated gypsiferous crumbly shale” (Reclamation, 1978). The collapse brecciais as much as 500 ft thick and overlain by more than 100 ft of alluvial deposits in some locations (Reclamation, 1978).

Top of the Salt of the Paradox Formation

The generalized configuration and altitude of the top of the salt in the Paradox Formation beneath the collapse breccia and cap rock in the Paradox Valley is shown in figure 8, which was modified from a regional map of that surface developed by Elston and Shoemaker (1961). Information from oil, gas, or brine test wells were used as control points to update the map for the Paradox Valley and surrounding area (well data published in Paschke and Mast, 2024). Local relief on the top surface of the salt is more than 12,000 ft, and the contour patterns reflect the structure of the underlying salt anticline (fig. 8).

Hydraulic and Storage Properties

The hydraulic and storage properties of the alluvial aquifer and collapse breccia of the Paradox Formation are estimated from previous constant-rate pumping tests and specific-capacity tests conducted at wells in the Paradox Valley (Reclamation, 1978; Paschke and Mast, 2024) and aquifer tests conducted by the USGS in 2013 (Newman, 2021) as described in the Methods section of this report.

Previous Estimates of Aquifer Properties

Constant-rate pumping tests of the alluvial aquifer and the collapse breccia were conducted during early investigations at the PVU (Reclamation, 1978). In addition, specific-capacity tests available from well permits for the Paradox Valley were compiled to estimate K for the alluvial aquifer (Paschke and Mast, 2024). The estimated K of the alluvial aquifer near the PVU ranged from about 44 to 161 feet per day (ft/d), based on analyses of one constant-rate pumping test, with a geometric mean of about 64 ft/d for all results (Reclamation, 1978). Results from specific-capacity tests conducted from 1973 to 1984 indicate slightly lesser K values than pumping test results for the alluvial aquifer ranging from 0.6 to 62 ft/d with a geometric mean of about 13 ft/d (Paschke and Mast, 2024). Spatial variations in estimated K for different sites indicates aquifer heterogeneity (Reclamation, 1978). Specific yield of the alluvial aquifer was not determined by the aquifer test but based on the sand and gravel lithology of the alluvium at the PVU, likely ranges from 10 to 25 percent. Results from two constant-rate pumping tests of the collapse

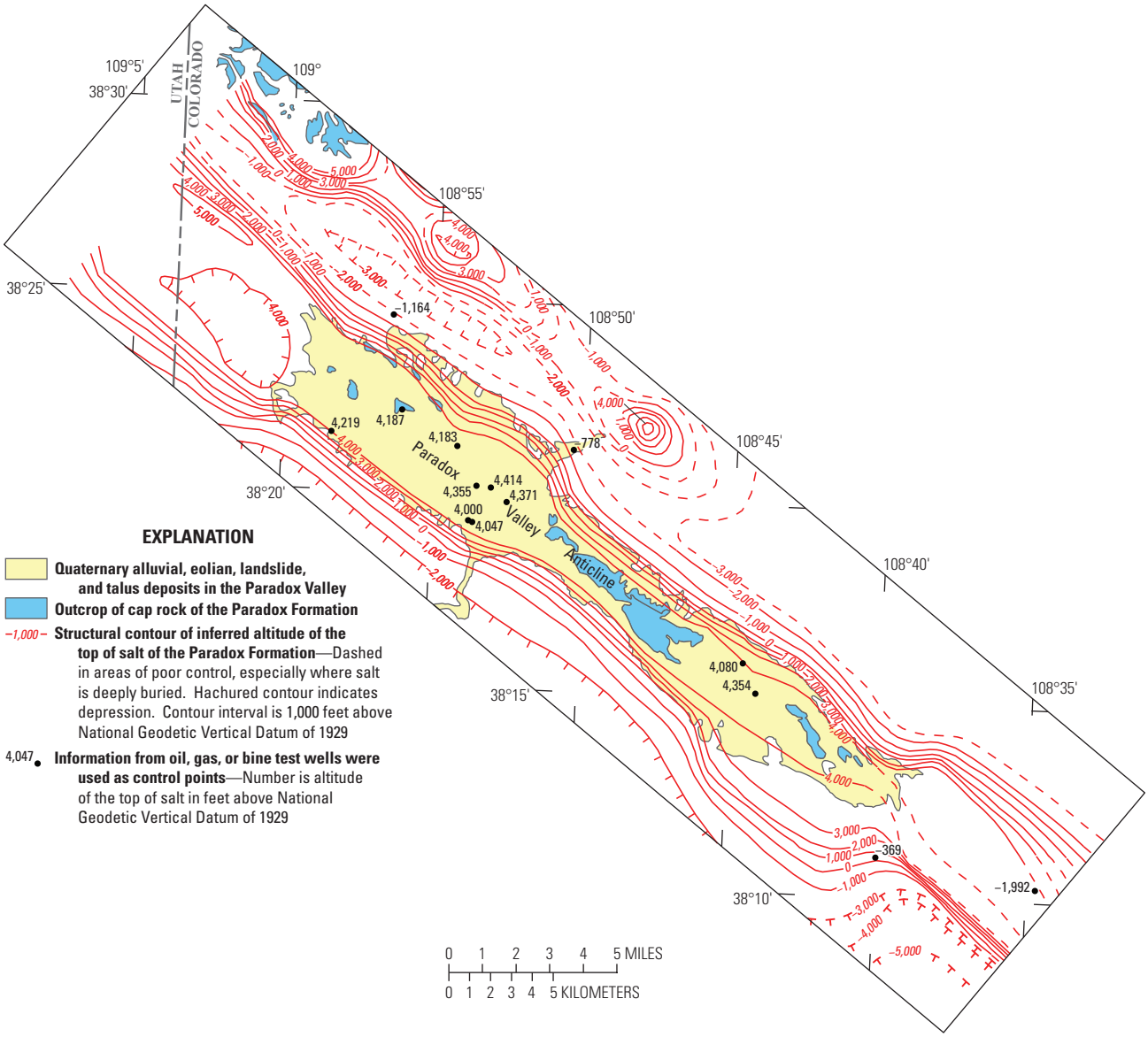

Figure 8. Generalized configuration and inferred altitude of the top of the salt of the Paradox Formation in the Paradox Valley, Montrose County, Colo.

breccia indicate K of the collapse breccia ranged from about 9 to 76 ft/d with a geometric mean of about 24 ft/d (Reclamation, 1978). The collapse breccia K values are similar in magnitude to those for the alluvial aquifer and are several orders of magnitude greater than K values reported for the unbrecciated cap rock, which ranged from 3.1 X 10^{-4} to 0.68 ft/d with a geometric mean of 3.5 X 10^{-2} ft/d (Wollitz and others, 1982).

Results of 2013 Aquifer Testing

Aquifer tests using both slug tests (Butler, 1997) and pumping tests (Kruseman and de Ridder, 1990) were conducted at the PVU in 2013 by the USGS, and the results were analyzed to estimate K as described in the "2013 Aquifer Testing" section of this report. Results of the 2013 aquifer tests are presented herein, and the underlying data are available in a USGS data release (Newman, 2021).

2013 Slug Tests

Well 8E25-D was the only well with slug-testing data suitable for analysis. Analysis of water-displacement data with the Bouwer-Rice and Springer-Gelhar methods yielded K values ranging from 4.6 ft/d to 130 ft/d with a median K of 19.1 ft/d. The large range in results is caused by the inclusion or exclusion of oscillatory behavior in the slug tests, which are handled differently by the Bouwer-Rice and Springer-Gelhar solutions. This range in K values is similar to the range of 2–175 ft/d reported in well permits (Colorado's Decision Support System, 2020). Calculated K values from the Springer-Gelhar method were consistently greater than calculated K values from the Bouwer-Rice method with ranges of 26–130 ft/d and 4.6–19 ft/d, respectively. These calculated K values from slug testing are compared to values derived from the pumping test in the "2013 Pumping Test" section of this report.

2013 Pumping Test

Water-level and pumping data from the 2013 large-scale pumping test of the Paradox Valley alluvial aquifer were analyzed using water-level modeling (Bakker and Schaars, 2019) and analytical approaches (Theis, 1935; Boulton, 1963) to explore potential variability in calculated hydraulic properties. Data analysis had the potential to be complicated by the numerous pumping wells that were pumped at variable rates throughout the test rather than the traditional aquifer-testing-methods, wherein a single well is pumped at a constant rate. Results of water-level modeling were thus used to indicate the pumping well (or groups of wells) that had the most statistically relevant effect on groundwater levels in each observation point. Water-level models, including extraction rates from the most statistically relevant pumping wells, generally accounted for more than 90 percent of the observed water-level displacement at observation points (table 5). Most observation points displayed water-level displacements that were primarily controlled by a single pumping well based on water-level modeling, and, in each instance, this was the pumping well nearest to the observation point. One shallow observation point had water-level displacements that were controlled by both the nearest pumping well and another nearby pumping well.

Groundwater-level data prior to the initiation of pumping indicated an upward hydraulic gradient within the aquifer where the groundwater-level altitude measured in the deeper observation wells was typically greater than the groundwater-level altitude at the shallower observation wells as illustrated in figure 9 for well 3E25-S and 3E25-D. Plots for other wells are included in Newman (2021). A higher groundwater-level altitude at depth in the aquifer promotes upward flow towards the land surface and the Dolores River. Groundwater-level altitudes in both the deep and shallow observation wells began to decrease within one hour after pumping was initiated (fig. 9).

Analysis of the pumping-test results from the Boulton and Theis solutions to pumping-induced water-level displacements resulted in K values ranging from 23.1 to 47.0 ft/d and 14.9 to 330 ft/d, respectively. These results are compared to results of slug testing in figure 10, and results for each observation point are summarized in table 5. Application of the Boulton solution to water-level displacements failed to converge (meaning the iterative calculations failed to reduce the difference between observations and idealized model behavior below the selected criterion) in several observation wells, culminating in fewer results for the Boulton solution than the Theis solution (fig. 10). Failure of the model to converge likely indicates that the Boulton solution was less applicable to conditions in the aquifer than the Theis solution. Where the Boulton solution did converge, calculated K values generally corresponded to K values from the slug-test analysis and have similar interquartile K values. Results of the Theis model overlap with the full range of the Boulton and slug tests but extend to greater calculated K values (fig. 10).

Spatial evaluation of the pumping-test results indicates that hydraulic properties of the alluvial aquifer vary both horizontally and vertically. Spatial comparison is made using

Table 5. Water-level modeling results indicating pumping wells identified as producing water-level displacements at observation points and results of hydraulic-property estimation (Newman, 2021).

[Observation and pumping well locations from figure 2. Pumping test solution from Theis (1935) and Boulton (1963). MF, model failure for a given well and analytical solution type]

Observation point name	Pumping well location explaining majority of water-level displacement	Percentage water-level displacement explained by net recharge, streamflow, and pumping	Hydraulic conductivity estimated by Theis pumping test solution (feet per day)	Hydraulic conductivity estimated by Boulton pumping test solution (feet per day)
3E25-D_Deep	3E	92.6	14.9	23.1
3E25-S_15	3E	98.0	27.8	47.0
8E25-D_Deep	9E	94.1	86.1	MF
8E25-S_14	9E	94.3	103	MF
8E250-D_Deep	9E	100.0	330	MF
8E250-S_14	8E, 9E	85.1	174	MF

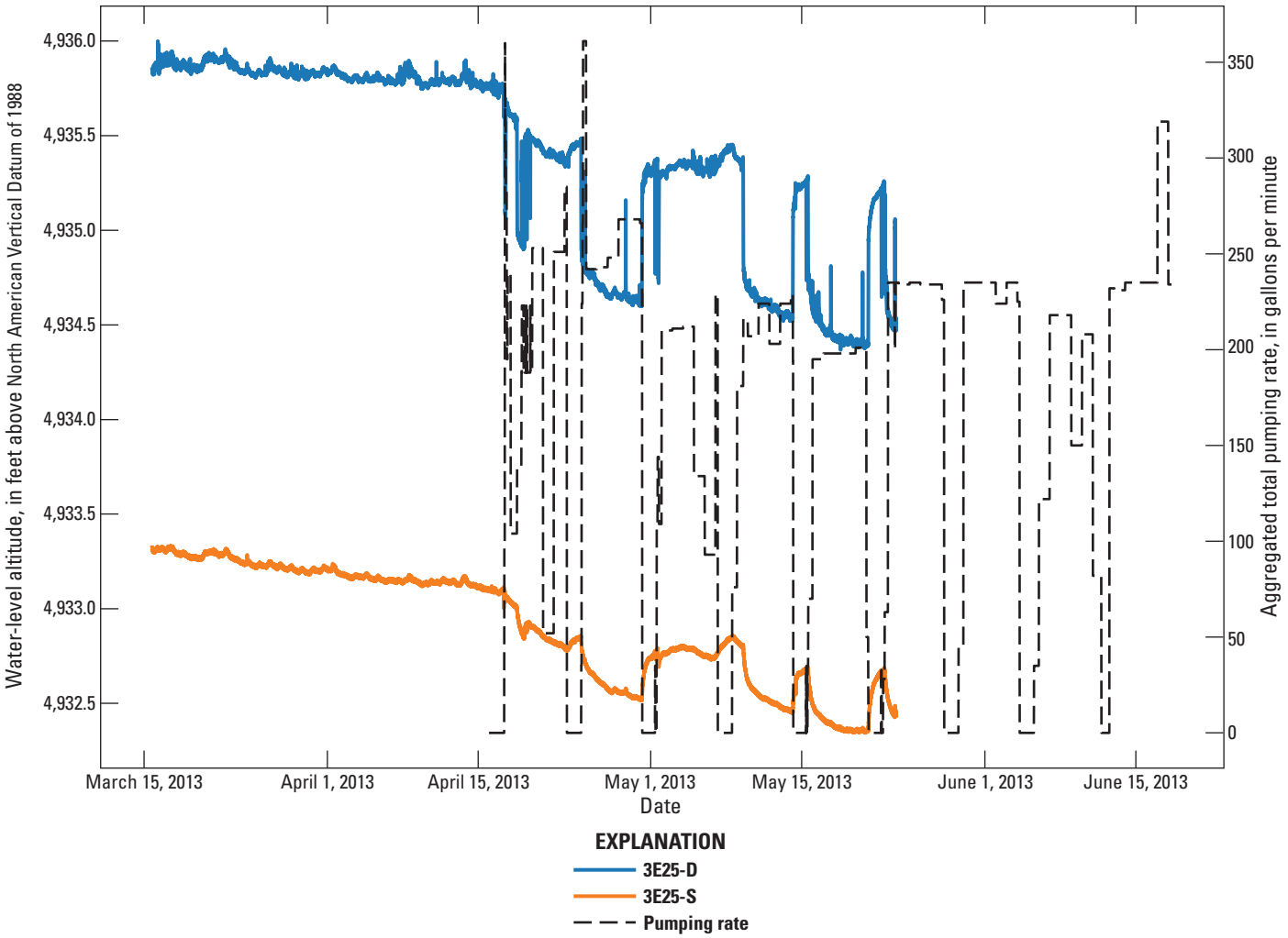

Figure 9. Groundwater-level altitudes in feet above North American Vertical Datum of 1988 in wells 3E25-S (shallow) and 3E25-D (deep) and aggregated total pumping rate from the Paradox Valley Unit pumping wells in the Paradox Valley, Montrose County, Colo. (Newman, 2021).

the results of the Theis solution because this solution produced results for all observation wells. Observation wells in the northern portion of the area included in aquifer testing (8E25D, 8E25S, 8E250D, 8E250S) had greater K values than the observation wells in the south (3E25D and 3E25S). In two of three shallow and deep observation well pairs, the shallower well had greater K values, whereas in the shallow and deep pair 8E250S and 8E250D, the deeper well had a K value about twice that of the shallower well (table 5). Greater K values in shallow wells are typical of conditions where increasing overburden pressure results in more aquifer compaction at depth, causing lower K values at depth (Freeze and Cherry, 1979). In observation well pair 8E250S and 8E250D, where the deeper well has a greater K value, the high K at depth may be caused by fracturing within the collapse breccia.

Limitations of the Analysis of Hydraulic Properties

This analysis of hydraulic properties of the alluvial aquifer in the Paradox Valley is subject to various uncertainties. First, during the period prior to the initiation of pumping, groundwater-level altitudes were slowly declining at several sites (fig. 9). In some instances, these initial trends can be removed from the data (Garcia and others, 2013), but that was not undertaken in this study because the goal was not to differentiate between pumping and non-pumping drawdowns (as was the goal of Garcia and others, 2013), but instead to quantify hydraulic properties based on the period of pumping data.

Second, during the data-collection period, the pumps cycled on and off. When the pumps were off, groundwater levels recovered slightly (fig. 9). However, the method of hydraulic-property analysis considers the entire period following initiation of pumping. This approach smooths the

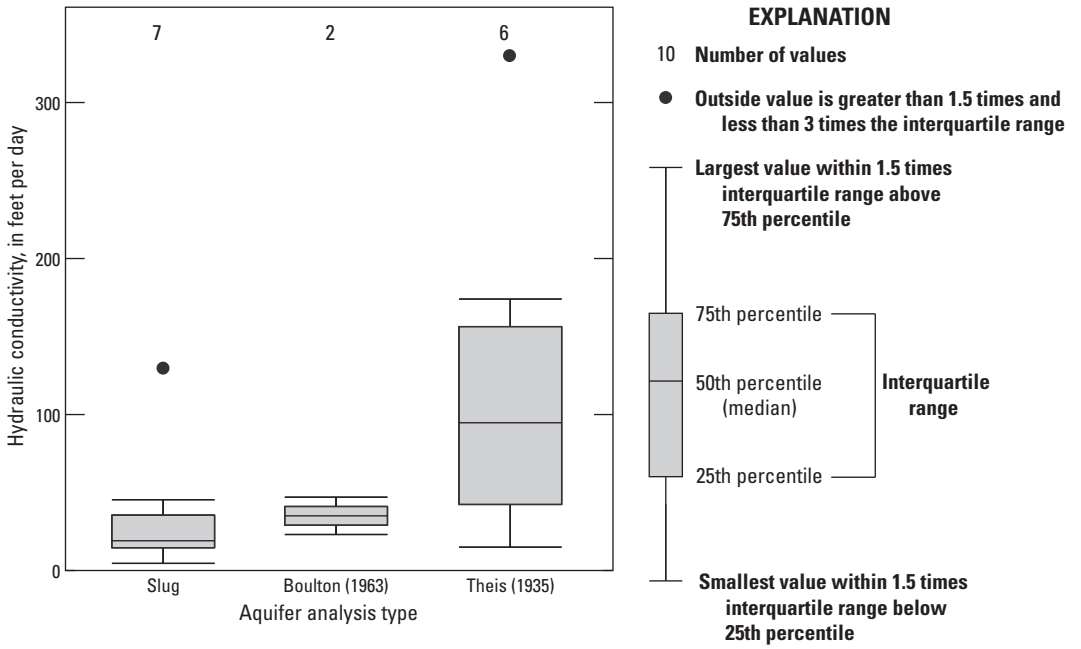

Figure 10. Results from slug tests and pumping tests estimated by Boulton (1963) and Theis (1935) solutions in the Paradox Valley, Montrose County, Colo. (Newman, 2021).

drawdown signal such that the small changes in water-level displacement at the end of the test are given the same weight in the solution as the initial water-level displacements (Newman, 2021). The results of the calculation therefore represent the long-term response of the system to testing as opposed to short-term variations related to pumping cycles in any one well.

Third, the effect of oscillatory responses in water-level displacement signals caused by variations in pumping were not assessed. Oscillatory signals in water-level displacement may be used to estimate hydraulic properties such as transmissivity and hydraulic diffusivity in three dimensions using Fourier transform analysis (Bakhos and others, 2014; Pozdniakov and others, 2021). Although these approaches may be useful in the future for characterizing the study area, no oscillatory signal analysis was completed as part of the current investigation.

Fourth, pumping interferences may complicate hydraulic-parameter estimation (Weber and Chapuis, 2013). Although interfering drawdowns were not explicitly calculated in this analysis, the water-level modeling results indicate that, in all observation wells considered but one (8E250-S_14), water-level displacements were best explained by a single pumping well. This indicates that the quantitative effects of pumping interferences were small.

Despite the various limitations on the 2013 pumping test and analysis, the range of resulting K values for the alluvial aquifer (from 23.1 to 47.0 ft/d and from 14.9 to 330 ft/d for the Boulton and Theis methods, respectively) are consistent with previous K estimates that range from 0.6 to about 161 ft/d (Reclamation, 1978; Paschke and Mast, 2024). The results are useful for conceptualizing the hydrologic system in the Paradox Valley and as estimated parameter values for a groundwater-flow model.

Groundwater Occurrence in the Paradox Valley

Groundwater occurrence in the Paradox Valley can be considered as two primary end members including freshwater in the alluvial aquifer and salt-saturated dense brine in the underlying salt cap rock and collapse breccia of the Paradox Formation (fig. 11). The alluvial aquifer is most extensive along the Dolores River and West Paradox Creek in the northwest half of the valley, where alluvial deposits form a freshwater water-table aquifer. The cap rock and collapse breccia at the top of the Paradox Formation are near the land surface in the Paradox Valley and contain a salt-saturated dense brine that is much older than the fresh groundwater as described in the "Groundwater Quality and Geochemical Indicators of Recharge Sources and Groundwater Age" section of this report. In the center of the valley, upward hydraulic

and density gradients drive flow of brine from the salt cap rock and collapse breccia into the alluvial aquifer and the Dolores River. This report section provides detailed information on groundwater occurrence in the two end members of the groundwater system in the Paradox Valley.

Alluvial Aquifer

The alluvial aquifer in the Paradox Valley exhibits unconfined (water-table) hydrologic conditions in the vicinity of the PVU and in the northwestern part of the valley. A generalized map of water-table altitude in this area was developed from limited groundwater-level data (Paschke and Mast, 2024) and indicates that groundwater in saturated parts of the alluvial aquifer flows from the northwest end of the valley toward the southeast generally following topography, the trend of West Paradox Creek, and the top of bedrock (figs. 5, 12). The alluvial aquifer ranges from 50 to 100 ft in thickness near the river based on data from well logs for the PVU pumping wells and is thickest, up to 170 ft in depth, near the center of the Paradox Valley in the collapse breccia feature (fig. 7). There is little to no alluvium southeast of the river along East Paradox Creek (Konikow and Bedinger, 1978).

Freshwater Recharge

The principal present-day sources of recharge to the alluvial aquifer include infiltration of incident precipitation in excess of soil moisture and evapotranspiration, infiltration of applied irrigation water in excess of crop consumptive use, leakage from irrigation canals and ponds, infiltration of surface water from West Paradox Creek, and infiltration of surface water from the Dolores River during high river stage. Mountain-block subsurface recharge from the foothills of the La Sal Mountains and groundwater movement along faults at the edges of the Paradox Valley are also plausible sources of recharge that were not evaluated as part of this investigation.

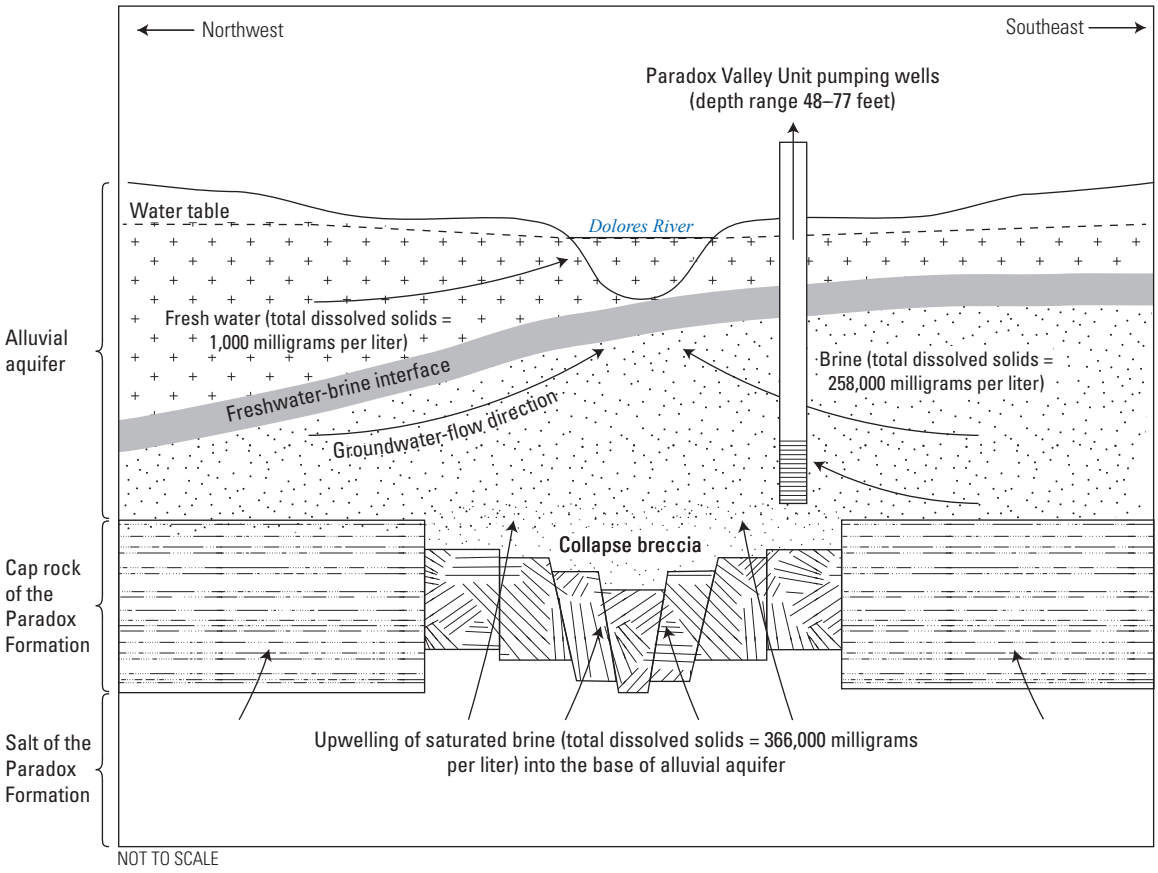

Figure 11. Conceptualized groundwater-flow directions and the variable-density groundwater system of the Paradox Valley. Thickness of the alluvial aquifer ranges from 50 to 100 feet and the cap rock of the Paradox Formation and brecciated gypsum (collapse breccia) average 500 and 300 feet, respectively, near the Dolores River. The salt of the Paradox Formation is up to 12,000 feet thick below the valley floor in the Paradox Valley, Montrose County, Colo. (Reclamation, 1978; Paschke and Mast, 2024; Elston and Shoemaker, 1961).

Recharge on the valley floor northwest of the Dolores River is a combination of infiltration of precipitation, infiltration of irrigation water, and infiltration of surface water primarily from West Paradox Creek. Annual precipitation on the valley floor averages 13.5 in, but much of this evaporates from the surface and soils or transpires. Recharge from infiltration of irrigation water likely occurs beneath about 2,730 acres of irrigated crop and pastureland northwest of the river (Colorado's Decision Support System, 2020). The primary source of water for irrigation in the valley is Buckeye Reservoir (fig. 1). Water is diverted from streams on the eastern slopes of the La Sal Mountains and stored in Buckeye Reservoir. Water released from Buckeye Reservoir flows into West Paradox Creek and is subsequently diverted for irrigation mainly through unlined canals in the valley. Releases from Buckeye Reservoir between 1988 and 2009 ranged from about 200 to 6,500 acre-feet per year (acre-ft/yr) and averaged about 3,420 acre-ft/year (Colorado's Decision Support System, 2020).

Infiltration of surface water is a primary source of recharge to the alluvial aquifer. West Paradox Creek, which originates in the La Sal Mountains, transmits natural snow-melt runoff from the mountains as well as irrigation water from Buckeye Reservoir to the Paradox Valley. West Paradox Creek loses water to the alluvial aquifer as it flows southwest toward its confluence with the Dolores River as evidenced by water-table maps (fig. 12) and mixed groundwater ages observed in wells adjacent to the creek as described in the "Groundwater Quality and Geochemical Indicators of Recharge Sources and Groundwater Age" section of this report.

Under present day conditions, the Dolores River flows across alluvial deposits, the collapse breccia, and the salt cap rock of the Paradox Formation. As the topographic low in the valley, the river is generally an area of groundwater discharge for both the alluvial aquifer and the underlying brine. However, reversal of freshwater gradients is observed during periods of high river stage, primarily during spring snowmelt runoff, and the river recharges the alluvial aquifer during

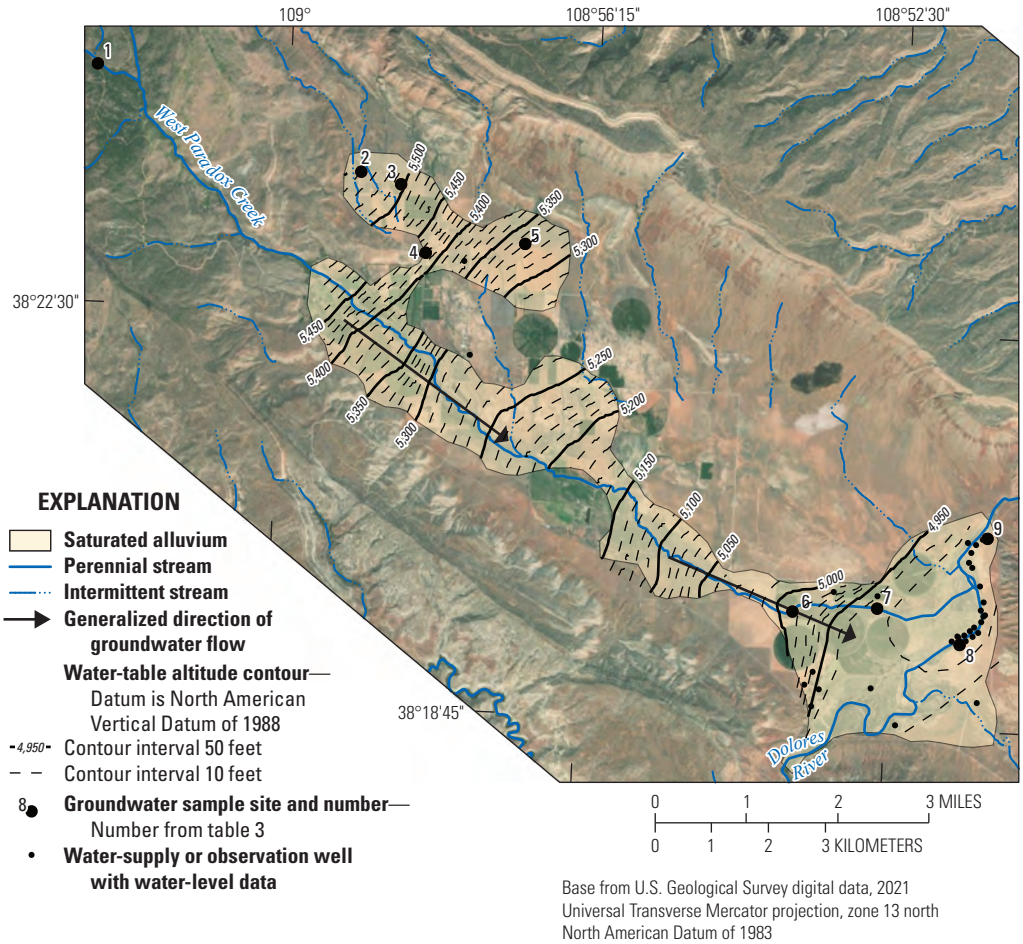

Base from U.S. Geological Survey digital data, 2021
Universal Transverse Mercator projection, zone 13 north
North American Datum of 1983

Figure 12. Generalized water-table altitude surface and extent of saturated alluvium in the alluvial aquifer in the Paradox Valley, Montrose County, Colo., 1961–2009. Water-level data for water-supply and observation wells are published in Paschke and Mast (2024). Groundwater sample data are published in Gardner and Newman (2023).

this gradient reversal (Mast and Terry, 2019). During valley formation and erosion of the Paradox Formation, the ancestral Dolores River was a likely source of recharge to the valley (Gutiérrez, 2004). Hunt (1956) concludes that the Dolores River has remained in its present course across the Paradox Valley since antecedent erosion of the valley began about 10–12 Ma. The geomorphic evolution of the valley along with groundwater ages estimated by this study, which indicate that the brine is more than 10,000 years old, support a hypothesis that the ancestral Dolores River was a source of recharge to the salt cap rock and contributed to brine formation during later stages of the Paradox Valley development (Cater and Craig, 1970; Gutiérrez, 2004).

Freshwater springs and wells at the northern end of the valley (fig. 1) are areas of groundwater discharge from the alluvial aquifer and surrounding uplands. The position of these springs along valley walls and grabens provides evidence that recharge occurs in upland areas surrounding the Paradox Valley and that groundwater flow in this part of the valley is likely fault controlled (fig. 5). Water-supply wells in the northern part of the valley (fig. 1) are completed in the alluvial aquifer and provide water supplies for domestic and stock uses (Colorado's Decision Support System, 2020). Water-supply wells in the southeastern part of the valley and along the sides of the valley are generally completed in Mesozoic sandstones.

Groundwater-Flow Directions and Saturated Thickness

Groundwater in the alluvial aquifer northwest of the Dolores River flows southeasterly toward the river where it discharges. The alluvial aquifer is thin to nonexistent and unsaturated southeast of the Dolores River where shales of the Chinle and Moenkopi Formation crop out at the land surface. The altitude of the water table near the northwestern corner of the valley is about 5,550 ft above NAVD 88 and about 4,930 ft at the Dolores River in the center of the valley (fig. 12). The approximate slope of the water-table surface (fig. 12) along West Paradox Creek from the northwestern end of the valley to the collapse feature is about 80 feet per mile (ft/mi) ([5,490−5,000] ft ÷ 6.1 mi ≈ 80 ft/mi), which is equivalent to a hydraulic gradient of about 0.015. The slope of the water table flattens within about 0.75 mi from the western edge of the collapse feature from about 80 ft/mi to about 11–18 ft/mi, which is equivalent to a hydraulic gradient of about 0.0021−0.0034. This change in slope implies that transmissivity of the alluvial aquifer is greater in the collapse feature than northwest of the collapse feature and is likely related to the greater saturated thickness of alluvial deposits within the collapse feature. At about 1.2 ft/mi, the slope of the water table parallel to the Dolores River as it crosses the collapse feature is relatively flat compared to gradients from the northwest part of the valley. The upstream flexure of water-table contours along the Dolores River shown on the May 2, 1977, water-table map of the PVU (Reclamation, 1978) indicates upward flow of brine from the collapse breccia to the alluvial aquifer as well as flow from the alluvial aquifer to the Dolores River.

Paradox Valley Brine

Brine in the Paradox Valley has TDS concentrations as high as 366,000 mg/L with sodium and chloride making up about 95 percent of the dissolved solids mass indicating that the brine is primarily derived from dissolution of halite in the Paradox Formation (Konikow and Bedinger, 1978; Reclamation, 1978). Large concentrations of dissolved solids can substantially increase the density of groundwater and, because the Paradox Valley brine is similar to a pure sodium-chloride solution, its density can be estimated from empirical relations (Weast, 1974). Increasing dissolved sodium-chloride concentration from 0 to about 350,000 mg/L increases the fluid density (ρ) by about 20 percent from 1.0 gram per cubic centimeter (g/cm^3) in freshwater to about 1.2 g/cm^3 in saturated brine. This difference in density between the brine and freshwater in the alluvial aquifer can affect groundwater gradients and discharge and indicates that the effects of variable densities warrant consideration when assessing or modeling groundwater flow in the Paradox Valley. The following subsections of this report provide theoretical background and applied presentations related to density-dependent groundwater flow in the Paradox Valley.

Equivalent Freshwater Head

When groundwater density varies along a flow path, it is helpful to correct hydraulic heads to a standard density for groundwater-flow computations, and the corrected heads are referred to as the equivalent freshwater head (Guo and Langevin, 2002). The concept of equivalent freshwater head explains upward gradients observed in the Paradox Valley and can be demonstrated by using groundwater levels measured in a well. Consider well B with a short-screened interval filled with saline groundwater (brine) with a density greater than that of pure water (fig. 13). The water altitude (h) in well B is an inverse function of the density of the water, and so if the mass of brine in well B is replaced with an equivalent mass of freshwater, the height of the water altitude (h_f) will increase as depicted for well A in figure 13 (Guo and Langevin, 2002). The water altitude in well A is a measure of head in terms of freshwater, which is referred to as equivalent freshwater head (Guo and Langevin, 2002). If the densities of freshwater and the brine are known, the equivalent freshwater head (h_f) of the brine in well B can be calculated from the measured head of the brine (h) with equation 1, modified from Guo and Langevin (2002).

$$h_f = h\,(\rho/\rho_f) - Z\,(\rho-\rho_f)/\rho_f \quad (1)$$

where

ρ is the density of the brine in the aquifer;
ρ_f is the density of pure water; and
Z is the altitude at the measurement point above the reference datum.

Water-table altitudes in the collapse breccia near the Dolores River measured May 2, 1977, were higher than those in freshwater in the alluvial aquifer at the PVU (Reclamation,

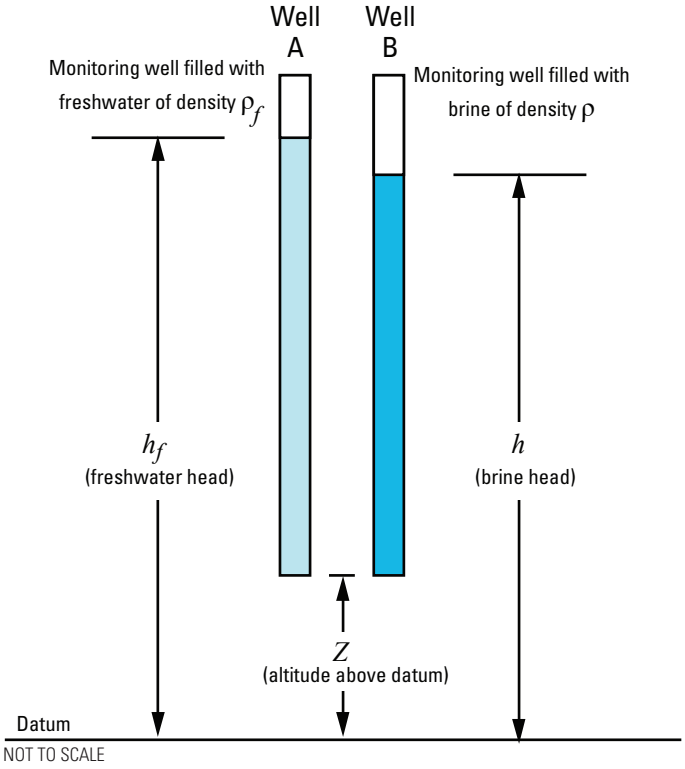

Figure 13. Head in two monitoring wells completed in a brine-filled aquifer. Well A head is filled with freshwater, and the well B head is filled with brine (modified from Guo and Langevin, 2002).

1978). Wells that were completed in the collapse breccia to average depths of about 225 ft were filled with brine with a density of 1.165 g/cm^3 (Reclamation, 1978). When corrected to equivalent freshwater heads, water-table altitudes in the collapse breccia were as much as about 40 ft higher than the measured water-table altitudes, which explains the upward density gradient from the collapse breccia to the alluvial aquifer and the Dolores River. The estimated vertical hydraulic gradient in the collapse breccia near the river at the PVU in these wells was about 0.18 (40 ft ÷ 225 ft).

Freshwater-Brine Interface

Freshwater and brine tend to mix at their contact by molecular diffusion and hydrodynamic dispersion. If the mixing (transition) zone is relatively thin, it can be treated mathematically as a sharp interface between the freshwater and brine, termed the freshwater-brine interface. At rest (hydrostatic condition), freshwater overlies brine with a horizontal interface (fig. 14*A*). However, if the water table has a gradient and is discharging to the river, the freshwater-brine interface will tilt upward in the direction of the freshwater flow (fig. 14*B*) because heads decrease in the direction of flow. The tangent of the angle of tilt of the interface (modified from Hubbert, 1953, p. 1,993) is given by equation 2.

$$dz/dx = \rho_f \div (\rho_f - \rho)\, dh_f/dx \qquad (2)$$

where

dz/dx is the tangent of the angle of tilt of the interface;
ρ_f is the density of the freshwater;
ρ is the density of the brine; and
dh_f/dx is the slope (hydraulic gradient) of the freshwater.

It is possible to have flowing freshwater in contact with static brine, if a hydrogeologic structure has a steeper angle of tilt than the freshwater-brine interface (Hubbert, 1953). Although Hubbert (1953) was discussing groundwater under confined conditions, it is assumed that this analysis also applies to unconfined conditions. By example for the Paradox Valley, assuming ρ_f = 1 g/cm^3, ρ is 1.165 g/cm^3, and dh_f/dx is 0.0028 (15 ft/mi, the slope of the water-table surface across the collapse feature), then dz/dx is −0.0171 [1 g/cm^3 ÷ (1 g/cm^3−1.165 g/cm^3) × 0.0028 = −0.171] or about −90 ft/mi. The slope of the freshwater-brine interface is in the opposite direction of the slope of the water table, and its absolute value is about six times greater or steeper than the slope of the water table. In the absence of a barrier, the brine flow will converge with the freshwater flow near the point of discharge at atmospheric pressure, which is the case in the Paradox Valley.

Upward Flow of Brine

Where vertical gradients are upward between a brine and an overlying freshwater aquifer, as is the case in the vicinity of the PVU, the rate of upward brine flow (q_z) will be less than that of freshwater for equivalent hydraulic gradients. For upward flow to occur, additional force is needed to overcome the frictional resistance of the more viscous brine and to lift the greater mass of the denser brine against the force of gravity (Massmann and others, 2006).

By convention, hydraulic gradients are considered positive in the direction of maximum decrease in value. The discussion in this section of this report applies to a density-stratified system in which less-dense groundwater overlies denser brine. Vertical flow of brine to an overlying freshwater body is a function of the equivalent freshwater hydraulic gradient and the density difference ratio $[(\rho_b-\rho_f)/\rho_f]$, where ρ_b is the density of brine and ρ_f is the density of the freshwater. When less-dense groundwater overlies denser brine, upward flow can occur only when the hydraulic gradient is upward and its magnitude is greater than the density difference ratio (Massmann and others, 2006). Although Massmann and others (2006) were discussing discharge of saline groundwater to an overlying freshwater surface-water body, their analysis is applicable to vertical flow within a porous medium. The

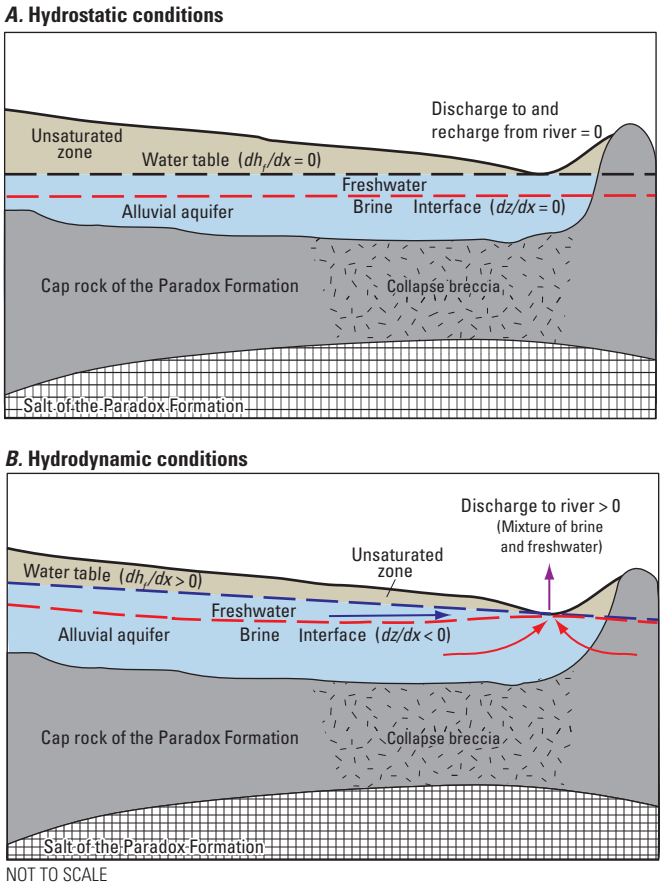

Figure 14. Position of the freshwater-brine interface (red dashed line) under *A*, hydrostatic conditions, and *B*, hydrodynamic conditions (modified from Hubbert, 1953; dh_f/dx is the slope [hydraulic gradient] of the freshwater; dz/dx is the tangent of the angle of tilt of the interface; >, greater than; <, less than; =, equal to).

mixed convection ratio (M) of Massmann and others (2006) is equivalent to the driving force ratio for vertical flow of Bear (1972, p. 654) and may be expressed as shown in equation 3.

$$M = (\Delta\rho/\rho_f)/(\Delta h_f/\Delta z) \quad (3)$$

where

$\Delta\rho/\rho_f$ is the difference between brine and freshwater densities;

Δh_f is the difference in equivalent freshwater head; and

Δz is the length along which Δh_f is measured.

Based on numerical simulations, when M is less than 1, the hydraulic gradient of equivalent freshwater head for saline groundwater is greater than the density ratio and is sufficient to overcome the opposing gravitational force. Consequently, brine flows upward. Conversely, when M is much greater than 1, flow is downward, and, when M is near 1, vertical flow is stagnant (Massmann and others, 2006). For example, assuming a freshwater density of 1 g/cm^3 and a brine density of 1.165 g/cm^3, the density difference ratio is 0.165 [(1.165 g/cm^3 − 1 g/cm^3) ÷ 1 g/cm^3 = 0.165] and the upward hydraulic gradient would have to be greater than 0.165 for upward flow of the brine ($M < 1$ if $\Delta h_f/\Delta z > \Delta\rho/\rho_f$). For PVU wells drilled into the collapse breccia, the estimated vertical hydraulic gradient in the collapse breccia near the river was about 0.18, which is greater than the estimated density gradient of 0.165, indicating that the brine can flow upward from the underlying cap rock and collapse breccia into the alluvial aquifer and eventually to the river.

Groundwater Pumping and the Freshwater-Brine Interface

Pumping of fresh groundwater underlain by brine can cause upconing of the freshwater-brine interface, depending on the magnitude of pumping (Bear, 1979). Upconing of the freshwater-brine interface has been studied extensively in coastal aquifers, where excessive pumping can cause the freshwater-sea-water interface to rise and move inland, potentially degrading water quality in aquifers used for public water supply. Analytical methods (Muskat, 1937; Bear and Dagan, 1964a, 1964b; Dagan and Bear, 1968; Bear, 1972) are often used to determine pumping rates that will not cause the interface or transition zone between freshwater and saline water to rise to the intake interval of a pumped well. There exists a critical steady pumping rate for a well pumping freshwater above a freshwater-brine interface, such that the interface can be maintained below the bottom of the well; however, if pumped at a higher rate, the interface rises and intercepts the screened interval of the well, which results in mixing freshwater and saline water (fig. 15).

By analogy, pumping brine from below a freshwater-brine interface, such as in the Paradox Valley, causes drawdown of the interface and intercepts freshwater that can dilute the pumped brine. Again, there is a critical pumping rate for wells with intake intervals below the freshwater-brine interface, such that the interface is maintained above the well intake to avoid mixing freshwater and brine (fig. 15). The PVU pumping wells, which are completed in the alluvial aquifer and below the freshwater-brine interface, are operated to maintain the interface above the perforated intake interval and to minimize pumping of freshwater.

Extent of Brine and Freshwater-Brine Interface in the Paradox Valley

On a larger scale, the distribution and mixing of freshwater and brine in the Paradox Valley is affected by the location of brine sources (cap rock and collapse breccia in the Paradox Formation), the distribution and hydraulic properties of hydrogeologic units, as well as hydrologic stresses on the freshwater alluvial aquifer. For example, changes in Dolores River streamflow as well as groundwater recharge and pumping all affect the extent of brine and the freshwater-brine

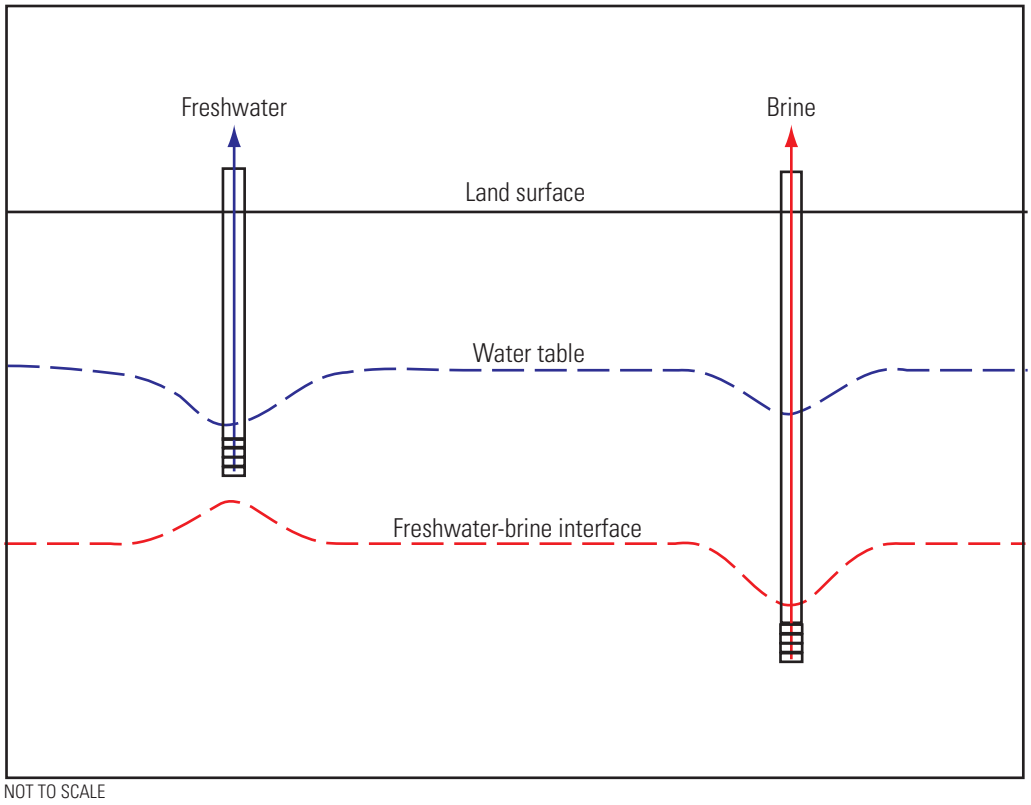

Figure 15. Effects of pumping wells perforated above and below the freshwater-brine interface (after Bear, 1979).

interface in the Paradox Valley. Understanding the extent of brine and the location of the freshwater-brine interface could be key to developing conceptual and numerical models of brine discharge to the Dolores River in the Paradox Valley. In October 2011, the USGS contracted an AEM survey across the majority of the Paradox Valley that contributed to ongoing hydrogeologic research in the valley (Ball and others, 2015). Descriptions of data acquisition and processing, as well as datasets of resistivity at set altitude intervals, are provided in Ball and others (2015). The AEM geophysical methods characterized the electrical resistivity of subsurface materials to depths of up to 985 ft below land surface and were used to map the three-dimensional distribution of brine in the alluvial aquifer and underlying cap rock (Ball and others, 2020).

Ball and others (2020) applied a combination of Bayesian and deterministic resistivity models to interpret the top of the freshwater-brine interface for October 2011 using resistivity thresholds that likely define changes in groundwater salinity. Three resistivity thresholds were established by Ball and others (2020) at 1 ohm meter (Ωm) or 3.28 ohm feet (Ωft), 3 Ωm (9.84 Ωft), and 9 Ωm (29.5 Ωft) (fig. 16). The 1-Ωm (3.28 Ωft) threshold is consistent with the observed TDS of the PVU pumping wells and likely represents the extent of brine with concentrations that exceed 200,000 mg/L. The 3-Ωm (9.84 Ωft), threshold represents a transition zone where TDS is likely less than 200,000 mg/L but above that of regional groundwater. The 9-Ωm (29.5 Ωft) threshold falls below resistivity values typical of the geologic background and delineates the region where TDS is likely above that of regional groundwater (Ball and others, 2020). The area has a diamond shape and extends nearly 2.5 mi away from the Dolores River parallel to the trend of the valley where it approaches the depth limits of the AEM. The 9-Ωm (29.5 Ωft) threshold is considered the most conservative interpretation of the extent of groundwater with elevated TDS and was used to develop a map of the altitude of the freshwater-brine interface by Ball and others (2020).

The resulting map of the freshwater-brine surface for October 2015 (fig. 17) indicates that the interface is shallowest near the Dolores River where it approaches the altitude of the land surface as it reaches its natural discharge area along the river (Ball and others, 2020). The brine extends away from the river to the northwest and southeast along the axis of the valley as well as towards the canyons where the river enters and exits the valley. At the depth limits of AEM of about 985 ft, the freshwater-brine interface appears to continue to dip into the subsurface. The brine is asymmetrical and is deeper northwest of the river, consistent with the presence of a substantial freshwater lens in the alluvial aquifer. The freshwater aquifer receives recharge from the northwest highland area in the foothills of the La Sal Mountains, West Paradox Creek as it enters the valley, and irrigated lands on the northwest side

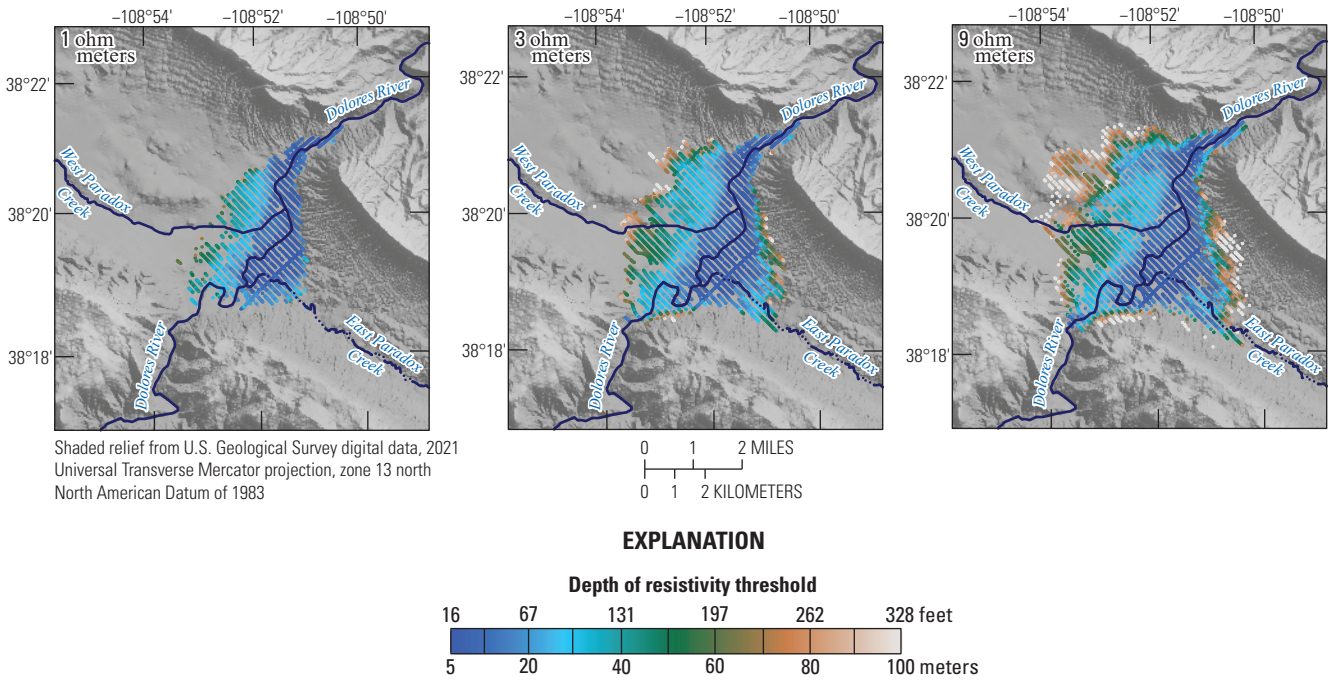

Figure 16. Depth to resistivity threshold picks for 1, 3, and 9 ohm meter (modified from fig. 5 in Ball and others, 2020).

of the valley. Southeast of the river, the alluvial aquifer and associated freshwater lens is much thinner or even nonexistent adjacent to the river, where shale confining units occur at the land surface and there is no alluvium. The freshwater-brine interface is near the land surface southeast of the river where outcrops of the shale confining unit may create vertical impermeable barriers to groundwater flow (Konikow and Bedinger, 1978).The AEM results confirm that the transition from freshwater to brine in the alluvial aquifer appears to be extremely abrupt near the Dolores River; however, away from these regions and particularly with distance from the river, the freshwater-brine interface becomes more diffuse (Ball and others, 2020).

Brine Discharge to the Dolores River

Brine from the cap rock and collapse breccia in the Paradox Formation exhibits an upward hydraulic gradient in the center of the Paradox Valley, such that it discharges naturally to the alluvial aquifer and Dolores River. It is this brine discharge that increases salinity in the river as it crosses the valley. This section of the report summarizes estimates of salinity load (Mast, 2017; Heywood and others, 2024a) and discusses controls on the spatial distribution of brine discharge from Mast and Terry (2019).

Total dissolved solids loading to the Dolores River is based on the differences between TDS loads computed at the two USGS streamgages that bracket flow in the Paradox Valley (Mast, 2017). The average annual increase in TDS load of the Dolores River across the Paradox Valley prior to test operations of the PVU (1980–1993) was estimated at about 137,900 tons per year (Mast, 2017), and the average annual increase in TDS load during PVU operation from 1997 to 2015 was estimated at 43,300 tons per year. These calculations represent a reduction in TDS load of 94,600 tons per year or about a 70 percent reduction in TDS loading to the Dolores River and compare closely to the average estimated mass of salt (104,000 tons per year) disposed of at the PVU injection well (Mast, 2017).

A synoptic survey of SC in the river between the upstream and downstream streamgages illustrates the magnitude and spatial variability of water quality in the river across the valley (fig. 18). The SC survey was conducted by Reclamation in June 2013 during an extremely dry period when SC values in the river were much greater than normal, accentuating the effect of brine discharge on the water quality of the river (Mast, 2017). At the upstream site where the river enters the valley, the SC was 1,990 microsiemens per centimeter (µS/cm) and increased to 31,000 µS/cm about 2 mi downstream as a result of brine discharge (Mast, 2017). This is the same area where results from Ball and others (2020) indicate brine in the upper 16 ft of the subsurface (fig. 17). Where the river flows past the PVU well field, the SC decreased to about 20,000 µS/cm, likely because freshwater from the alluvial aquifer discharges into this reach of the river from the northwest and because of PVU operations. Downstream from the PVU well field, the SC in the river increased to 60,000 µS/cm

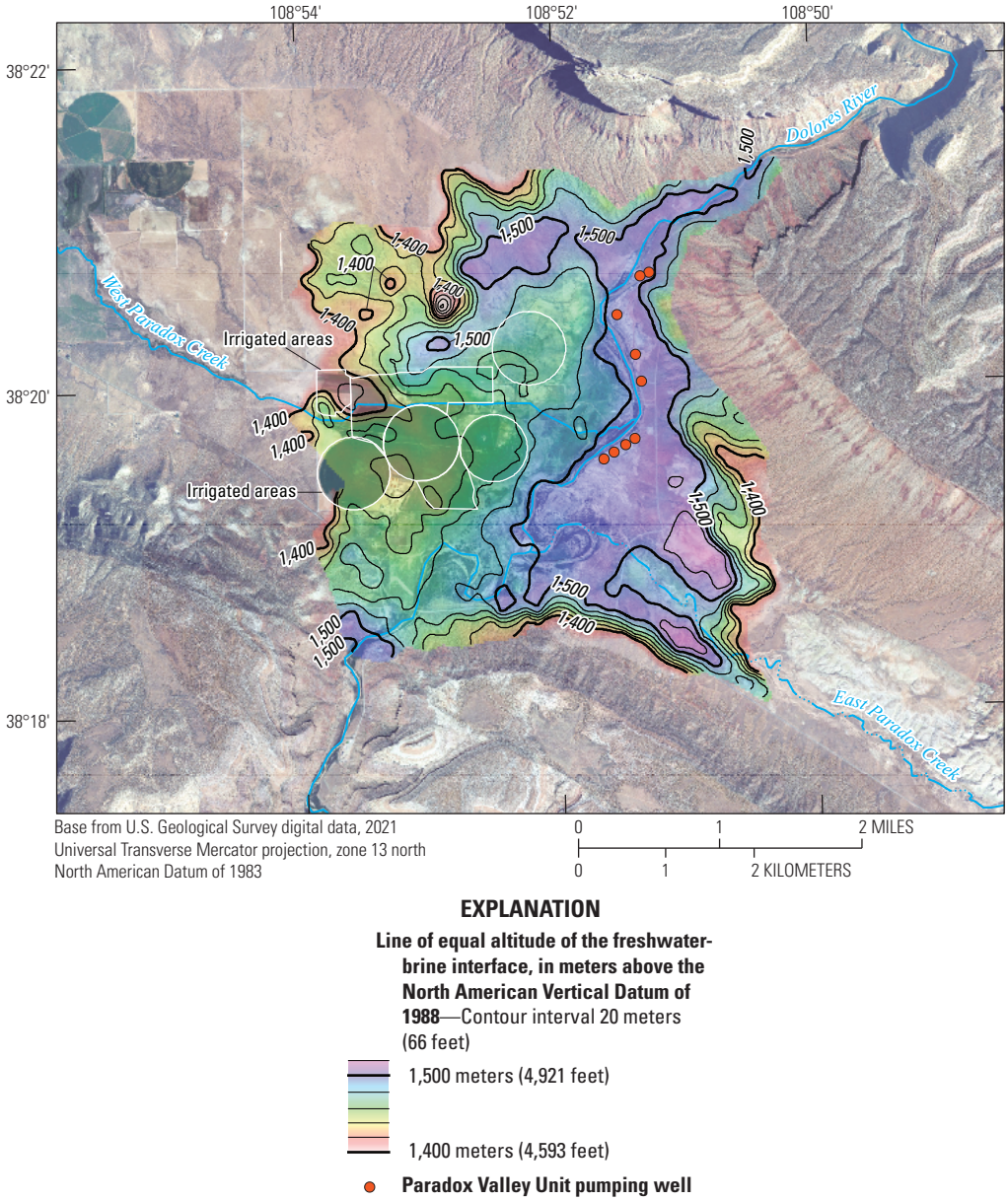

Figure 17. Equal altitude of the freshwater-brine interface in the Paradox Valley, Montrose County, Colo., October 2011 (modified from fig. 6 in Ball and others, 2020).

(more than 30 times greater than at the upstream site) because of additional brine discharge from the alluvial aquifer that is not captured by the PVU (Mast, 2017).

In 2017, the USGS, in cooperation with Reclamation, conducted a study to improve the characterization of processes controlling spatial and temporal variations in brine discharge to the Dolores River (Mast and Terry, 2019). For the study, three geophysical surveys were conducted in March, May, and September 2017, and water levels were monitored in selected ponds and groundwater wells from November 2016 to May 2018. River-based continuous resistivity profiling and frequency domain electromagnetic induction surveys were made during high- and low-flow conditions, and results indicate dynamic groundwater-surface-water interactions along the Dolores River that vary spatially and temporally. Spatially, during winter low-flow conditions, a zone of low resistivity interpreted as brine-rich groundwater was observed close to the riverbed along an approximately 2.5-mi reach of the river consistent with the results of Ball and others (2015) (Mast and Terry, 2019). Also consistent with the findings of Ball and others (2015), direct current electrical resistivity surveys conducted by Mast and Terry (2019) showed that freshwater in the alluvial aquifer overlying the brine is much thicker (up to 32 ft) on the northwest riverbank than on the southeast

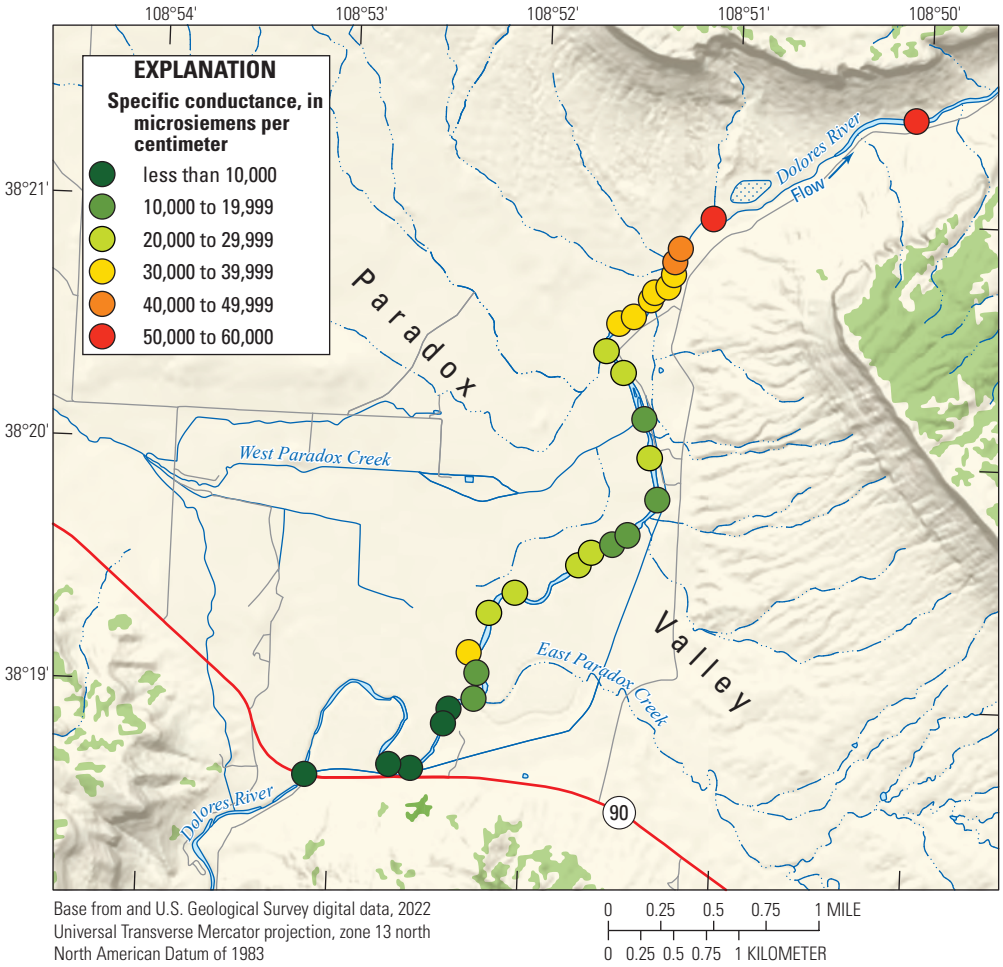

Figure 18. Specific-conductance survey of the Dolores River through the Paradox Valley, Montrose County, Colo., conducted by the Bureau of Reclamation on June 24–25, 2013 (from Mast, 2017).

bank (less than 16 ft). A large low-conductivity anomaly located about 2 mi upstream from the downstream streamgage (09171100) was observed in all surveys that may represent a freshwater discharge zone or a losing reach of the river (Mast and Terry, 2019).

Brine discharge also varies seasonally in response to changes in river stage caused by an annual cycle of spring snowmelt runoff and winter low-flow conditions (Mast and Terry, 2019). Results from geophysical surveys during high-flow conditions (March 2017) indicate that when the river stage is highest during spring snowmelt runoff, the layer of fresh groundwater underlying the river is thickest (Mast and Terry, 2019). During this time, the freshwater-brine interface was depressed as much as 6 ft below the riverbed during high-flow conditions, and brine discharge to the river was reduced to a minimum (Mast and Terry, 2019). During fall and winter low-flow conditions, the freshwater layer thins, the freshwater-brine interface rises closer to the land surface near the river, and brine discharge is greater than during the high-flow period (Mast and Terry, 2019). Groundwater-level monitoring showed there was an active exchange of water between the river and the adjacent alluvial aquifer that was consistent with the seasonal variation observed by the geophysical surveys. When river stage was low, groundwater flowed towards the river, and brine discharge to the river increased (Mast and Terry, 2019). When the river stage was high, the gradient was reversed, and fresh surface water from the Dolores River recharged the alluvial aquifer, minimizing brine discharge (Mast and Terry, 2019). Most of the TDS load to the river occurred during the winter and appeared to be enhanced by diurnal stage fluctuations (Mast and Terry, 2019).

Groundwater Quality and Geochemical Indicators of Recharge Sources and Groundwater Age

In June 2011, nine groundwater samples were collected from selected wells and springs in the Paradox Valley (table 3), and the samples were analyzed for a suite of major

constituents and environmental tracers that are described in more detail in appendix 1. Results for sample chemical analyses are available from the USGS NWIS database (U.S. Geological Survey, 2020a) using the USGS identification numbers from table 3 from the Methods section of this report, and the groundwater-age calculations for noble gases and carbon isotopes are provided in a USGS data release (Gardner and Newman, 2023).

Geochemical data interpretations are presented here that conceptualize sources of recharge, identify groundwater-flow paths, and estimate groundwater ages, and these data interpretations are used to constrain the conceptual model of fresh groundwater and brine occurrence in the Paradox Valley. The sample sites include one spring, five domestic wells, one irrigation well, and two PVU pumping wells (table 3; fig. 12). The spring is located in the northwest part of the valley and likely receives recharge from uplands northwest of the valley on the basis of its location and topographic position (fig. 12). The eight sample sites on the valley floor are located along a gradient of the general groundwater-flow direction from the northwestern end of the valley toward the Dolores River. The sites represent both the freshwater and brine parts of the groundwater system, as described in the "Water Quality of Groundwater" section of this report.

General Groundwater Quality

Results from groundwater samples collected during June 2011 for field parameters, major ions, and selected water-quality indicators (table 6) can be used to describe general water-quality conditions in the study area and to define freshwater and brine end members of the groundwater system. The analytical results are shown in table 6 and are generally consistent with initial water-quality assessments in the Paradox Valley reported by Reclamation (1978).

Seven of the samples (sites 1 through 7) represent fresh groundwater with TDS concentrations less than 3,000 mg/L, and the remaining two samples, from sites 8 and 9, represent brine at the base of the alluvial aquifer with TDS concentrations of 283,000 and 272,000 mg/L, respectively. Sample sites 1, 2, and 3 are farthest upgradient with TDS concentrations less than 500 mg/L. Site 1 is a spring located in the uplands northwest of the valley that discharges from the Dakota Sandstone. Sites 2 and 3 are wells located in the upgradient (northwestern) corner of the valley, which periodically is recharged by infiltration of runoff from the uplands. Dissolved-solids concentrations increase substantially in a downgradient direction (toward the southeast from sites 2 and 3). Sites 4 and 5 have respective dissolved-solids concentrations of 2,910 and 1,310 mg/L. The downgradient increases in TDS concentrations may result from longer flow paths, which allow more time for dissolution of minerals as groundwater moves through the aquifer, or by interception and mixing with brine from the underlying salt in the Paradox Formation. Shallow groundwater farther downgradient—near the confluence of West Paradox Creek and the Dolores River—at sites 6 and 7 has TDS concentrations of 898 and 820 mg/L, respectively. The relatively low concentrations of TDS at sites 6 and 7 compared to sites 4 and 5 likely result from infiltration of surface water from nearby West Paradox Creek. Sites 8 and 9, PVU pumping wells 2E and 8E, are completed in the alluvial aquifer within the collapse feature and pump brine from respective depths of 77.5 and 48 ft below land surface (table 3). Dissolved-solids concentrations at sites 8 and 9 were 283,000 and 272,000 mg/L, respectively, which is consistent with the brine concentrations pumped from the PVU (Mast, 2017).

Characterization of the water samples using the relative percentages of dissolved major ions shown in a Piper diagram (Piper, 1944) indicates three distinct groups: (1) calcium-magnesium-bicarbonate (Ca-Mg-HCO_3) water at sites 1–3, (2) calcium-magnesium-sulfate (Ca-Mg-SO_4) water at sites 4–7, and (3) sodium-chloride (Na-Cl) water at sites 8 and 9 (fig. 19). Upgradient samples with the lowest dissolved-solids concentrations (sites 1–3) are Ca-Mg-HCO_3 type waters and are located nearest to areas of recharge and have primarily been in contact with sandstone and shallow alluvium. Farther downgradient, Ca-Mg-SO_4 type waters are found throughout a large part of the valley (sites 4–7). The replacement of HCO_3 with SO_4 as the primary anion may indicate that groundwater is dissolving SO_4-bearing evaporite minerals (anhydrite and gypsum) as it flows down valley or is mixing with groundwater that was in contact with SO_4-bearing evaporite minerals from the underlying cap rock. The brine captured by the PVU pumping wells is predominantly Na-Cl type water but contains substantial concentrations of calcium, potassium, and sulfate (table 6).

Stable Isotopes of Water

Stable-isotope values of hydrogen (δ^2H) and oxygen ($\delta^{18}O$) in fresh groundwater samples from the Paradox Valley indicate that fresh groundwater is sourced from high-altitude precipitation. Isotopic ratios range from −113 to −108 parts per thousand (per mil) for δ^2H and −15.3 to −14.6 per mil for $\delta^{18}O$ (table 6; fig. 20) and are tightly clustered along the Global Meteoric Water Line (see app. 1 for more details). The narrow range of stable-isotope ratios is similar to those measured in groundwater from the nearby Moab-Spanish Valley area, which receives recharge sourced from precipitation at high altitudes in the La Sal Mountains (Gardner, 2004). Stable-isotope ratios of brine samples are shifted above the Global Meteoric Water Line by about 10 per mil in figure 20. The shift in δ^2H between the brine and freshwater samples could be caused by the presence of hydrogen sulfide (H_2S), which is noted in PVU pumping wells. Isotopic exchange with H_2S at low temperatures is known to increase δ^2H values of water because of large $^2H/^1H$ fractionation factors between water and H_2S (Horita, 2005).

Table 6. Field measurements, major-ion concentrations, and stable isotopes of water for groundwater samples collected during June 2011 in the Paradox Valley, Montrose County, Colo.

[Data from U.S. Geological Survey (2020a).°C, degrees Celsius; µS/cm, microsiemens per centimeter at 25 degrees Celsius; mg/L, milligrams per liter; $CaCO_3$, calcium carbonate; SiO_2; silicon dioxide; $\delta^{18}O$, stable-isotope ratio of oxygen-18; δ^2H, stable-isotope ratio of hydrogen; per mil, parts per thousand; —, not measured]

Constituent	Site number (table 3 and fig. 12)								
	1	2	3	4	5	6	7	8	9
Water temperature, °C	8	13.9	12.9	12.8	—	11.6	8	16.4	16.9
Specific conductance, µS/cm	357	577	562	2,920	1,670	1,250	1,170	226,000	225,000
pH, standard units	7.3	7	7.3	6.7	7	7	7.1	6	6
Dissolved oxygen, mg/L	4.9	1	0.4	0.1	0.2	0	0.1	0.4	0.5
Total dissolved solids, mg/L	208	332	328	2,910	1,310	898	820	283,000	272,000
Alkalinity, mg/L as $CaCO_3$	181	314	283	333	216	288	253	204	207
Calcium, mg/L	43	51.3	55.1	568	148	168	128	1,350	1,350
Magnesium, mg/L	13.2	39.3	35.1	163	118	53	75.2	1,620	1,660
Sodium, mg/L	10.7	15	13.5	33.8	70	46.8	30.8	86,000	86,400
Potassium, mg/L	1.75	7.23	6.15	11.1	23.7	3.8	3.73	4,610	4,580
Chloride, mg/L	3.37	5.37	5.07	13.3	33.4	28.4	26.5	182,000	171,000
Sulfate, mg/L	14	12.9	30.1	1,910	776	410	390	6,550	7,070
Silica, mg/L as SiO_2	12.5	11.8	12	14.4	8.09	13.4	12.5	6.46	6.43
$\delta^{18}O$, per mil	−14.8	−14.8	−15.3	−15.2	−14.8	−14.6	−14.8	−14.8	−14.7
δ^2H, per mil	−110	−110	−113	−112	−111	−108	−110	−100	−98

Tritium (^3H) and Tritium/Helium ($^3H/^3He$) Ages

Tritium (^3H) results are presented for the samples of fresh groundwater only (sites 1–7). The large amounts of hydrogen sulfide in the samples from sites 8 and 9 corroded the stainless-steel flasks used in the analyses and prohibited ^3H measurements of the brine samples. Tritium concentrations are either less than or equal to 0.2 tritium units (TU) or greater than or equal to 1.0 TU for all samples of fresh groundwater (table 7). Samples with tritium concentrations less than or equal to 0.2 TU are considered pre-modern (greater than about 60 years in age) and contain little to no tritium, because they were recharged prior to above-ground nuclear testing in the 1950s (Michel, 1989). Samples with tritium concentrations greater than or equal to 1.0 TU were recharged in the last 60 years, since the 1950s (Michel, 1989) and are considered modern. Site 1, a spring located in the upland area above the valley floor, has a ^3H of 2.3 TU and a tritium to helium-3 ($^3H/^3He$) age of 16 years (see app. 1 for additional details on groundwater-age dating). Sites 2, 3, and 5 have ^3H less than or equal to 0.2 TU and are classified pre-modern with respect to their $^3H/^3He$ ages indicating that, at a minimum, freshwater recharge takes more than 60 years to travel to wells in the northwestern end of the Paradox Valley.

Although site 4 has 1.0 TU, it also contains elevated concentrations of terrigenic helium-4 ($^4He_{terr}$) (discussed in the "Terrigenic Helium-4" section of this report), indicating that it is a mixture of modern groundwater with substantially older groundwater and cannot be assigned a $^3H/^3He$ age. Site 4 is a flowing well in a groundwater-discharge area where brine likely flows upward from the underlying cap rock of the Paradox Formation and mixes with freshwater. Nearby and downgradient from site 4, shale of the Paradox Formation crops out at the surface. It is likely that the small component of young water in this sample is derived from nearby recharge sourced from upgradient irrigation within the valley. Sample sites 6 and 7, respectively, have 3.1 and 2.9 TU and $^3H/^3He$ ages of 8.6 and 15 years. These wells have the youngest water of the sampled sites but are farther downgradient, a seeming contradiction that likely results from their proximity to infiltration of water from West Paradox Creek, which would have recently been released from Buckeye Reservoir.

Terrigenic Helium-4 ($^4He_{terr}$)

Concentrations of $^4He_{terr}$ and helium (He) isotope ratio measurements (expressed as R/R_a) are useful when making interpretations about groundwater age (Solomon, 2000). As discussed in appendix 1 of this report, $^4He_{terr}$ was not used to assign specific ages to groundwater in this study, but rather was used as an indicator of relative age that can be considered along with $^3H/^3He$ and radiocarbon-age estimates. The rate that groundwater acquires $^4He_{terr}$ from aquifer materials may vary from one location to another across the study area, and determining these rates is beyond the scope of this study. Regardless, a sample containing more than about

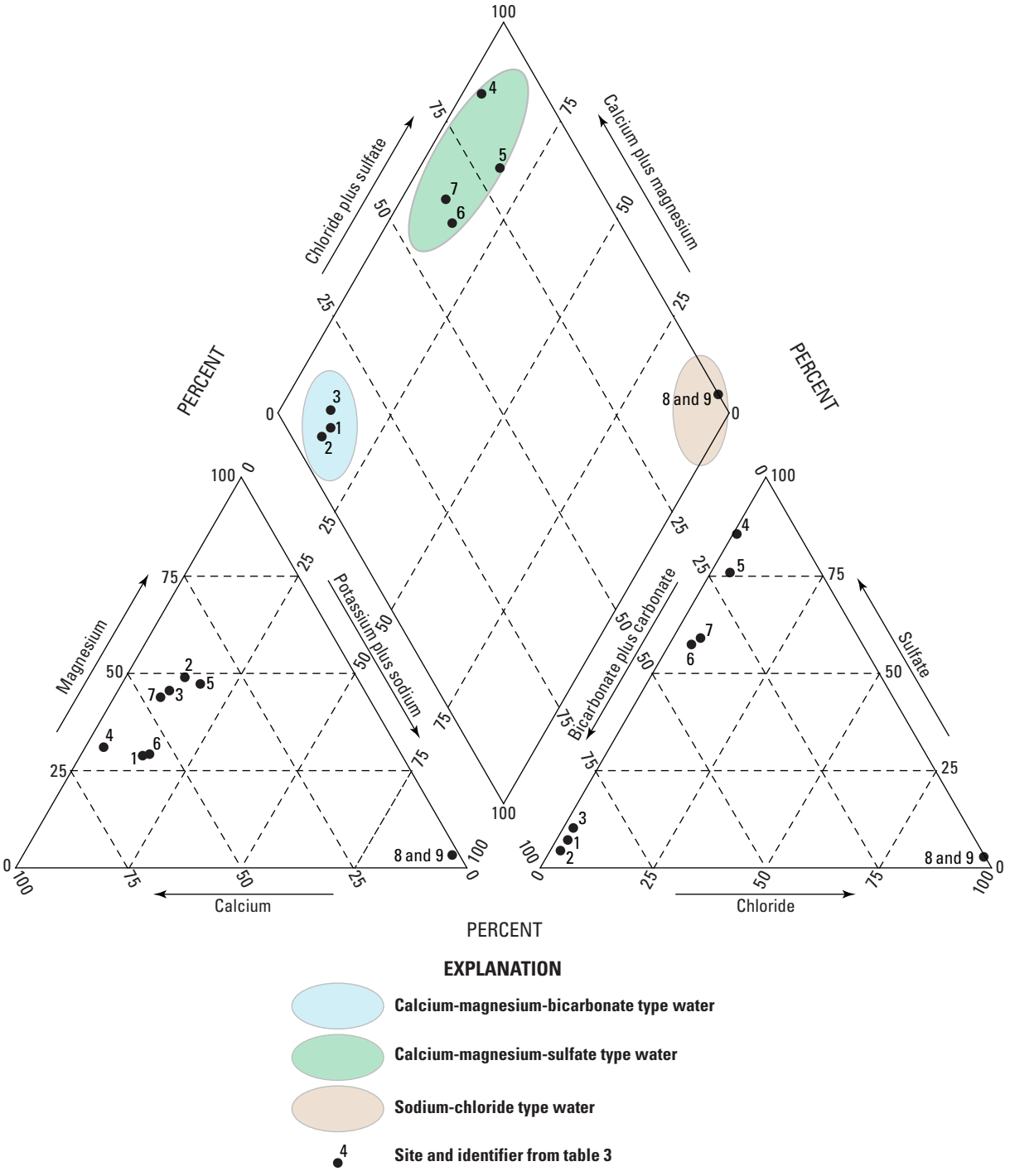

Figure 19. Percentage of major cations and anions in groundwater samples collected during June 2011 in the Paradox Valley, Montrose County, Colo. Site numbers from table 3 (U.S. Geological Survey, 2020a).

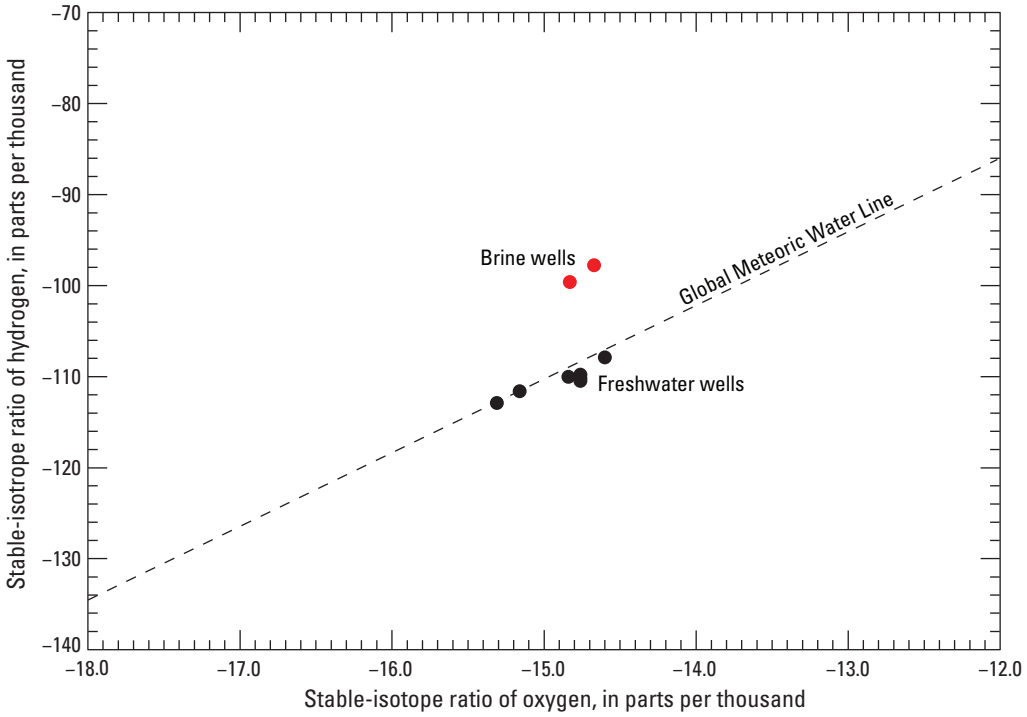

Figure 20. Stable-isotope ratio values of hydrogen and oxygen in groundwater samples collected during June 2011 in the Paradox Valley, Montrose County, Colo., (U.S. Geological Survey, 2020a) plotted with the Global Meteoric Water Line (Craig, 1961).

2.0×10^{-8} cubic centimeters at standard temperature and pressure per gram of water (ccSTP/g) of $^{4}He_{terr}$ most likely has a minimum average age of more than 1,000 years (Solomon, 2000). Because $^{4}He_{terr}$ is an interpreted value (derived by subtracting the solubility and excess air components from the total measured ^{4}He), measured $^{3}He/^{4}He$ expressed as R/R_a provides a useful check on the assumption that $^{4}He_{terr}$ correlates with time spent in the aquifer (Solomon, 2000). Where crustal He makes up the majority of the He_{terr}, the R/R_a value of groundwater will systematically be less than 1 as it acquires He_{terr} from time spent in contact with the aquifer solids.

Samples from sites 1, 6, and 7 contain modern water (^{3}H greater than or equal to 1.0 TU and less than 60 years in age), have low $^{4}He_{terr}$ concentrations less than about 5.0×10^{-9} ccSTP/g, and have R/R_a values of slightly more than 1 (fig. 21). Groundwater from site 4, previously noted as a mixture of modern and much older water, is the exception. Although the 1.0 TU of ^{3}H in the sample from site 4 indicates a modern fraction of water that is less than 60 years old, the $^{4}He_{terr}$ of 9.6×10^{-8} ccSTP/g is more than an order of magnitude greater than that of the other samples containing tritium, indicating that this water also contains a substantial fraction of water that is thousands of years old. Groundwater from site 3 has an R/R_a of 1.02 and a $^{4}He_{terr}$ of only 5.0×10^{-9} ccSTP/g, indicating that it is nearly modern, even though it is categorized as pre-modern by having low ^{3}H (0.2 TU). Groundwater from sites 2 and 5 have low R/R_a ratios (0.27 and 0.08, respectively) and high concentrations of $^{4}He_{terr}$ (2.9×10^{-7} and 6.7×10^{-7} ccSTP/g, respectively), indicating that they are at least thousands of years old. Lastly, samples from the PVU pumping wells, sites 8 and 9, have $^{4}He_{terr}$ of more than 1.0×10^{-6} ccSTP/g (three orders of magnitude greater than that of modern samples) and R/R_a of only 0.04, indicating that the brine contains a substantial fraction of water that is much older than all other groundwater sampled during this study.

Carbon-14 and Radiocarbon Ages

Carbon-14 activity, measured in dissolved inorganic carbon (DIC), ranges from 25.8 to 92.7 percent modern carbon (pmC) (table 7), indicating a broad range of ages for groundwater in the Paradox Valley. The highest activities, 65.6–92.7 pmC, were measured in samples determined to be modern by $^{3}H/^{3}He$ age dating (sites 1, 6, and 7). Intermediate activities of 60.4–62.5 pmC were measured in samples from sites 3 and 4, and the lowest activities of 25.8–33.5 pmC were measured in samples with substantially elevated concentrations of $^{4}He_{terr}$ (sites 2, 5, 8, and 9). This pattern is generally consistent with expected trends wherein modern water can have a range of ^{14}C activities depending on the degree of

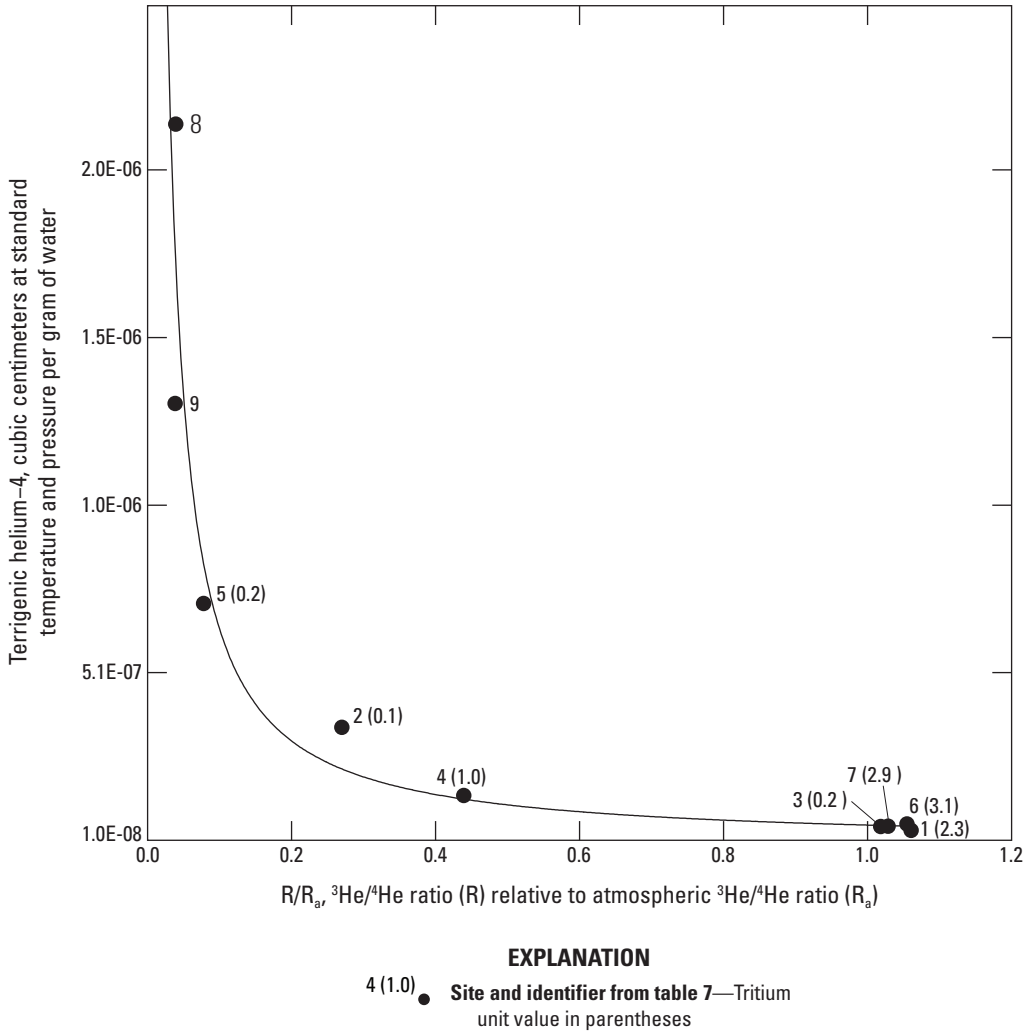

Figure 21. Terrigenic helium-4 compared with measured tritium to helium-4 ratio ($^3He/^4He$) to atmospheric $^3He/^4He$ ratio (R/Ra) for groundwater samples collected during June 2011 in the Paradox Valley, Montrose County, Colo. (Gardner and Newman, 2023).

chemical reaction in the soil and unsaturated zones, and pre-modern water will have lower ^{14}C activities with increasing age (Kalin, 2000).

Unadjusted and adjusted radiocarbon ages for these samples are listed in table 7 and described in Gardner and Newman (2023). The modern age designation is used for groundwater with adjusted ^{14}C ages that are less than zero, which results from the uncertainty in age adjustments (generally less than ±1,500 years). The range of adjusted ages determined by Gardner and Newman (2023) represents the minimum and maximum ages determined using the formula-based adjustment models of Ingerson and Pearson (1964); Tamers (1975); and Fontes and Garnier (1979). These radiocarbon-age adjustment models require ^{14}C and delta carbon-13 ($\delta^{13}C$) values of soil zone carbon dioxide (CO_2) and carbonate minerals that are available to react with or add to the dissolved inorganic carbon of the groundwater (Kalin, 2000). In all cases, ^{14}C activity was assumed to be 100 pmC, and soil zone CO_2 was assumed to have a $\delta^{13}C$ value of −22.0 per mil, the average isotopic value reported for similar terrains in nearby Utah (Hart and others, 2010). Carbonate minerals were assumed to have 0 pmC ^{14}C because of their age (Middle Cambrian to Permian) and a $\delta^{13}C$ value of 0, approximately the worldwide average for marine limestone (Keith and Weber, 1964).

Unadjusted radiocarbon ages of the groundwater samples range from 10,900 to 600 years (table 7). The largest age adjustments (difference between unadjusted and adjusted minimum radiocarbon ages) range from 7,500 to 600 years, giving adjusted minimum ages of 8,100 to modern. Adjusted radiocarbon ages indicate that samples from sites 1, 3, 6, and 7 are modern. This is in direct agreement with $^3H/^3He$ ages for sites 1, 6, and 7, and reinforces that site 3 is nearly modern despite having low ^3H. The adjusted radiocarbon age range for

Table 7. Radio-isotope data used to estimate groundwater ages at sites sampled during June 2011 in the Paradox Valley, Montrose County, Colo.

[Data from U.S. Geological Survey (2020a); Gardner and Newman (2023). Groundwater ages are in years before present. TU, tritium units; ^{3}H, tritium; ^{3}He, helium-3; ccSTP/g, cubic centimeters at standard temperature and pressure per gram of water; R/Ra, measured $^{3}He/^{4}He$ ratio to atmospheric $^{3}He/^{4}He$ ratio; ^{14}C, carbon-14; pmC, percent modern carbon; <, less than; >, greater than; —, not determined; pre-modern, groundwater recharged prior to nuclear weapons testing in the 1950s; modern, groundwater with adjusted ^{14}C ages less than zero]

Site number (table 3 and fig. 12)	Tritium (TU)	Tritiogenc helium-3 (TU)	Apparent $^{3}H/^{3}He$ age (years)	Terrigenic helium-4 (ccSTP/g)	R/Ra	Carbon-14 (pmC)	Unadjusted ^{14}C age (years)	Adjusted ^{14}C age (years)	Interpreted age range (years)
1	2.3	3.5	16	3.24E−09	1.06	65.6	3,400	modern	<20
2	0.1	—	pre-modern	2.90E−07	0.27	33.5	8,800	4,800–3,600	4,800–3,600
3	0.2	—	pre-modern	5.19E−09	1.02	62.5	3,800	modern	<1,000 and >60
4	1.0	—	mixture	9.61E−08	0.44	60.4	4,100	1,100–modern	mix (>1,000 + <60)
5	0.2	—	pre-modern	6.69E−07	0.08	25.8	10,900	6,900–3,500	6,900–3,500
6	3.1	1.9	8.6	1.10E−09	1.05	92.7	600	modern	<10
7	2.9	3.6	15	4.63E−09	1.03	89.4	900	modern	<20
8	—	—	—	2.11E−06	0.04	32.5	9,000	8,100–6,700	mix (>10,000 + <60)
9	—	—	—	1.31E−06	0.04	32.6	9,000	8,100–7,600	mix (>10,000 + <60)

site 4 is 1,100 years to modern, consistent with the hypothesis that this flowing well discharges a mixture of modern and pre-modern groundwater. Samples from sites 2 and 5 in upper Paradox Valley have adjusted radiocarbon ages of 4,800 to 3,600 and 6,900 to 3,400 years, respectively. The oldest adjusted radiocarbon ages are around 7,000 to 8,000 years for the brines from sites 8 and 9, respectively. Despite not being able to accurately confirm the age of the brine, the measured $^{4}He_{terr}$ of more than 1×10^{-6} ccSTP/g strongly indicates that these samples contain a fraction of much older water than is indicated by ^{14}C.

Groundwater with $^{4}He_{terr}$ of 1×10^{-6} ccSTP/g for a well in Rush Valley, Utah, had an associated ^{14}C activity of 2.2 pmC and adjusted radiocarbon ages of 32,000–22,000 years (Gardner and Kirby, 2011). Thomas and others (2003) report a total ^{4}He for Big Spring in Ash Meadows, Nevada, of 1.8×10^{-6} ccSTP/g. The reported ^{14}C activity at Big Spring was 2.2–3.0 pmC. Also, groundwater in the Snake Valley area of western Utah and eastern Nevada with $^{4}He_{terr}$ accumulations from 10^{-7} to 10^{-6} ccSTP/g typically have ^{14}C activities of less than 4 pmC and adjusted ^{14}C ages greater than 10,000 years (Gardner and Heilweil, 2014). It has been previously proposed that the near-surface brine in the vicinity of the Dolores River is a mixture of deeper salt-saturated brine with freshwater (Reclamation, 1978). The maximum reported TDS concentration in groundwater in the Paradox Valley was 365,900 mg/L from Jensen brine well #2 (original data available in Paschke and Mast [2024]). The concentration of dissolved solids in brine from the PVU pumping wells typically is about 258,000 mg/L (Reclamation, 1978). The lower concentration of the brine produced by the PVU well field (258,000 mg/L) relative to that of brine from Jensen brine well #2 (365,900 mg/L) implies that extracted brine is a mixture of less-saline water and saturated brine. However, the source of the freshwater to wells and how and where it mixes with saturated brine is not well characterized. The mixture previously postulated would require about 30 percent freshwater to dilute the saturated brine to the concentration of dissolved solids observed in brine at the PVU. Assuming that modern freshwater has little to no $^{4}He_{terr}$ and 100 pmC of ^{14}C and that the older, underlying brine has around 2.0×10^{-6} ccSTP/g of $^{4}He_{terr}$ and a ^{14}C activity of about 4 pmC, a 30:70 mixture of modern freshwater and old brine would also explain the incongruent ^{14}C and $^{4}He_{terr}$ measured at sites 8 and 9.

Interpreted Groundwater-Age Summary

A preliminary assessment of groundwater ages, such as this report, does not allow for a detailed assessment of the uncertainty associated with the age estimates. Factors related to this uncertainty include mixing of groundwater of different ages, imprecise knowledge of $^{4}He_{terr}$ production rates, unclear understanding of the chemical reactions affecting ^{14}C activity, and assumptions made about ^{14}C and $\delta^{13}C$ values of soil zone CO_2 and carbonate minerals that are available to react with dissolved inorganic carbon (Kalin, 2000). Focused age-related studies can resolve much of this uncertainty. However,

generalized patterns of groundwater age interpreted using multiple age-related tracers can still reveal key features of a groundwater-flow system.

The final column of table 7 lists interpreted age ranges for the nine groundwater samples as derived by Gardner and Newman (2023). These interpreted age ranges convey the relevant conclusions drawn from considering all age-related tracers analyzed in this study (^{3}H, $^{3}He_{trit}$, $^{4}He_{terr,}$ and ^{14}C) while acknowledging the associated uncertainty. Samples from sites 1, 6, and 7 are interpreted to be less than 20, less than 10, and less than 20 years old, respectively, based on their modern $^{3}H/^{3}He$ ages, R/R_a values approximately equal to 1, low $^{4}He_{terr}$, and ^{14}C activities of more than 65 pmC. These samples represent recent groundwater recharge to freshwater in the alluvial aquifer. Although the sample from site 3 has low ^{3}H, indicating that it is more than 60 years old, it is similar to the samples from sites 1, 6, and 7 with respect to R/R_a, $^{4}He_{terr}$, and ^{14}C, indicating that it is likely less than 1,000 years old. Samples from sites 2 and 5 are from wells located in the upper Paradox Valley and exhibit all the characteristics of relatively fresh water. Both samples have very low ^{3}H, low R/R_a, high $^{4}He_{terr}$, and low ^{14}C, and are interpreted to be several thousands of years old. The sample from site 4 is the flowing well interpreted to be a mixture of modern water (based on its ^{3}H content) with water that is thousands of years old based on its intermediate R/R_a and $^{4}He_{terr}$ similar to samples from sites 2 and 5. Lastly, based on very high values for $^{4}He_{terr}$, samples from sites 8 and 9 appear to contain primarily pre-modern water greater than 10,000 years old mixed with modern water less than 60 years old. The estimated age of pre-modern water for sites 8 and 9 suggests groundwater circulation during the Pleistocene as a source of recharge in the generation of brine.

Noble-Gas Recharge Temperatures

Dissolved noble-gas concentrations and noble-gas recharge temperatures (T_r) are presented for all freshwater samples in table 8. Measured gas concentrations were unreliable in brine samples from the PVU pumping wells because of excessive degassing of dissolved H_2S during sample collection. Because degassing strips the noble gases to a degree that prevents T_r calculations, the measured concentrations are presented in the table with the caveat that they represent minimum concentrations.

The range of possible T_r values calculated for the seven freshwater sites is shown in figure 22. In figure 22, the left and right points for each sample represent the minimum (T_{rmin}) and maximum (T_{rmax}) temperatures, respectively. Because T_r represents the temperature of the water table at the location of recharge, the values are compared to valley water-table temperatures to examine whether the samples appear to be mountain or valley recharge. Measured groundwater temperatures from six of the valley wells, assumed to represent the water-table temperature, ranged from 11.6 to 16.9 °C with an average value of 14.1 °C (fig. 22). The water temperatures from sample sites 1 and 7 (both 8.0 °C) were excluded from this group. Site 1 is a spring in the uplands at an altitude about 1,575–2,200 ft higher than sample sites in the valley. The anomalously cool water temperature of the sample from site 7 likely resulted from infiltration of surface water from nearby West Paradox Creek.

Minimum dissolved-gas recharge temperatures (T_{rmin}) range from 0 (near freezing) to 6.8 °C, and maximum dissolved-gas recharge temperatures (T_{rmax}) range from 2.1 to 10.0 °C (table 8). All T_r values are clearly cooler than the range of measured valley water-table temperatures (fig. 22). In fact, the average recharge temperature (T_{ravg}), which is derived using a median altitude for the basin and is likely closer to the true T_r than T_{rmin} or T_{rmax}, is less than 8.0 °C, the measured water temperature of Willow Basin Creek Spring (site 1), which certainly contains 100 percent upland recharge. These data provide another line of evidence to support a conceptual model in which the source of present-day recharge to the freshwater system northwest of the Dolores River is from snowmelt plausibly from the mountains or uplands northwest of the valley or from the San Juan Mountains where the Dolores River originates. Sites 6 and 7 have the coolest T_r of any samples, and as previously discussed, are thought to reflect recharge from surface water derived from high-altitude snowmelt outside the valley.

Conceptual Model of Groundwater Occurrence and Brine Discharge in the Paradox Valley

The hydrogeologic data provided herein—along with the most recent loading analysis for the Dolores River in the Paradox Valley (Mast, 2017; Heywood and others, 2024a; 2024b) and the conceptual model for brine discharge to the river developed by Mast and Terry (2019)—are used to present a conceptual model of groundwater occurrence in the Paradox Valley at three different scales. On a basin-wide scale, hydrogeology of the Paradox Valley can be conceptualized as an unconfined aquifer in alluvial deposits containing mostly modern recharge underlain by a pre-modern brine more than 10,000 years old that occurs in the brecciated cap rock and underlying salt deposits of the Paradox Formation. At the near-river scale of groundwater-surface-water interaction, seasonal variations in the stage of the Dolores River control brine discharge to the river both annually and interannually (Mast and

Table 8. Dissolved noble-gas and recharge-temperature data for groundwater samples collected during June 2011 in the Paradox Valley, Montrose County, Colo.

[Data from U.S. Geological Survey (2020a);°C, degrees Celsius; ccSTP/g, cubic centimeters at standard temperature and pressure per gram of water; —, not determined]

Site number (table 3 and fig. 12)	Water temperature (°C)	Neon (^{20}Ne) (ccSTP/g)	Argon (^{40}Ar) (ccSTP/g)	Krypton (^{84}Kr) (ccSTP/g)	Xenon (^{129}Xe) (ccSTP/g)	Helium (^{4}He) (ccSTP/g)	Noble gas recharge temperature range (T_r) (°C)
1	8.0	1.41E−07	3.22E−04	4.38E−08	2.86E−09	3.92E−08	4.7 to 7.2
2	13.9	2.09E−07	3.64E−04	4.97E−08	3.20E−09	3.46E−07	2.2 to 7
3	12.9	1.76E−07	3.77E−04	4.65E−08	2.98E−09	5.03E−08	6.8 to 9.8
4	12.8	1.82E−07	3.56E−04	4.57E−08	3.12E−09	1.43E−07	3.8 to 8.4
5	—	1.78E−07	3.25E−04	4.37E−08	2.93E−09	7.16E−07	4.3 to 10
6	11.6	2.28E−07	4.15E−04	5.19E−08	3.66E−09	5.84E−08	0.2 to 5.1
7	8.0	1.90E−07	4.17E−04	5.69E−08	3.97E−09	5.15E−08	0 to 2.1
[1]8	16.4	2.64E−08	1.20E−04	3.29E−08	2.74E−09	2.15E−06	—
[1]9	16.9	1.60E−08	9.51E−05	2.72E−08	2.52E−09	1.31E−06	—

[1]Because of excessive degassing of dissolved hydrogen sulfide, noble-gas concentration may be unreliable. These values represent minimum concentrations.

Terry, 2019). At the finest scale, diurnal fluctuations in river stage drive exchange of freshwater with saltier pore water in the hyporheic zone, which appears to enhance brine discharge to the river during the winter (Mast and Terry, 2019).

Basin wide, groundwater occurrence in the Paradox Valley can be considered as two primary end members: (1) an unconfined aquifer in alluvial deposits containing components of recently recharged freshwater; and (2) an underlying dense sodium-chloride brine more than 10,000 years old that occurs in the brecciated cap rock and underlying salt deposits of the Paradox Formation. The alluvial aquifer is most extensive along the Dolores River and West Paradox Creek in the northwest half of the valley, where groundwater in saturated parts of the aquifer generally flows from northwest to southeast toward the Dolores River. The alluvial aquifer ranges from 50 to 100 ft in thickness near the river based on well logs for the pumping wells and is thickest, up to 170 feet in depth, near the center of the Paradox Valley in a collapse breccia feature. Hydraulic conductivity of the alluvial aquifer, determined from aquifer tests at the PVU, ranged from 23.1 to 47.0 ft/d and from 14.9 to 330 ft/d for the Boulton and Theis pumping-test analysis methods, respectively, consistent with previous estimates. Infiltration of surface water is a primary source of recharge to the alluvial aquifer. West Paradox Creek, which originates in the La Sal Mountains, transmits natural snowmelt runoff from the mountains as well as irrigation water from Buckeye Reservoir to the Paradox Valley. West Paradox Creek loses water to the alluvial aquifer as it flows southwest toward its confluence with the Dolores River as evidenced by water-table maps (fig. 12) and modern groundwater ages observed in wells adjacent to the creek. The Dolores River is a source of recharge during periods of high stage during spring snowmelt runoff.

Groundwater composition in the alluvial aquifer evolves in a downgradient direction from the northwest part of the valley with TDS concentrations and groundwater age increasing in a downgradient direction. Groundwater discharging from a spring in the most upgradient (northwest) part of valley represents recently recharged water, which exhibited TDS concentrations less than 500 mg/L, was characterized as a calcium-magnesium-bicarbonate type water and had an estimated groundwater age of 16 years. As groundwater in the alluvial aquifer moves downgradient toward the southeast, TDS concentrations increase substantially, water types shift to calcium-magnesium-sulfate, and groundwater ages of thousands of years are indicated. Calcium-magnesium-sulfate type waters are found throughout a large part of the valley in the alluvial aquifer. The replacement of bicarbonate with sulfate as the primary anion may indicate that groundwater is dissolving sulfate-bearing evaporite minerals (anhydrite and gypsum) as it flows down valley, or the alluvial groundwater is mixing with older water that was in contact with sulfate-bearing evaporite minerals from the underlying cap rock. Concentrations of TDS and groundwater-age tracers in downgradient parts of the alluvial aquifer indicate mixtures of modern groundwater with substantially older groundwater. At sample site 4, upward flow from the underlying brine is indicated by artesian well conditions, and $^{4}He_{terr}$ concentrations indicate that groundwater contains a substantial fraction of water that is thousands of years old. Shallow groundwater farthest downgradient—near the confluence of West Paradox Creek and the Dolores River—has TDS concentrations of about 800–900 mg/L and exhibits groundwater ages on the order of 20 years likely as the result from infiltration of surface water from nearby West Paradox Creek. Alluvial aquifer water-table fluctuation and groundwater discharge to the Dolores River exhibit seasonal cycles affected by seasonal snow-melt runoff and river stage.

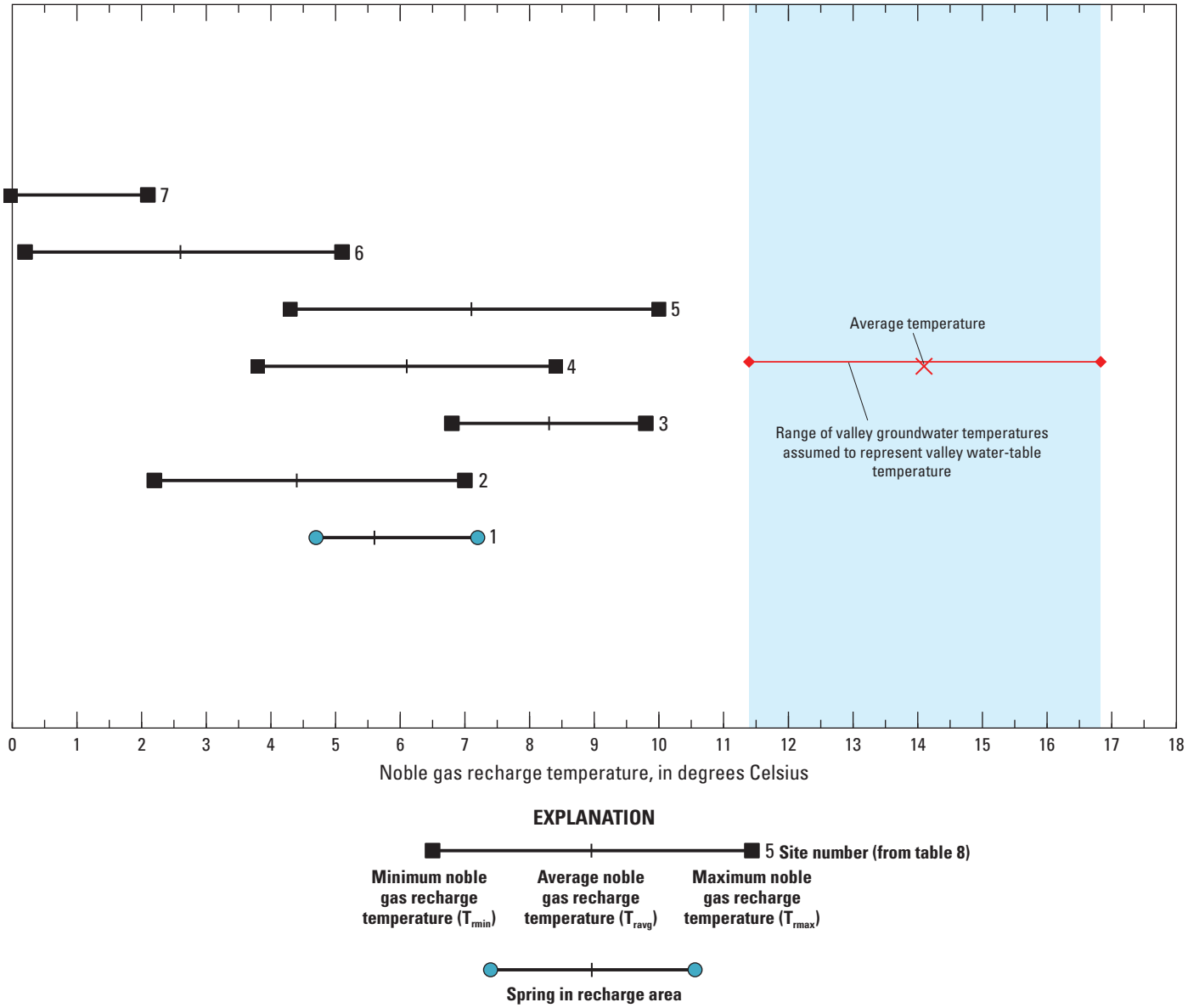

Figure 22. Noble-gas recharge temperature of groundwater samples collected during June 2011 in the Paradox Valley, Montrose County, Colo. (Gardner and Newman, 2023).

The cap rock and collapse breccia at the top of the Paradox Formation are near the land surface in the Paradox Valley and contain a sodium-chloride saturated dense brine that is much older than all other groundwater sampled during this study. Density-dependent gradients in the brine support upward flow toward the Dolores River, and freshwater from both the alluvial aquifer and brine discharge to the river. As the Dolores River crosses the Paradox Valley, it gains salinity, or TDS, from discharge of the brine. To mitigate brine discharge and reduce TDS concentrations in the Dolores River, Reclamation operates the PVU, which extracts brine from nine pumping wells adjacent to river. The pumped brine is piped to a deep injection well for disposal about 3 miles southwest of the Paradox Valley.

A valley wide AEM survey from 2011 lends insight to the extent and distribution of brine in the upper 985 ft beneath the valley floor (Ball and others, 2015; 2020), and geophysical and hydrologic observations along the Dolores River (Mast and Terry, 2019) have informed understanding of brine discharge to the river. Based on drilling records and the AEM survey, a prominent collapse feature filled with brecciated salt and alluvial sediments is observed beneath the center of the valley and this feature provides hydraulic connection between the brine in the cap rock and the surrounding alluvial aquifer. Spatial patterns of the freshwater-brine interface indicate that the brine is nearest to land surface along the river and southeast of the river (Ball and others, 2020), where the occurrence of shale bedrock may be a vertical impermeable

barrier to groundwater flow (Konikow and Bedinger, 1978). Specific-conductance measurements in the river indicate brine discharges to the river upstream and downstream from the PVU (Mast and Terry, 2019) such that the PVU pumping wells do not intercept all the brine flowing toward the river.

Total dissolved solids concentration of the brine is about 366,000 mg/L based on data from Jensen brine well #2 (Paschke and Mast, 2024), and the heavy brine density creates upward hydraulic gradients, which drive upward and lateral flow of brine toward the river. As the topographic low area in the Paradox Valley, the Dolores River is incised into the near-surface cap rock and forms a natural discharge area for the brine (fig. 11). The brine mixes with freshwater at the base of the alluvial aquifer reducing TDS concentrations to around 258 g/L in the vicinity of the PVU pumping wells (Reclamation, 1978). Groundwater samples of brine from two PVU pumping wells appear to contain about 30 percent modern water, likely from the freshwater system, mixed with about 70 percent pre-modern water that is likely more than 10,000 years old based on its very high values for $^{4}He_{terr}$. The origin and occurrence of brine including the relation between the brine and present-day sources of recharge are not completely understood because of a lack of hydrologic monitoring data from the cap rock and underlying salt. Groundwater-age dating results for the brine suggest that it was recharged more than 10,000 years ago during the Pleistocene (table 4) likely in response to erosion and groundwater circulation associated with regional glaciation and increased flows in the ancestral Dolores River during later stages of the Paradox Valley development. (Cater and Craig, 1970; Gutiérrez, 2004).

At the near-river scale of groundwater-surface-water interaction, geologic features as well as seasonal changes in river stage and saturated thickness of the alluvial aquifer control the discharge of brine to the Dolores River. Groundwater in the alluvial aquifer forms a freshwater lens on top of the brine, and both freshwater and brine discharge to the Dolores River at the low point in the valley. Upward gradients from the brine to the alluvial aquifer, as well as the greater K of the alluvial aquifer and collapse breccia in the center of valley, provide a hydraulic connection between the brine and the freshwater alluvial aquifer. River stage varies seasonally in response to the annual cycle of spring snowmelt runoff and winter low-flow (base flow) conditions, and this variation in river stage affects thickness of the freshwater lens in the alluvial aquifer as well as brine discharge (Mast and Terry, 2019). River stage is highest, and the freshwater layer is thickest, during spring and summer high-flow conditions, when the brine can be depressed as much as 7 ft below the riverbed, and brine discharge is reduced to a minimum (Mast and Terry, 2019). When the river stage is lower during fall and winter low-flow conditions, the freshwater layer thins, the freshwater-brine interface rises closer to the land surface, and brine discharge is enhanced (Mast and Terry, 2019). These results indicate that, during the high-flow spring snowmelt runoff period when brine discharge is naturally minimized, brine extraction from the PVU pumping wells does not substantially affect salinity in the Dolores River. Brine discharge to the river is greatest during the winter low-flow months, with as much as 70 percent of the annual salinity gain occurring from December through March (Mast and Terry, 2019). Winter increases in brine discharge likely result from declining river stage and saturated thickness of the freshwater lens which causes the freshwater-brine interface to move closer to the riverbed (Mast and Terry, 2019). In addition, large diurnal fluctuations of SC are observed in response to diurnal river-stage fluctuations (Mast and Terry, 2019). These fluctuations may be caused by freezing and thawing of the river upstream from and within the Paradox Valley and are contemporaneous with periods of increased brine discharge (Mast and Terry, 2019). These observations indicate that, at the finest scale, diurnal fluctuations in river stage caused by daily winter freeze-thaw cycles cause exchange of freshwater with saltier pore water in the hyporheic zone, which appears to enhance salt flux to the river during winter months (Mast and Terry, 2019).

Summary

Salinity, or total dissolved solids (TDS), in the Colorado River Basin is a major concern in southwestern United States where the river provides water to about 40 million people for municipal and industrial use and is used to irrigate about 5.5 million acres of land. Much of the salinity in the Upper Colorado River Basin is derived from surface water and groundwater interactions with various geologic materials (rocks, soils, and alluvial deposits). The Dolores River is a major tributary of the Colorado River that historically accounts for about 6 percent of the TDS load to the Colorado River. The primary source of salinity to the Dolores River is the Paradox Valley, where discharge of brine from the underlying salt deposits increases TDS concentrations in the river as it flows across the valley. The Paradox Valley, one of several salt-anticline valleys in the region, is a fault-bounded topographic basin aligned with and exposing an underlying salt-anticline core. Salt deposits in the Pennsylvanian Paradox Formation of the Hermosa Group form an elongated salt diapir oriented northwest to southeast that is up to 12,000 feet (ft) thick beneath the present valley floor. Surface erosion, groundwater circulation, and weathering during Tertiary and Quaternary valley formation contributed to development of a cap rock, collapse features, breccia, and brine at the top of the exposed salt diapir. Today (2023), brine occurring in the brecciated cap rock and underlying salt deposits is in hydraulic connection with a freshwater alluvial aquifer and the Dolores River, discharges to the river, and causes the observed increase in TDS as the river crosses the Paradox Valley.

To reduce TDS concentrations in the Dolores River, the Bureau of Reclamation (Reclamation) operates the Paradox Valley Unit (PVU). The PVU consists of nine pumping wells located adjacent to the river along its southeast banks.

When operational, brine is withdrawn from the pumping wells, collected, and piped to a deep-injection disposal well about 3 miles southwest of the PVU. The PVU became fully operational July 1, 1996, and by 2015, the PVU had reduced brine discharge to the Dolores River by as much as 70 percent compared to pre-PVU conditions. In response to a 4.5 magnitude earthquake, injection operations, and thus PVU pumping, were suspended from March 2019 to June 2022. A trial period of operation began in June 2022 with a reduced injection rate, and thus PVU pumping rate, of about two-thirds capacity to gather additional information and guide future operational decisions.

This report, prepared in cooperation with Reclamation, presents results from U.S. Geological Survey (USGS) investigations and provides the current (2023) understanding of groundwater and brine occurrence and discharge to the Dolores River in the Paradox Valley. Water-quality and groundwater-level data, maps, and geographic information systems datasets were compiled from existing data including generalized maps of the base of the alluvial aquifer, the top of the salt in the Paradox Formation, and the extent and altitude of the alluvial-aquifer water table. In June 2011, groundwater-quality samples were collected from springs, domestic and irrigation wells, and PVU pumping wells in the valley, and the samples were analyzed for a suite of groundwater-age tracers and other constituents to lend insight to general water quality as well as groundwater age, recharge, and occurrence in the valley. In 2013, the USGS measured groundwater levels in PVU pumping and observation wells as a large-scale aquifer pumping test, and the results, which were analyzed in 2020, are presented as estimates of alluvial-aquifer hydraulic conductivity. The hydrogeologic data provided herein, along with the most recent loading analysis for the Dolores River in the Paradox Valley, and a previous conceptual model for brine discharge to the river, are used to present a conceptual model of groundwater occurrence in the Paradox Valley at three different scales – a basin-wide hydrogeologic setting, near-river groundwater-surface-water interaction, and fine-scale hyporheic zone flow.

On a basin-wide scale, hydrogeology of the Paradox Valley can be conceptualized as an unconfined aquifer in alluvial deposits, containing components of recent recharge, underlain by a pre-modern brine more than 10,000 years old that occurs in the brecciated cap rock and underlying salt deposits of the Paradox Formation. Groundwater in the alluvial aquifer forms a freshwater lens on top of the brine, primarily in the northwest part of the valley, and both freshwater and brine discharge to the Dolores River at the low point in the valley. Infiltration of surface water from West Paradox Creek, which originates as snow-melt runoff in the La Sal Mountains, is a primary source of recharge to the alluvial aquifer as evidenced by water-table maps and mixed groundwater ages observed in wells adjacent to the creek. Groundwater flow in the alluvial aquifer is generally from the northwest part of the valley to the southeast and the Dolores River. The cap rock and collapse breccia at the top of the Paradox Formation are near the land surface in the Paradox Valley and contain a sodium-chloride saturated dense brine that is much older than all other groundwater sampled during this study. The heavy brine density creates upward hydraulic gradients, which drive upward and lateral flow of brine into the base of the alluvial aquifer and the Dolores River. Based on drilling records and an aerial electromagnetic survey, a prominent collapse feature filled with breccia is observed beneath the center of the valley and this feature provides hydraulic connection between the brine in the cap rock and the surrounding alluvial aquifer. Groundwater samples of brine from two PVU pumping wells appear to contain about 30 percent modern water, likely from the freshwater system, mixed with about 70 percent pre-modern water. Based on very high values for $^{4}He_{terr}$ measured for these wells, the pre-modern component is likely more than 10,000 years old. The origin and occurrence of brine including the relation between the brine and present-day sources of recharge are not completely understood because of a lack of hydrologic monitoring data from the cap rock and underlying salt. Groundwater-age dating results indicate that the brine received recharge and developed during the Pleistocene likely during later stages of the Paradox Valley development.

At the near-river scale of groundwater-surface-water interaction, geologic features as well as seasonal changes in river stage and saturated thickness of the alluvial aquifer control the discharge of brine to the Dolores River. River stage varies seasonally in response to the annual cycle of spring snowmelt runoff and winter low-flow (base flow) conditions, and this variation in river stage affects thickness of the freshwater lens in the alluvial aquifer as well as brine discharge. River stage is highest, and the freshwater layer is thickest, during spring and summer high-flow conditions, when the brine can be depressed as much as 7 ft below the riverbed, and brine discharge is reduced to a minimum. When the river stage is lower during fall and winter low-flow conditions, the freshwater layer thins, the freshwater-brine interface rises closer to the land surface, and brine discharge increases. These results indicate that, during the high-flow spring snowmelt runoff period when brine discharge is naturally minimized, brine extraction from the PVU pumping wells does not substantially affect salinity in the Dolores River. During winter low-flow winter conditions, spatial patterns of the freshwater-brine interface indicate that brine discharges to the river upstream and downstream from the PVU such that the PVU does not intercept all the brine flowing toward the river.

At the finest scale, baseflow and hyporheic zone flow affect TDS loading during low-flow conditions. Brine discharge to the river is greatest during the winter low-flow months, with as much as 70 percent of the annual TDS gain occurring from December through March. Winter increases in brine discharge likely result from declining river stage and saturated thickness of the freshwater lens, which causes the freshwater-brine interface to move closer to the riverbed. In addition, large diurnal fluctuations of specific conductance are observed in response to diurnal river-stage fluctuations. These fluctuations may be caused by freezing and thawing of

the river upstream from and within the Paradox Valley and are contemporaneous with periods of increased brine discharge. These observations indicate that, at the finest scale, diurnal fluctuations in river stage caused by daily winter freeze-thaw cycles cause exchange of freshwater with saltier pore water in the hyporheic zone, which appears to enhance salt flux to the river during winter months.

References Cited

Bakhos, T., Cardiff, M., Barrash, W., and Kitanidis, P.K., 2014, Data processing for oscillatory pumping tests: Journal of Hydrology, v. 511, p. 310–319, accessed December 17, 2020, at https://doi.org/10.1016/j.jhydrol.2014.01.007.

Bakker, M., and Schaars, F., 2019, Solving groundwater flow problems with time series analysis—You may not even need another model: Groundwater, v. 57, no. 6, p. 826–833, accessed December 17, 2020, at https://doi.org/10.1111/gwat.12927.

Ball, L.B., Bedrosian, P.A., and Minsley, B.J., 2020, High-resolution mapping of the freshwater–brine interface using deterministic and Bayesian inversion of airborne electromagnetic data at Paradox Valley, USA: Hydrogeology Journal, v. 28, p. 941–954, accessed December 17, 2020, at https://doi.org/10.1007/s10040-019-02102-z.

Ball, L.B., Bloss, B.R., Bedrosian, P.A., Grauch, V.J.S., and Smith, B.D., 2015, Airborne electromagnetic and magnetic survey data of the Paradox and San Luis Valleys, Colorado: U.S. Geological Survey Open-File Report 2015–1024, 19 p., accessed December 17, 2020, at https://doi.org/10.3133/ofr20151024.

Bear, Jacob, 1972, Dynamics of fluids in porous media: American Elsevier Publishing Company, Inc., New York, 764 p.

Bear, Jacob, 1979, Hydraulics of groundwater: Dover Publications, Inc., Mineola, New York, 569 p.

Bear, Jacob, and Dagan, Gedeon, 1964a, Some exact solutions of interface problems by means of the hodograph method: Journal of Geophysical Research, v. 69, no. 8, p. 1563–1572, accessed December 17, 2020, at https://doi.org/10.1029/JZ069i008p01563.

Bear, Jacob, and Dagan, Gedeon, 1964b, Moving interface in coastal aquifers: Proceedings of American Society of Civil Engineers, v. 99, p. 193–215.

Baars, D.L., and Doelling, H.H., 1987, Moab salt-intruded anticline, east-central Utah; Geological Society of America Centennial Field Guide, Rocky Mountain Section, 1987, 6 p.

Block, L.V., Wood, C.K., Yeck, W.L., and King, V.M., 2015, Induced seismicity constraints on subsurface geological structure, Paradox Valley, Colorado: Geophysical Journal International, v. 200, no. 2, p. 1172–1195, accessed December 17, 2020, at https://doi.org/10.1093/gji/ggu459.

Boulton, N.S., 1963, Analysis of data from non-equilibrium pumping tests allowing for delayed yield from storage: Proceedings of the Institution of Civil Engineers, v. 26, no. 3, p. 469–482, accessed December 17, 2020, at https://doi.org/10.1680/iicep.1963.10409.

Bouwer, H., and Rice, R.C., 1976, A slug test for determining hydraulic conductivity of unconfined aquifers with completely or partially penetrating wells: Water Resources Research, v. 12, no. 3, p. 423–428. [Also available at https://doi.org/10.1029/WR012i003p00423.]

Bureau of Reclamation, [Reclamation], 1978, Paradox Valley Unit—Definite plan report: Bureau of Reclamation, Colorado River Basin Salinity Control Project, accessed November 12, 2020, at https://www.usbr.gov/uc/progact/paradox/docs/DPR-1978.pdf.

Bureau of Reclamation, [Reclamation], 2020, Colorado River Basin Salinity Control Program—Paradox Valley Unit: Bureau of Reclamation, Interior Region 7, Upper Colorado Basin, accessed November 17, 2020, at http://www.usbr.gov/uc/progact/salinity/index.html.

Bureau of Reclamation, [Reclamation], 2022, Paradox Valley Unit website: Bureau of Reclamation, Upper Colorado Basin, Interior Region 7, Upper Colorado Basin, accessed June 7, 2022, at https://www.usbr.gov/uc/progact/paradox/index.html.

Butler, J.J., 1997, The design, performance, and analysis of slug tests: Boca Raton, Fla., Lewis Publishers, 250 p., accessed November 17, 2020, at https://doi.org/10.1201/9781482229370.

Carter, W.D., and Gualtieri, J.L., 1957, Geologic map of the Mount Peale 1 SE quadrangle, Montrose County, Colorado, and San Juan County, Utah: U.S. Geological Survey Miscellaneous Field Studies Map MF–123, scale 1:24,000.

Carter, W.D., and Gualtieri, J.L., 1965, Geology and uranium-vanadium deposits of the La Sal quadrangle, San Juan County, Utah, and Montrose County, Colorado: U.S. Geological Survey, Professional Paper 508, 82 p.

Carter, W.D., Gualtieri, J.L., and Shoemaker, E.M., 1958, Preliminary geologic map of the Mount Peale 1 NE quadrangle, San Juan County, Utah, and Montrose County, Colorado: U.S. Geological Survey, Mineral Investigations Field Studies Map MF–139, scale 1:24,000.

Cater, F.W., Jr., 1954, Geology of the Bull Canyon quadrangle, Colorado: U.S. Geological Survey Quadrangle Map GQ–33, scale 1:24,000.

Cater, F.W., Jr., 1955a, Geology of the Davis Mesa quadrangle, Colorado: U.S. Geological Survey Quadrangle Map GQ–71, scale 1:24,000.

Cater, F.W., Jr., 1955b, Geology of the Naturita NW quadrangle, Colorado: U.S. Geological Survey Quadrangle Map GQ–65, scale 1:24,000.

Cater, F.W., Jr., 1955c, Geology of the Anderson Mesa quadrangle, Colorado: U.S. Geological Survey Quadrangle Map GQ–77, scale 1:24,000.

Cater, F.W., Jr., Butler, A.P., Jr., and McKay, E.J., 1955, Geology of the Uravan quadrangle, Colorado: U.S. Geological Survey Quadrangle Map GQ–78, scale 1:24,000.

Cater, F.W., and Craig, L.C., 1970, Geology of the salt anticline region in southwestern Colorado: U.S. Geological Survey Professional Paper 637, 80 p., 2 plates, accessed November 17, 2020, at https://doi.org/10.3133/pp637.

Clark, I.D., and Fritz, P., 1997, Environmental isotopes in hydrogeology: New York, CRC Press, 318 p.

Cohen, K.M., Finney, S.C., Gibbard, P.L., and Fan, J.-X., 2013; updated: The ICS International Chronostratigraphic Chart. Episodes 36: 199-204, accessed April 9, 2023, at http://www.stratigraphy.org/ICSchart/ChronostratChart2020-03.pdf.

Collenteur, R.A., Bakker, M., Caljé, R., Klop, S.A., and Schaars, F., 2019, Pastas—Open source software for the analysis of groundwater time series: Groundwater, v. 57, no. 6, p. 877–885, accessed December 17, 2020, at https://doi.org/10.1111/gwat.12925.

Colorado's Decision Support System, 2020, Colorado's Decision Support Systems data and tools: Colorado Water Conservation Board, Division of Water Resources, accessed December 17, 2020, at https://dwr.state.co.us/Tools/Home.

Colorado Department of Public Health and Environment, 2020, Colorado Department of Public Health and Environment: Denver, Colo. Colorado Department of Public Health and Environment, accessed December 17, 2020, at https://cdphe.colorado.gov/.

Colorado Oil and Gas Conservation Commission, 2020, Colorado Oil and Gas Conservation Commission: Denver, Colo., Colorado Oil and Gas Conservation Commission, accessed December 17, 2020, at https://cogcc.state.co.us/#/home.

Craig, H., 1961, Isotopic variations in meteoric waters: Science, v. 133, p. 1702–1703.

Dagan, Gedeon, and Bear, Jacob, 1968, Solving the problem of local interface upconing in a coastal aquifer by the method of small perturbations: Journal of Hydraulic Research, v. 6, no. 1, p. 15–44, accessed December 17, 2020, at https://doi.org/10.1080/00221686809500218.

Day, W.C., Green, G.N., Knepper, D.H., Jr., and Phillips, R.C., 1999, Spatial geologic data model for the Gunnison, Grand Mesa, Uncompaghre National Forests mineral resource assessment area, southwestern Colorado and digital data for the Leadville, Montrose, Durango, and Colorado parts of the Grand Junction, Moab, and Cortez 1° × 2° geologic maps: U.S. Geological Survey Open-File Report 99–427, variously paged.

Denlinger, R.P., and O'Connell, D.R.H., 2020, Evolution of faulting induced by deep fluid injection, Paradox Valley, Colorado: Bulletin of the Seismological Society of America, v. 110, no. 5, p. 2308–2327, accessed December 17, 2020, at https://doi.org/10.1785/0120190328.

Doelling, H.H., 2002, Geologic map of the Moab and eastern part of the San Rafael Desert 30' × 60' quadrangles, Grand and Emery Counties, Utah, and Mesa County, Colorado: Utah Geological Survey Geologic Map 180, scale 1:100,000, 3 sheets.

Doelling, H.H., 2004, Geologic map of the La Sal 30' × 60' quadrangle, San Juan, Wayne, and Garfield Counties, Utah, and Montrose and San Miguel Counties, Colorado: Utah Geological Survey Geologic Map 205, scale 1:100,000, 2 sheets.

Duffield, G.M., 2007, AQTESOLV for Windows version 4.5 user's guide: Reston, Va., HydroSOLVE, Inc., 529 p., accessed December 17, 2020, at https://hwbdocuments.env.nm.gov/Los%20Alamos%20National%20Labs/General/37764.pdf.

Elston, D.P., and Shoemaker, E.M., 1961, Preliminary structure contour map on top of salt in the Paradox Formation of the Hermosa Group in the salt anticline region, Colorado and Utah: U.S. Geological Survey Oil and Gas Investigations Map OM 209, scale 1:250,000.

Epis, R.C., Scott, G.R., Taylor, R.B., and Chapin, C.E., 1980, Summary of Cenozoic geomorphic, volcanic and tectonic features of central Colorado and adjoining areas in Kent, H.C. and Porter, K.W., eds., ColoradoGeology, Rocky Mountain Association of Geologists 1980 Symposium, Denver, CO, p. 135-156.

Esri, 1999–2009, ArcMap Version 10.3, accessed December 17, 2020, at https://www.esri.com/en-us/home.

Fenneman, N.M., 1931, Physiography of western United States: New York, McGraw-Hill Book Co., 534 p.

Fishman, M.J., and Friedman, L.C., 1989, Methods for determination of inorganic substances in water and fluvial sediments: U.S. Geological Survey Techniques of Water-Resources Investigations 05–A1, accessed December 17, 2020, at https://doi.org/10.3133/twri05A1.

Fontes, J.C., and Garnier, J.M., 1979, Determination of initial 14C activity of the total dissolved carbon—A review of existing models and a new approach: Water Resources Research, v. 5, no. 2, p. 399–413, accessed December 17, 2020, at https://doi.org/10.1029/WR015i002p00399.

Freethey, G.W., and Cordy, G.E., 1991, Geohydrology of Mesozoic rocks in the upper Colorado River basin in Arizona, Colorado, New Mexico, Utah, and Wyoming, excluding the San Juan Basin: U.S. Geological Survey Professional Paper 1411–C, 118 p., 6 plates, accessed December 17, 2020, at https://doi.org/10.3133/pp1411C.

Freeze, R.A., and Cherry, J.A., 1979, Groundwater: Prentice Hall, Inc., 604 p.

Garcia, C.A., Halford, K.J., and Fenelon, J.M., 2013, Detecting drawdowns masked by environmental stresses with water-level models: Groundwater, v. 51, no. 3, p. 322–332, accessed December 17, 2020, at https://doi.org/10.1111/gwat.12042.

Gardner, P.M., 2004, Environmental tracer investigation of groundwater conditions at the Scott M. Matheson Wetland Preserve near Moab, Utah: Salt Lake City, University of Utah, master's thesis, 160 p.

Gardner, P.M., and Heilweil, V.M., 2014, A multiple-tracer approach to understanding regional groundwater flow in the Snake Valley area of the eastern Great Basin, USA: Applied Geochemistry, v. 45, p., 33–49, accessed September 29, 2023, at https://doi.org/10.1016/j.apgeochem.2014.02.010.

Gardner, P.M., and Kirby, S.M., 2011, Hydrogeologic and geochemical characterization of groundwater resources in Rush Valley, Tooele County, Utah: U.S. Geological Survey Scientific Investigations Report 2011–5068, 68 p., accessed December 17, 2020, at https://doi.org/10.3133/sir20115068.

Gardner, P.M., and Newman, C.P., 2023, Recharge temperatures and groundwater-age models for the Paradox Valley alluvial aquifer, 2011, Colorado: U.S. Geological Survey data release, accessed February 7, 2023, at https://doi.org/10.5066/P9FMWX2J.

Gardner, P.M., and Solomon, D.K., 2009, An advanced passive diffusion sampler for the determination of dissolved gas concentrations: Water Resources Research, v. 45, 12 p.

Geldon, A.L., 2003a, Geology of Paleozoic rocks in the upper Colorado River basin in Arizona, Colorado, New Mexico, Utah, and Wyoming, excluding the San Juan Basin: U.S. Geological Survey Professional Paper 1411–A, 85 p., 17 plates, accessed December 17, 2020, at https://doi.org/10.3133/pp1411A.

Geldon, A.L., 2003b, Hydrologic properties and groundwater flow systems of the Paleozoic rocks in the upper Colorado River basin in Arizona, Colorado, New Mexico, Utah, and Wyoming, excluding the San Juan Basin: U.S. Geological Survey Professional Paper 1411–B, 153 p., 13 plates, accessed December 17, 2020, at https://doi.org/10.3133/pp1411B.

Geological Associates, 2007, Final report shallow seismic survey Piñon Ridge Project, Montrose County, Colorado: Albuquerque, N. Mex., Geological Associates, 12 p.

Golder Associates Inc., 2008a, Evaporation pond design report Piñon Ridge project, Montrose County, Colorado: Golder Associates Inc., Lakewood, Colo., 183 p.

Golder Associates Inc., 2008b, Phase 3 long-term pumping tests data report Piñon Ridge Project, Montrose County, Colorado: Golder Associates Inc., Lakewood, Colo., 131 p.

Golder Associates Inc., 2009, Hydrogeologic report Piñon Ridge Project, Montrose County, Colorado: Golder Associates Inc., Lakewood, Colo., 39 p.

Guo, Weixing, and Langevin, C.D., 2002, User's guide to SEAWAT—A computer program for simulation of three-dimensional variable-density ground-water flow: U.S. Geological Survey Techniques of Water-Resources Investigations, book 6, chap. A7, 77 p., accessed March 30, 2023, at https://fl.water.usgs.gov/PDF_files/twri_6_A7_guo_langevin.pdf.

Gutiérrez, F., 2004, Origin of the salt valleys in the Canyonlands section of the Colorado Plateau—Evaporite-dissolution collapse versus tectonic subsidence: Geomorphology v. 57, no. 3–4, p. 423–435, accessed December 17, 2020, at https://doi.org/10.1016/S0169-555X(03)00186-7.

Hart, R., Nelson, S.T., and Eggett, D., 2010, Uncertainty in ^{14}C model ages of saturated zone waters—The influence of soil gas in terranes dominated by C_3 plants: Journal of Hydrology, v. 392, no. 1–2, p. 83–95, accessed December 17, 2020, at https://doi.org/10.1016/j.jhydrol.2010.08.001.

Heywood, C.E., Mast, M.A., and Paschke, S.S., 2024a, MODFLOW-6 model of variable-density groundwater flow and brine discharge to the Dolores River in Paradox Valley, Colorado: U.S. Geological Survey data release, at https://doi.org/10.5066/P9ZW0FH5.

Heywood, C.E., Paschke, S.S., Mast, M.A., and Watts, K.R., 2024b, Simulation of groundwater flow and brine discharge to the Dolores River in Paradox Valley, Montrose County, Colorado: U.S. Geological Survey Scientific Investigations Report 2024–5038, 44 p., https://doi.org/10.3133/sir20245038.

Hite, R.J., and Lohman, S.W., 1973, Geologic appraisal of Paradox basin salt deposits for waste emplacement: U.S. Geological Survey Open-File Report 73–114, 75 p.

Horita, J., 2005, Saline water, chap. 17 *of* Aggarwal, P.K., Gat, J.R., and Froehlich, K.F., eds., Isotopes in the water cycle—Past, present and future of a developing science: Springer, 381 p.

Hubbert, M.K., 1953, Entrapment of petroleum under hydrodynamic conditions: American Association of Petroleum Geologists Bulletin v. 37, no. 8, p. 1954–2026.

Hunt, B., and Scott, D., 2005, Extension of Hantush and Boulton solutions: Journal of Hydrologic Engineering, v. 10, no. 3, p. 223–236, accessed December 17, 2020, at https://doi.org/10.1061/(ASCE)1084-0699(2005)10:3(223).

Hunt, C.B, 1958, Structural and igneous geology of the LaSal Mountains, Utah: U.S. Geological Survey Professional Paper 294–I, p. 305–364, accessed December 17, 2020, at https://doi.org/10.3133/pp294I.

Hunt, C.B., 1969, Geologic history of the Colorado River: U.S. Geological Survey Professional Paper 669–C, p. 59–130, https://doi.org/10.3133/pp669C.

Ingerson, R., and Pearson, F.J., 1964, Estimation of age and rate of motion of groundwater by the 14C method, *in* Miyake, Y., and Koyama, T., eds., Recent research in the field of hydrosphere, atmosphere, and nuclear geochemistry: Tokyo, Japan, Marusen, 404 p.

Kalin, R.M., 2000, Radiocarbon dating of groundwater systems, chap. 4 *of* Cook, P.G., and Herczeg A.L., eds., Environmental tracers in subsurface hydrology: Boston, Kluwer Academic Publishers, 529 p.

Keith, M.L., and Weber, J.N., 1964, Carbon and oxygen isotopic composition of selected limestones and fossils: Geochimica et Cosmochimica Acta, v. 28, no. 10–11, p. 1787–1816, accessed December 17, 2020, at https://doi.org/10.1016/0016-7037(64)90022-5.

Kelley, V.C., 1958, Tectonics of the region of the Paradox Basin, *in* Sanborn, A.F, ed., Guidebook to the geology of the Paradox Basin: Ninth Annual Field Conference, Intermountain Association of Petroleum Geologists, Salt Lake City, p. 31–38.

Kenney, T.A., Gerner, S.J., Buto, S.G., and Spangler, L.E., 2009, Spatially referenced statistical assessment of dissolved-solids load sources and transport in streams of the Upper Colorado River Basin: U.S. Geological Survey Scientific Investigations Report 2009–5007, 50 p., accessed December 17, 2020, at https://doi.org/10.3133/sir20095007.

King, V.M., Block, L.V., Yeck, W.L., Woode, C.K., and Derouin, S.A., 2014, Geological structure of the Paradox Valley Region, Colorado, and relationship to seismicity induced by deep well injection: Journal of Geophysical Research—Solid Earth, v. 199, no. 6, p. 4955–4978, accessed December 17, 2020, at https://doi.org/10.1002/2013JB010651.

Kleinfelder, 2008, Geotechnical design recommendations mill and infrastructure Piñon Ridge Project, Montrose County, Colorado: Kleinfelder West, Inc., Golden, Colo.

Kleinfelder, 2009, Geologic report, revision 0: Kleinfelder West, Inc., Albuquerque, New Mexico, June 9, 2009, 467 p.

Konikow, L.F., and Bedinger, M.S., 1978, Evaluation of hydrogeologic aspects of proposed salinity control in Paradox Valley, Colorado: U.S. Geological Survey Open-File Report 78–27, 23 p., accessed December 17, 2020, at https://doi.org/10.3133/ofr7827.

Kruseman, G.P., and de Ridder, N.A., 1990, Analysis and evaluation of pumping test data: Publication 47, International Institute for Land Reclamation and Improvement, Wageningen, The Netherlands, accessed February 7, 2023, at https://www.hydrology.nl/images/docs/dutch/key/Kruseman_and_De_Ridder_2000.pdf.

Lindner-Lunsford, J.B., Kimball, B.A., Chafin, D.T., and Bryant, C.G., 1989, Hydrogeology of aquifers of Paleozoic age, Upper Colorado River Basin, excluding the San Juan Basin, in Colorado, Utah, Wyoming, and Arizona: U.S. Geological Survey Hydrologic Atlas HA–702, scale 1:5,000,000, 2 sheets, accessed December 17, 2020, at https://doi.org/10.3133/ha702.

Massmann, Gudrun, Simmons, Craig, Love, Andrew, Ward, James, and James-Smith, Julianne, 2006, On variable density surface water–groundwater interaction—A theoretical analysis of mixed convection in a stably-stratified fresh surface water–saline groundwater discharge zone: Journal of Hydrology, v. 329, no. 3–4, p. 390–402, accessed December 17, 2020, at https://doi.org/10.1016/j.jhydrol.2006.02.024.

Mast, M.A., 2017, Estimation of salt loads for the Dolores River in the Paradox Valley, Colorado, 1980–2015: U.S. Geological Survey Scientific Investigations Report 2017–5059, 20 p., accessed December 17, 2020, at https://doi.org/10.3133/sir20175059.

Mast, M.A., and Terry, N., 2019, Controls on spatial and temporal variations of brine discharge to the Dolores River in the Paradox Valley, Colorado, 2016–18: U.S. Geological Survey Scientific Investigations Report 2019–5058, 25 p., accessed December 17, 2020, at https://doi.org/10.3133/sir20195058.

McKay, E.J., 1955, Geology of the Red Canyon quadrangle, Colorado: U.S. Geological Survey, Geologic Quadrangle Map GQ–58, scale 1:24000.

Michel, R.L., 1989, Tritium deposition over the continental United States, 1953–1983, *in* Atmospheric deposition: International Association of Hydrological Sciences, p. 109–115.

Muskat, M., 1937, The flow of homogeneous fluids through porous media: McGraw-Hill, New York, 736 p.

Newman, C.P., 2021, Water-level and pumping data, water-level models, and estimated hydraulic properties for the Paradox Valley alluvial aquifer: U.S. Geological Survey data release, accessed February 7, 2023, at https://doi.org/10.5066/P9NV5U6F.

Paschke, S.S., and Mast, M.A., 2024, Geospatial datasets developed for a hydrogeologic conceptual model of brine discharge to the Dolores River, Paradox Valley, Colorado: U.S. Geological Survey data release, accessed February 7, 2023, at https://doi.org/10.5066/P9CJQDDU.

Piper, A.M., 1944, A graphic procedure in the geochemical interpretation of water-analyses: EOS Transactions American Geophysical Union, v. 25, no. 6, p. 914–928, accessed December 17, 2020, at https://doi.org/10.1029/TR025i006p00914.

Pozdniakov, S., Ivanov, P., Davis, P., and Sizov, N., 2021, Use of groundwater level fluctuations near an operating water supply well to estimate aquifer transmissivity: Groundwater, v. 29, no. 21, p. 49–58, accessed December 17, 2020, at https://doi.org/10.1111/gwat.13018.

PRISM Climate Group, 2021, PRISM climate data website: Corvallis, Oreg., Oregon State University, accessed July 31, 2021, at https://prism.oregonstate.edu.

R Core Team, 2020, R—A language and environment for statistical computing: Vienna, Austria, R Foundation for Statistical Computing, accessed December 17, 2020, at https://www.R-project.org.

Sanford, W.E., Shropshire, R.G., Solomon, D.K., 1996, Dissolved gas tracers in groundwater—Simplified injection, sampling, and analysis: Water Resources Research, v. 32, no. 6, p. 1635–1642, accessed December 17, 2020, at https://doi.org/10.1029/96WR00599.

Shoemaker, E.M., 1956, Geology of the Rock Creek quadrangle, Colorado: U.S. Geological Survey, Geologic Quadrangle Map, GQ–83, scale 1:24,000.

Solomon, D.K., 2000, ^{4}He in groundwater, chap. 14 *of* Cook, P.G., and Herczeg A.L., eds., Environmental tracers in subsurface hydrology: Boston, Kluwer Academic Publishers, 529 p.

Springer, R.K., and L.W.Gelhar, 1991, Characterization of large-scale aquifer heterogeneity in glacial outwash by analysis of slug tests with oscillatory response, Cape Cod, Massachusetts: U.S. Geological Survey Water Resources Investigations Report 91–4034, p. 36–40.

Stute, M., and Schlosser, P., 2000, Atmospheric noble gases, chap. 11 *of* Cook, P.G., and Herczeg, A.L., eds., Environmental tracers in subsurface hydrology: Boston, Mass., Kluwer Academic Publishers, p. 349–377.

Tamers, M.A., 1975, Validity of radiocarbon dates on ground water: Geophysical Surveys, v. 2, p. 217–239, accessed December 17, 2020, at https://doi.org/10.1007/BF01447909.

Theis, C.V., 1935, The relation between the lowering of the Piezometric surface and the rate and duration of discharge of a well using ground-water storage: Transactions American Geophysical Union, v. 16, no. 2, p. 519–524, accessed December 17, 2020, at https://doi.org/10.1029/TR016i002p00519.

Thomas, J.M., Hudson, G.B., Stute, M., and Clark, J.F., 2003, Noble gas loss may indicate groundwater flow across flow barriers in southern Nevada: Environmental Geology, v. 43, p. 568–579, accessed December 17, 2020, at https://doi.org/10.1007/s00254-002-0681-1.

Tuttle, M.L., and Grauch, R.I., 2009, Salinization of the upper Colorado River—Fingerprinting geologic salt sources: U.S. Geological Survey Scientific Investigations Report 2009–5072, 62 p., accessed December 17, 2020, at https://doi.org/10.3133/sir20095072.

University of Utah, 2022, Noble gas lab: Salt Lake City, Utah, University of Utah, College of Mines and Earth Sciences, accessed March 24, 2022, at https://noblegaslab.utah.edu.

U.S. Geological Survey [USGS], 2008, Field measurements, (edited by Wilde, F.D.): U.S. Geological Survey Techniques of Water-Resources Investigations, book 9, chap. A6, accessed March 24, 2022, at https://doi.org/10.3133/twri09A6.

U.S. Geological Survey [USGS], 2020a, USGS water data for the nation: U.S. Geological Survey National Water Information System database, accessed December 17, 2020, at https://doi.org/10.5066/F7P55KJN.

U.S. Geological Survey [USGS], 2020b, The national map: U.S. Geological Survey National Geospatial Program, accessed December 17, 2020, at https://www.usgs.gov/core-science-systems/national-geospatial-program/national-map.

Voggesser, Garrit, 2001, The Dolores Project, Bureau of Reclamation history; accessed July 3, 2023, at https://www.usbr.gov/projects/pdf.php?id=113

Watts, K.R., 2000, Effects of the Paradox Valley Unit on dissolved solids, sodium, and chloride in the Dolores River near Bedrock, Colorado, water years 1988–98: U.S. Geological Survey Water-Resources Investigations Report 00–4011, 8 p., accessed December 17, 2020, at https://pubs.usgs.gov/wri/wri00-4011/.

Weast, R.C., ed., 1974, Handbook of chemistry and physics (54th ed.): Cleveland, Ohio, CRC Press Division of the Chemical Rubber Co., 2,405 p.

Weber, S., and Chapuis, R.P., 2013, Interpretation of a pumping test with interference from a neighboring well: Groundwater, v. 51, no. 6, p. 935–944, accessed December 17, 2020, at https://doi.org/10.1111/gwat.12014.

Weir, I.E., Jr., Maxfield, E.B., and Zimmerman, E.A., 1983, Regional hydrology of the Dolores River basin, eastern Paradox Basin, Colorado and Utah: U.S. Geological Survey Water-Resources Investigations Report 83–4217, 53 p.

Williams, P.L., 1964, Geology, structure, and uranium deposits of the Moab quadrangle, Colorado and Utah: U.S. Geological Survey, Miscellaneous Geologic Investigations Map I–360, scale 1:250,000, 2 sheets, accessed December 17, 2020, at http://ngmdb.usgs.gov/Prodesc/proddesc_1388.htm.

Withington, C.F., 1955, Geologic map of the Paradox quadrangle, Colorado: U.S. Geological Survey Geologic Quadrangle GQ–72, scale 1:24,000.

Wollitz, L.E., Thordarson, W, Whitfield M.S., Jr., and Weir, J.E., Jr.,1982, Results of hydraulic tests in U.S. Department of Energy's wells DOE-4, 5, 6, 7, 8, and 9, Salt Valley, Grand County, Utah: U.S. Geological Survey Open-File Report 82–346, 71 p., accessed December 17, 2020, at https://doi.org/10.3133/ofr82346.

Appendix 1. Application of Environmental Tracers to Determine Groundwater Recharge Sources and Age

Oxygen-18 and Deuterium

The stable isotopes of water were examined to investigate recharge sources to groundwater in the Paradox Valley. Most water molecules are made up of hydrogen (^{1}H) and oxygen-16 (^{16}O). However, some water molecules (less than 1 percent) contain the heavier isotopes of deuterium (^{2}H or D) and oxygen-18 (^{18}O). Heavier refers to the condition when there are additional neutrons in the nucleus of the hydrogen or oxygen atom, thereby increasing the mass or atomic weight of the water molecule (Coplen, 1994).

Stable isotopes are analyzed by measuring the ratio of the heavier, less abundant isotope to the lighter, more abundant isotope and are reported as differences relative to a known standard. The isotope ratios are reported as delta (δ) values expressed as parts per thousand. The δ value for an isotope ratio, R, is determined as shown in equation 1.1.

$$\delta R = (R\text{sample}/R\text{standard} - 1) \times 1{,}000 \qquad (1.1)$$

where

δR is the δ value for a specific isotope in the sample (^{2}H or ^{18}O);

Rsample is the ratio of the rare isotope to the common isotope for a specific element in the sample; and

Rstandard is the ratio of the rare isotope to the common isotope for the same element in the standard reference material. The reference standard used in this report is Vienna Standard Mean Ocean Water (Craig, 1961b; Coplen, 1994).

A positive δR value indicates that the sample is enriched in the heavier isotope with respect to the standard (Coplen, 1994). A negative δR value indicates that the sample is depleted in the heavier isotope with respect to the standard. Heavier isotopes are more difficult to evaporate and easier to condense; for example, liquid contains more heavy isotopes than the vapor evaporated from the liquid. Because of this effect, water vapor in the atmosphere that condenses and falls as precipitation will become increasingly depleted in the heavier isotopes at cooler temperatures and at higher altitudes. The proportional depletion of ^{2}H and ^{18}O results in isotopic compositions of precipitation (and groundwater sourced from precipitation) that plot along a trend referred to as a meteoric water line when the deuterium excess ($\delta^{2}H$) is plotted compared to the ^{18}O excess ($\delta^{18}O$) (Craig, 1961a; Clark and Fritz, 1997).

Cooler (or high-altitude) precipitation values usually plot lower on the trend line and warmer (or low-altitude) precipitation values plot higher on the trend line. The trend line for worldwide precipitation defines the Global Meteoric Water Line (GMWL) and is described by equation 1.2.

$$\delta^{2}H = 8(\delta^{18}O) + d \qquad (1.2)$$

where

d is defined as the ^{2}H excess (Dansgaard, 1964).

The mean global value for d in freshwater is 10 (Craig, 1961a).

In addition to temperature, isotopic composition of meteoric water is also affected by evaporation, particularly during irrigation or time spent in open-water bodies. Evaporation creates preferential enrichment in ^{18}O relative to ^{2}H, resulting in a shift from and a slope less than the GMWL. Groundwater with evaporated stable isotope compositions can often be identified as containing recharge from distinct sources such as lakes or irrigation canals (Gonfiantini and others, 1998).

Tritium and Helium-3

Tritium (^{3}H) and tritiogenic helium-3 ($^{3}He_{trit}$) were used in this study to identify relatively young groundwater and to estimate the apparent age of groundwater that is less than about 60 years old. Tritium is a radioactive isotope of hydrogen with a half-life of 12.32 years that decays to $^{3}He_{trit}$. Tritium is present in water as part of the water molecule, whereas its decay product, $^{3}He_{trit}$, exists as a noble gas dissolved in water. During the 1950s and 1960s, large amounts of ^{3}H were released into the atmosphere and introduced into the hydrologic cycle by above-ground nuclear weapons testing. Concentrations of ^{3}H in precipitation in the northern hemisphere peaked during 1963–64 at three orders of magnitude above natural background concentrations (Michel, 1989).

Comparison of reconstructed initial ^{3}H concentrations with atmospheric concentration data is used to distinguish between groundwater recharged before or after the beginning of weapons testing in the mid-1950s. By using the concentrations of both ^{3}H and $^{3}He_{trit}$, the age of groundwater (time elapsed since recharge to the water table) can be estimated to an apparent recharge year. These ages are referred to as "apparent," because they can differ from the true average age of the sample when it contains a mixture of water of different ages. Mixtures of modern (post mid-1950s recharge) and pre-modern (before mid-1950s recharge) water typically have

apparent ages that represent the age of the young fraction of the sample, because dilution with pre-modern water will leave the ratio of ^{3}H to $^{3}He_{trit}$ virtually unchanged. Details of this groundwater-dating method are presented in Solomon and Cook (2000).

Tritium concentrations typically are reported in tritium units (TU), where 1 TU is equivalent to one molecule of tritiated water ($^{3}H^{1}HO$) in 10^{18} molecules of $^{1}H_2O$. In a sample of pre-modern groundwater, ^{3}H will have decayed from background pre-nuclear weapons testing concentrations of about 6–8 TU to less than 0.3 TU, which approaches the detection limit of the best analytical methods used to quantify ^{3}H (Lindsey and others, 2019). Samples collected during this study with concentrations of less than 0.2 TU are interpreted to contain no modern water, whereas samples with more than 1 TU are interpreted to contain a substantial fraction of modern water. Apparent $^{3}H/^{3}He$ ages were generally computed for samples having concentrations of 1.0 TU or greater.

Terrigenic Helium

In addition to ^{3}He derived from ^{3}H decay, groundwater accumulates dissolved helium (He) that is produced by the radioactive decay of naturally occurring uranium- and thorium-series elements in aquifer solids and by the upward advection and diffusion of primordial helium from the Earth's mantle. The former of these components is referred to as "crustal He" and the latter as "mantle He." Crustal and mantle helium are collectively referred to as "terrigenic He" (He_{terr}) (Solomon, 2000). Crustal- and mantle-sourced helium are distinguishable by their relative abundance of ^{3}He and ^{4}He isotopes. These values are generally expressed as a $^{3}He/^{4}He$ ratio (R) relative to the atmospheric $^{3}He/^{4}He$ ratio (R_a). Because crustal He has an R/R_a value of approximately 0.02 and mantle He has an R/R_a value of approximately 10–30, the R/R_a of a water sample provides information on the relative amount of crustal compared to mantle sources of He_{terr}. Modern groundwater has an R/R_a value approximately equal to 1, indicating that it contains atmospheric concentrations of He isotopes. In most aquifers, crustal He makes up the majority of the He_{terr}. Where this is the case, the R/R_a value of groundwater will fall below 1 as it acquires He_{terr} from time spent in contact with the aquifer solids. Because He_{terr} concentrations generally increase with lengthening residence time, dissolved $^{4}He_{terr}$ concentrations are useful as a semi-quantitative tool for dating groundwater with ages from 1,000 to more than one million years (Mazor and Bosch, 1992; Solomon, 2000).

Solomon (2000) reports average crustal ^{4}He production rates ranging from 0.28 to 2.4 micro cubic centimeters per cubic meter per year at standard temperature and pressure. At these rates, groundwater will most likely not acquire substantial concentrations of $^{4}He_{terr}$ (more than about 2×10^{-8} cubic centimeters at standard temperature and pressure per gram of water) until it has been in contact with the aquifer materials for more than about 1,000 years. Therefore, even without precise knowledge of local ^{4}He production rates, ^{4}He concentrations more than atmospheric solubility are useful as qualitative measures of groundwater age.

Carbon-14

Carbon-14 (^{14}C) was used in this study to examine the relative distribution of groundwater age and to examine flow rates. Carbon-14 is a naturally occurring radioactive isotope of carbon with a half-life of 5,730 ± 40 years that can be used to determine the apparent age of groundwater on time scales ranging from several hundred to more than 30,000 years. The method of radiocarbon dating used in this study is based on the radioactive decay of the ^{14}C isotope of the dissolved inorganic carbon (DIC) in groundwater. Kalin (2000) provides a comprehensive review of the radiocarbon groundwater dating method, a summary of which is included in the following paragraphs.

Carbon-14 (^{14}C) is produced in the upper atmosphere as cosmic rays react with nitrogen-14 (^{14}N) and then mixes into the lower atmosphere in the form carbon dioxide (CO_2). Any material using or reacting with atmospheric CO_2 (plants and water) attains a ^{14}C activity (effective concentration) equal to the atmospheric $^{14}CO_2$. Carbon-14 activity is reported as percent modern carbon (pmC) and, by convention, the pre-1950 (pre-modern) activity of atmospheric ^{14}C is 100 pmC. The DIC in precipitation has a ^{14}C activity in equilibrium with atmospheric CO_2. As precipitation infiltrates the subsurface, the ^{14}C activity is modified by exchange with soil-zone CO_2 and by reaction with carbon-bearing minerals in the unsaturated zone. After entering the saturated zone, interaction with soil-zone carbon ceases, and the ^{14}C in the DIC decays with time.

In addition to radioactive decay, the ^{14}C activity of groundwater in the saturated zone can be affected by several processes. Chemical reactions in the saturated zone can introduce carbon (for example, from the dissolution of limestone) having essentially 0 pmC to groundwater, thus decreasing the ^{14}C activity of the DIC and causing a sample to appear older than it is. These reactions can greatly decrease the ^{14}C activity of groundwater. For example, in terrains where carbonate rocks are present in the recharge area, modern carbon in groundwater may be diluted with dissolved ^{14}C-free carbonate minerals to the extent that very young groundwater can have ^{14}C activities as low as 50 pmC (Clark and Fritz, 1997). Mixing of groundwater of varying ages also needs to be considered, especially when samples are collected from wells with large-screened intervals or from regional discharge areas where groundwater-flow paths converge. Lastly, the apparent radiocarbon age of groundwater is also affected by the historical variation of atmospheric ^{14}C activity. For these reasons, age adjustments may be needed to account for their effects on ^{14}C activity and improve the accuracy of radiocarbon ages.

Dissolved Noble Gases

Stute and Schlosser (2000) provide a comprehensive review of how dissolved noble gases are used as groundwater tracers. In this study, dissolved noble gases were analyzed to evaluate groundwater recharge temperature (the temperature of recharging water as it crosses the water table) with the goal of identifying mountain compared to valley recharge. Most noble gases that are dissolved in groundwater originate in the atmosphere. As recharging water enters the aquifer, it becomes isolated from the atmosphere, and the dissolved concentrations of neon, argon, krypton, and xenon become essentially static according to their solubility relations to the temperature, pressure, and salinity conditions that existed at the water table at the time of recharge (Aeschbach-Hertig and others, 1999; Ballentine and Hall, 1999; Stute and Schlosser, 2000).

Because these gases are generally nonreactive along flow paths in the subsurface, their concentrations in groundwater provide a record of the physical conditions (recharge temperature [T_r] and recharge pressure [P_r]) that existed at the time of recharge. The P_r is nearly equal to the atmospheric pressure at the land surface above the point of recharge and thus is directly related to the recharge altitude (H_r). The T_r is the ground temperature at the water table at the point of recharge and is often close to the average annual air temperature (T_a) at the land surface above the point of recharge. Water-table temperatures (and thus T_r) are generally 1–3 degrees Celsius (°C) warmer than the average annual air temperature at the land surface for typical water-table depths of less than about 50 meters (164 feet [ft]) (Domenico and Schwartz, 1998). Because temperature decreases as altitude increases, modern (or Holocene) mountain recharge most likely has T_r values cooler than the temperature at the water table in the valley. Deep water tables (more than 300 ft) may be influenced by the geothermal gradient (the natural warming of the earth with depth) and are often substantially warmer than T_a.

Measured concentrations of dissolved neon-20 (^{20}Ne), argon-40 (^{40}Ar), krypton-84 (^{84}Kr), and xenon-129 (^{129}Xe) were used in a closed-system equilibration model (CE model; Aeschbach-Hertig and others, 2000; Kipfer and others, 2002) to calculate noble gas recharge temperatures (assumed to equal T_r), excess air (A_e), and a fractionation factor (F), related to the partial dissolution of trapped air bubbles. The three unknown parameters (T_r, A_e, and F) were solved for by optimization of an overdetermined system of equations that relates them to the measured dissolved-gas concentrations in each sample. In this system of equations, H_r serves as the proxy for P_r used for the gas solubility calculations in the CE model. Both H_r and T_r are highly correlated parameters, meaning that different combinations can produce nearly the same set of dissolved-gas concentrations, and thus the values cannot be solved for simultaneously. By specifying H_r ahead of time, the remaining unknown recharge parameters can be solved. In areas of high topographic relief, it is generally not possible to know H_r ahead of time. Therefore, a range of T_r values is calculated for each sample using a range of possible H_r values. The minimum recharge altitude (H_{rmin}) for each sample was assumed to be the land-surface altitude at the sample site, and the maximum recharge altitude (H_{rmax}) was chosen to approximate the highest possible recharge altitude within the surface basin (10,500 ft). Using this method, the uncertainty in the calculated T_r values is approximately plus or minus 1 °C (Manning and Solomon, 2003).

References Cited

Aeschbach-Hertig, W., Peeters, F., Beyerle, U., and Kipfer, R., 1999, Interpretation of dissolved atmospheric noble gases in natural waters: Water Resources Research, v. 35, no. 9, p. 2779–2792, accessed December 17, 2020, at https://doi.org/10.1029/1999WR900130.

Aeschbach-Hertig, W., Peeters, F., Beyerle, U., and Kipfer, R., 2000, Paleotemperature reconstruction from noble gases in ground water taking into account equilibration with entrapped air: Nature, v. 405, p. 1040–1044, accessed December 17, 2020, at https://doi.org/10.1038/35016542.

Ballentine, C.J., and Hall, C.M., 1999, Determining paleotemperature and other variables by using an error-weighted, nonlinear inversion of noble gas concentrations in water: Geochimica et Cosmochimica Acta, v. 63, no. 16, p. 2315–2336, accessed December 17, 2020, at https://doi.org/10.1016/S0016-7037(99)00131-3.

Clark, I.D. and Fritz, P., 1997, Environmental isotopes in hydrogeology: New York, CRC Press, 342 p.

Coplen, T.B., 1994, Reporting of stable hydrogen, carbon, and oxygen isotopic abundances: Pure and Applied Chemistry, v. 66, no. 2, p. 273–276, accessed December 17, 2020, at https://doi.org/10.1351/pac199466020273.

Craig, H., 1961a, Isotopic variations in meteoric waters: Science, v. 133, no. 3465, p. 1702–1703, accessed December 17, 2020, at https://doi.org/10.1126/science.133.3465.1702.

Craig, H., 1961b, Standard for reporting concentrations of deuterium and oxygen-18 in natural waters: Science, v. 133, no. 3467, p. 1833–1834, accessed December 17, 2020, at https://doi.org/10.1126/science.133.3467.1833.

Dansgaard, W., 1964, Stable isotopes in precipitation: Talus, v. 16, p. 436–468.

Domenico, P.A., and Schwartz, F.W., 1998, Physical and chemical hydrogeology: New York, John Wiley and Sons, 506 p.

Gonfiantini, R., Fröhlich K., Araguás-Araguás, L., and Rozanski, K., 1998, Isotopes in groundwater hydrology, chap. 7 *of* Kendall, C., and McDonnel, J.J., eds, Isotope tracers in catchment hydrology: Elsevier, p. 203–246, accessed December 17, 2020, at https://doi.org/10.1016/B978-0-444-81546-0.50014-8.

Kalin, R.M., 2000, Radiocarbon dating of groundwater systems, chap. 4 *of* Cook, P.G., and Herczeg A.L., eds., Environmental tracers in subsurface hydrology: Boston, Kluwer Academic Publishers, 529 p.

Kipfer, R., Aeschbach-Hertig, W., Peeters, F., and Stute, M., 2002, Noble gases in lakes and ground waters, *in* Porcelli, D., Ballentine, C.J., and Wieler, R., eds., Noble gases in geochemistry and cosmochemistry: Mineralogical Society of America, p. 615–700, accessed December 17, 2020, at https://doi.org/10.1515/9781501509056-016.

Lindsey, B.D., Jurgens, B.C., and Belitz, K., 2019, Tritium as an indicator of modern, mixed, and premodern groundwater age: U.S. Geological Survey Scientific Investigations Report 2019–5090, 18 p., accessed March 26, 2022, at https://doi.org/10.3133/sir20195090.

Manning, A.H., and Solomon, D.K., 2003, Using noble gases to investigate mountain-front recharge: Journal of Hydrology, v. 275, p. 194–207, accessed December 17, 2020, at https://doi.org/10.1016/S0022-1694(03)00043-X.

Mazor, E., and Bosch, A., 1992, Helium as a semi-quantitative tool for groundwater dating in the range of 104–108 years, in isotopes of noble gases as tracers in environmental studies, *in* A consultants meeting on isotopes of noble gases as tracers in environmental studies organized by the International Atomic Energy Agency, Vienna, Austria, May 29 to June 2, 1989, Proceedings: Vienna, Austria, International Atomic Energy Agency, p. 163–178.

Michel, R.L., 1989, Tritium deposition over the continental United States, 1953–1983, *in* Atmospheric deposition: International Association of Hydrological Sciences, p. 109–115.

Solomon, D.K., 2000, ^{4}He in groundwater, chap. 14 *of* Cook, P.G., and Herczeg A.L., eds., Environmental tracers in subsurface hydrology: Boston, Kluwer Academic Publishers, 529 p.

Solomon, D.K., and Cook, P.G., 2000, 3H and ^{3}He, chap. 13 *of* Cook, P.G., and Herczeg A.L., eds., Environmental tracers in subsurface hydrology: Boston, Kluwer Academic Publishers, p. 397–424.

Stute, M., and Schlosser, P., 2000, Atmospheric noble gases, chap. 11 *of* Cook, P.G., and Herczeg, A.L., eds., Environmental tracers in subsurface hydrology: Boston, Mass., Kluwer Academic Publishers, p. 349–377.

For more information concerning the research in this report, contact the

Director, USGS Colorado Water Science Center
Box 25046, Mail Stop 415
Denver, CO 80225
(303) 236-6901

Or visit the Colorado Water Science Center website at

https://www.usgs.gov/centers/colorado-water-science-center

Publishing support provided by the Denver and Reston Publishing Service Centers

ISSN 2328-0328 (online)
https://doi.org/10.3133/sir20235094